

ACCEPTED MANUSCRIPT • OPEN ACCESS

## 2026 Roadmap on Next-Generation Solid Electrolytes for Battery Applications

To cite this article before publication: Florian Strauss *et al* 2026 *Mater. Futures* in press <https://doi.org/10.1088/2752-5724/ae5120>

### Manuscript version: Accepted Manuscript

Accepted Manuscript is “the version of the article accepted for publication including all changes made as a result of the peer review process, and which may also include the addition to the article by IOP Publishing of a header, an article ID, a cover sheet and/or an ‘Accepted Manuscript’ watermark, but excluding any other editing, typesetting or other changes made by IOP Publishing and/or its licensors”

This Accepted Manuscript is © 2026 The Author(s). Published by IOP Publishing Ltd on behalf of the Dongguan Institute of Materials Science and Technology, CAS.



As the Version of Record of this article is going to be / has been published on a gold open access basis under a CC BY 4.0 licence, this Accepted Manuscript is available for reuse under a CC BY 4.0 licence immediately.

Everyone is permitted to use all or part of the original content in this article, provided that they adhere to all the terms of the licence <https://creativecommons.org/licenses/by/4.0>

Although reasonable endeavours have been taken to obtain all necessary permissions from third parties to include their copyrighted content within this article, their full citation and copyright line may not be present in this Accepted Manuscript version. Before using any content from this article, please refer to the Version of Record on IOPscience once published for full citation and copyright details, as permissions may be required. All third party content is fully copyright protected and is not published on a gold open access basis under a CC BY licence, unless that is specifically stated in the figure caption in the Version of Record.

View the [article online](#) for updates and enhancements.

---

**2026 Roadmap on Next-Generation Solid Electrolytes for  
Battery Applications**

Journal:	<i>Materials Futures</i>
Manuscript ID	MF-101084.R1
Manuscript Type:	Roadmap
Keywords:	Energy storage, Solid state batteries, Inorganic electrolytes

SCHOLARONE™  
Manuscripts

Accepted Manuscript

# 2026 Roadmap on Next-Generation Solid Electrolytes for Battery Applications

Florian Strauss<sup>1,\*</sup>, Torsten Brezesinski<sup>1,\*</sup>, Saneyuki Ohno<sup>2,3</sup>, Yi Huang<sup>2</sup>, Peng Song<sup>2</sup>, Xabier Martinez de Irujo-Labalde<sup>4</sup>, Wolfgang G. Zeier<sup>4,5</sup>, Jelena Popovic-Neuber<sup>6</sup>, Hugo Braun<sup>7,8</sup>, Arndt Remhof<sup>7,8</sup>, Corsin Battaglia<sup>7,9,10</sup>, Theodosios Famprikis<sup>11,a</sup>, Marnix Wagemaker<sup>11</sup>, Ke Huang<sup>12</sup>, Yan Zeng<sup>12</sup>, Bin Ouyang<sup>12</sup>, Juhyoun Park<sup>13</sup>, Yoon Seok Jung<sup>13,14</sup>, Jingui Yang<sup>1</sup>, Siyuan Guo<sup>1</sup>, Shuo Wang<sup>15</sup>, Shu-Bo Wang<sup>15</sup>, Eric McCalla<sup>16</sup>, Benjamin Mercier-Guyon<sup>17</sup>, Ove Korjus<sup>17</sup>, Patrice Perrenot<sup>17</sup>, Claire Villevieille<sup>17</sup>, H. Martin R. Wilkening<sup>18</sup>, Kerstin Wissel<sup>19</sup> and Oliver Clemens<sup>19</sup>

- <sup>1</sup> Institute of Nanotechnology, Karlsruhe Institute of Technology (KIT), Kaiserstr. 12, 76131 Karlsruhe, Germany.
- <sup>2</sup> Institute of Multidisciplinary Research for Advanced Materials, Tohoku University, Miyagi 980-8577, Japan.
- <sup>3</sup> Department of Frontier Sciences for Advanced Environment, Graduate School of Environmental Studies, Tohoku University, Miyagi 980-8572, Japan.
- <sup>4</sup> Institute of Inorganic and Analytical Chemistry, University of Münster, Corrensstr. 28/30, 48149 Münster, Germany.
- <sup>5</sup> Institute of Energy Materials and Devices (IMD), IMD-4: Helmholtz Institute Münster, Forschungszentrum Jülich GmbH, 48149 Münster, Germany.
- <sup>6</sup> Department of Energy and Petroleum Engineering, University of Stavanger, Stavanger, Norway.
- <sup>7</sup> Empa - Swiss Federal Laboratories for Materials Science and Technology, Duebendorf, Switzerland.
- <sup>8</sup> Institute for Inorganic and Analytical Chemistry, University of Freiburg, Freiburg, Germany.
- <sup>9</sup> Department of Information Technology and Electrical Engineering, ETH Zurich, Zurich, Switzerland.
- <sup>10</sup> Institute of Materials, School of Engineering, EPFL, Lausanne, Switzerland.
- <sup>11</sup> Radiation Science and Technology, Faculty of Applied Sciences, Delft University of Technology, Delft, The Netherlands.
- <sup>12</sup> Department of Chemistry & Biochemistry, Florida State University, Tallahassee, FL 32306, USA.
- <sup>13</sup> Department of Chemical and Biomolecular Engineering, Yonsei University, Seoul 03722, South Korea.
- <sup>14</sup> Department of Battery Engineering, Yonsei University, Seoul 03722, South Korea.
- <sup>15</sup> School of Materials Science and Engineering, Wuhan University of Technology, Wuhan 430070, China.
- <sup>16</sup> Department of Chemistry, McGill University, Montreal, Canada.
- <sup>17</sup> Université Grenoble Alpes, Université Savoie Mont Blanc, CNRS, Grenoble INP, LEPMI, 38000 Grenoble, France.
- <sup>18</sup> Institute of Chemistry and Technology of Materials, Stremayrgasse 9, Graz University of Technology, 8010 Graz, Austria.
- <sup>19</sup> University of Stuttgart, Institute for Materials Science, Heisenbergstr. 3, 70569 Stuttgart, Germany.

\*E-mail: [florian.strauss@kit.edu](mailto:florian.strauss@kit.edu) and [torsten.brezesinski@kit.edu](mailto:torsten.brezesinski@kit.edu)

<sup>a</sup> Current address: Inorganic Chemistry Laboratory, Department of Chemistry, University of Oxford, Oxford, United Kingdom.

## Abstract

The global transition to sustainable energy systems requires breakthroughs in electrochemical storage technologies that are not only safe, but also resource-efficient. Solid-state batteries (SSBs), which use superionic solid electrolytes (SEs) instead of flammable liquid electrolytes, are at the forefront of this transformation. In general, SEs promise increased safety, access to high-voltage cathode and metal anode chemistries, and new avenues for circular design and recyclability. However, to reach their full potential, intertwined challenges related to ion transport, (electro)chemical stability, manufacturing, processing, and cost must be overcome. This “2026 Roadmap on Next-Generation Solid Electrolytes for Battery Applications” outlines new directions that will contribute to research in the field of SSBs over the next decade. It provides an overview of the current state of the art in sulfide- and halide-based solid electrolytes for Li and Na systems, examines post-Li/Na chemistries (K, Mg, and others), and highlights advances in hydroborates, fully reduced (irreducible), and compositionally complex (high-entropy) electrolytes, as well as glass-ceramic electrolytes. Beyond material innovation, the paper emphasizes the critical role of redox activity in SEs, scalable processing, high-throughput synthesis, and machine learning, as well as *operando* analytics and nuclear magnetic resonance spectroscopy to accelerate discoveries and gain a better understanding of structure-property relationships. Finally, the growing importance of recycling and circular design for ensuring sustainability is highlighted. By combining insights from chemistry, materials science, data (computational) science, and manufacturing, this article assumes that future SEs will progressively evolve from passive components to active design elements in high-energy-density electrochemical systems. The integration of multidisciplinary innovations will be crucial to realizing the potential of SSBs in practical technologies that power a decarbonized world.

Keywords: electrochemical energy storage, solid-state batteries, superionic conductors, synthesis, characterization, recycling

## Outline

1. Introduction
2. Sulfide solid electrolytes: materials-to-devices perspectives
3. Perspectives on halide-based solid electrolytes
4. Post-Li/Na inorganic solid-state electrolytes
5. Hydroborate solid electrolytes
6. Fully reduced (irreducible) solid electrolytes
7. Amorphous solid electrolytes: ionic conductivity and conduction mechanisms
8. Glass-ceramic solid electrolytes: halides
9. Redox-active solid electrolytes
10. Processing/large-scale manufacturing
11. Outlook for high-throughput and machine learning guided synthesis of solid electrolytes
12. Advanced *operando* investigation of solid-state batteries
13. NMR as a key to unlocking defect structure and dynamics in emerging solid electrolytes
14. Recycling of solid electrolytes in solid-state batteries

# 1. Introduction

Florian Strauss<sup>1,\*</sup> and Torsten Brezesinski<sup>1,\*</sup>

<sup>1</sup> Institute of Nanotechnology, Karlsruhe Institute of Technology (KIT), Kaiserstr. 12, 76131 Karlsruhe, Germany.

\*E-mail: florian.strauss@kit.edu and torsten.brezesinski@kit.edu

As the world moves towards electrification and the integration of renewable energies, the need for storage technologies that are intrinsically safe, energy dense, and sustainable is more urgent than ever. One of the most groundbreaking developments in this area is solid-state batteries (SSBs), in which the liquid electrolyte is replaced by an ionically conductive solid, i.e., a superionic solid electrolyte (SE). This paradigm shift promises not only a significant increase in performance, but also a fundamental rethinking of the design, manufacture, and recycling of electrochemical energy storage devices. Especially inorganic SEs appear to be capable of unlocking the potential of high-capacity anodes and high-voltage cathodes, which are currently limited by their incompatibility with conventional liquid electrolytes [1–3]. Over the past decade, a wide variety of SEs have been developed as Li-, Na-, and K-ion conductors and beyond (**Figure 1a**), including sulfides, halides, oxides, hydroborates, and other material classes (**Figure 1b**), each with unique advantages and challenges [4, 5]. The research field has evolved from (isolated) seminal discoveries of high room-temperature ionic conductivity, for example, in  $\text{Li}_{10}\text{GeP}_2\text{S}_{12}$  (LGPS), similar to that of leading liquid electrolytes [6], to an increasingly differentiated understanding of structure-property relationships, defect chemistry, migration mechanisms, and interfacial phenomena.

However, the community is now at a critical turning point. The next phase of SE research must go beyond the search for superionic conductivity alone and focus on integrated solutions that balance (electro)chemical stability, mechanical resilience, manufacturability, and recyclability. The focus is shifting slowly from “what works in the laboratory?” to “what can be scaled up in practice?”. This change requires not only material innovations, but also a system-level perspective that combines design at the atomic scale with implementation on an industrial scale.

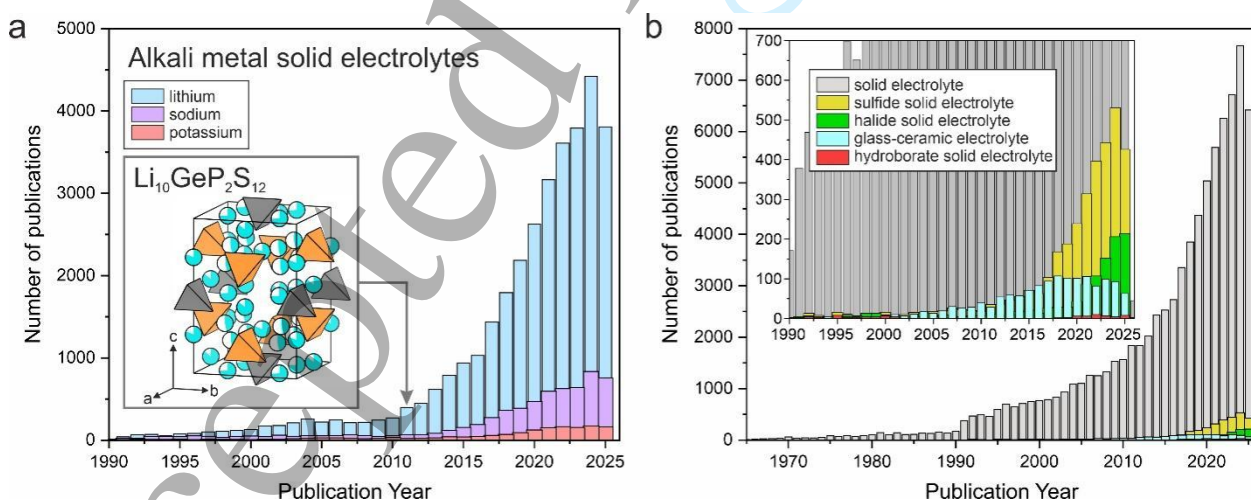


**Figure 1.** Number of publications per year for (a) alkali metal SEs and (b) various classes of SEs according to the keywords indicated in the inset. The data contained herein is sourced from Web of Science™, Copyright (2025), Clarivate.

In this article, we outline the new frontiers that will define the next generation of inorganic SEs and their use in practical battery environments. We begin with sulfide-based systems, which continue

1 to set the standard for high room-temperature ionic conductivity in both lithium and sodium SEs.  
2 Halide electrolytes have recently attracted attention due to their high electrochemical (anodic) stability  
3 and mechanical softness. Post-Li/Na chemistries, such as potassium, magnesium, or other multivalent  
4 systems, offer sustainable (abundant) alternatives for solid-state electrochemical energy storage. In  
5 addition to these families, hydroborates and fully reduced electrolytes expand the design space with  
6 unique transport properties and improved electrochemical stability. Amorphous ion conductors  
7 introduce disorder to increase mobility and structural robustness. Glass-ceramic electrolytes combine  
8 high ion conductivity of the crystalline phase(s) with flexibility provided by the amorphous matrix,  
9 thus improving processability and chemo-mechanical behavior. Redox-active SEs blur the boundary  
10 between electrolyte and electrode active material, thereby enabling an increase in cell capacity and  
11 facilitating redox mediation in the solid state.  
12

13  
14 Beyond the discovery of new materials and their tailoring, progress will depend on systems that  
15 are easily scalable and can be used in cost-effective processing techniques (compatible with industrial  
16 manufacturing). Furthermore, high-throughput experimentation, modeling/simulation, and machine  
17 learning will likely make SE design a predictive and automated process. *In situ* and *operando*  
18 characterization techniques and advanced nuclear magnetic resonance (NMR) spectroscopy further  
19 enable real-time observation of interfacial dynamics and degradation processes. Finally, recycling  
20 strategies are emerging to ensure sustainable life cycles and the recovery of materials within SSB  
21 ecosystems.  
22  
23

24 As the field of SE research for batteries enters a phase of rapid growth, the convergence of  
25 materials science, data science, and manufacturing technology will drive the development of advanced  
26 SSBs. The roadmap for 2026 envisions a future in which the SE is no longer passive but active,  
27 enabling transformative electrochemical systems that are developed at the atomic level, integrated  
28 across multiple scales, and embedded in a circular, sustainable energy economy. The breakthroughs of  
29 the next decade will likely emerge from interdisciplinary collaboration, bringing together insights from  
30 crystallography, computer science, interfacial chemistry, and industrial engineering to push the  
31 boundaries of what is possible in solid-state electrochemical energy storage.  
32  
33

34 The potential commercialization of advanced SEs depends crucially on the development of cost-  
35 effective manufacturing processes, including the availability of low-cost precursors and low-  
36 temperature synthesis routes. Currently, only a few sulfide-, oxide-, and halide-based materials are  
37 commercially available for research and development purposes (in kg quantities) at relatively high  
38 prices. However, if SSBs are to become a widespread technology, production costs must be drastically  
39 reduced. Although the development of new synthesis routes (or the use of existing ones) may well be  
40 feasible, the price of certain precursors can be a serious obstacle, e.g., in the case of hydroborate or  
41 sulfide SEs. For the latter, the price of battery-grade  $\text{Li}_2\text{S}$  remains high, as it is produced mainly from  
42  $\text{Li}_2\text{SO}_4$  using an energy-intensive carbothermal reduction process [7]. Furthermore, it remains  
43 questionable whether the materials currently synthesized using mechanochemical processes can be  
44 scaled up to have a far-reaching impact on future SSB technologies, or whether they are more suited  
45 to niche market applications, where cost is not a primary consideration. Since this roadmap focuses on  
46 SEs that are just emerging from academic research and are of more fundamental interest, commercial  
47 and industrial considerations would be highly speculative and are therefore not the focus.  
48  
49

50 Overall, this article serves both as a snapshot of the current state of knowledge and as a strategic  
51 compass for future research by highlighting the challenges and opportunities that lie ahead. The vision  
52 is clear: by leveraging the full diversity of the chemical space, utilizing computational and analytical  
53 methods, and considering sustainability from design to disposal, the next generation of superionic SEs  
54 can redefine the future of batteries, and therefore, also the energy systems that will power our world.  
55  
56  
57  
58  
59  
60

**Acknowledgment**

F.S. is grateful to the German Federal Ministry of Research, Technology and Space (BMFTR) for funding within the project MELLi (03XP0447).

**Conflict of Interest**

The authors declare no conflict of interest.

Accepted Manuscript

For Review Only

## 2. Sulfide solid electrolytes: materials-to-devices perspectives

Saneyuki Ohno<sup>1,2,\*</sup>, Yi Huang<sup>1</sup> and Peng Song<sup>1</sup>

<sup>1</sup> Institute of Multidisciplinary Research for Advanced Materials, Tohoku University, Miyagi 980-8577, Japan.

<sup>2</sup> Department of Frontier Sciences for Advanced Environment, Graduate School of Environmental Studies, Tohoku University, Miyagi 980-8572, Japan.

\*E-mail: saneyuki.ohno.c8@tohoku.ac.jp

### Status

Sulfide-based solid electrolytes (SEs), alongside oxides, represent one of the most historically established and practically relevant classes of solid-state ionic conductors. The prominence of sulfide-based electrolytes stems from two intrinsic advantages: the exceptionally high ionic conductivity enabled by the high polarizability of sulfide anions, and their mechanical softness, which allows the formation of percolating ion-conduction pathways under simple cold pressing at room temperature [8]. Among them, thiophosphate-based glasses and crystalline electrolytes, such as  $\text{Li}_{10}\text{GeP}_2\text{S}_{12}$  (LGPS) [6] and argyrodites ( $\text{Li}_6\text{PS}_5\text{X}$ , X = Cl, Br, I) [9], have been regarded as particularly promising, attracting intensive research from fundamental studies of transport mechanisms to applied demonstrations in solid-state batteries (SSBs).

The research trajectory of sulfide electrolytes can be traced back to glassy systems. Building upon work on  $\text{Ag}^+$  and  $\text{Cu}^+$  conductors in the 1970s, studies in the 1980s on  $\text{Li}_2\text{S}$ - $\text{P}_2\text{S}_5$  glasses [10], thio-silicates [11], and halogen-substituted systems [12] ignited the field of lithium-ion conducting sulfide electrolytes. The exploration of crystalline phases expanded in the 2000s with the report of LISICON-type  $\text{Li}_4\text{SiS}_4$ , followed by the discovery of lithium superionic argyrodites in 2008 and  $\text{Li}_7\text{P}_3\text{S}_{11}$  in 2009 [13, 14], both of which were inspired by silver superionic conductors. A major breakthrough came in 2011 with the identification of LGPS [6], a LISICON-derived compound, which triggered a surge of activity in solid-state battery research. Subsequent studies demonstrated the potential of sulfide-based SSBs for high-power operation and thick-electrode designs, marking a turning point in the field [15, 16].

Over the past decades, tremendous efforts have been devoted not only to the discovery of new compounds, but also to elucidating ion transport mechanisms and establishing rational design principles. **Figure 2** summarizes the transport properties of representative crystalline sulfide electrolytes discovered during this period. Notably, several sulfide conductors have been reported with room-temperature ionic conductivities exceeding  $10 \text{ mS cm}^{-1}$ . Looking forward, alongside the development of scalable production techniques for practical applications, continued exploration of new materials and mechanistic insights to fully utilize the developed materials will remain central to advancing the field. In the following section, we focus particularly on the effect of (i) crystallinity, (ii) AI-driven materials discovery, (iii) high-entropy design, (iv) reproducibility of functionality, and (v) safety assessment, and discuss the present status and future challenges of sulfide SEs.

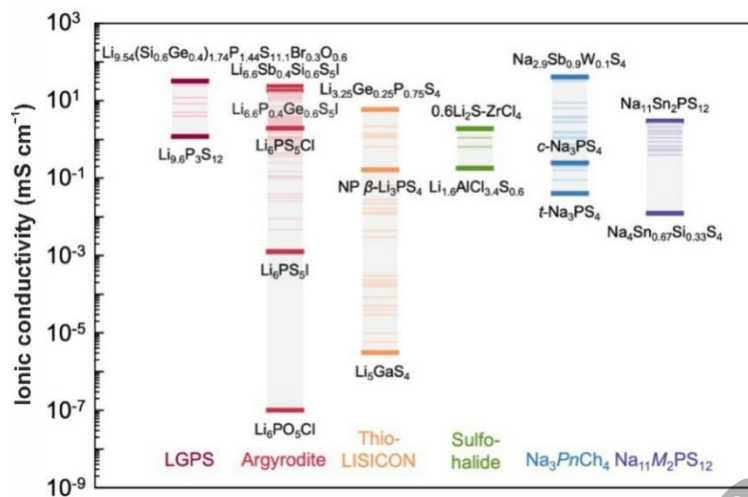


**Figure 2.** Overview of the achieved ionic conductivity over classes of electrolytes for Li- and Na-ion conductors. Adopted from [8], Copyright (2020), with permission from IOP Publishing Ltd and modified with data in the latest reports.

### Current and Future Challenges

Ionic conductivity is a prerequisite for any material to function as a SE in batteries, yet thermal, chemical, and electrochemical stability are equally critical. Sulfide-based SEs, while offering exceptionally high ionic conductivities, remain challenged by limited thermodynamic stability. As in liquid electrolyte systems, their performance after compositing with active materials and additives, and upon cycling, is strongly governed by interfacial states. Considerable research has addressed oxidative decomposition near high-voltage cathodes or reductive decomposition near lithium anodes, including gas evolution phenomena. However, we highlight another difficult descriptor to formalize in this context, which is crystallinity.

A key advantage of sulfide electrolytes lies in their ability to form metastable phases, including glassy interphases, that nevertheless retain appreciable ionic transport. The intrinsic drawback of such glasses is their inferior thermodynamic stability compared to crystalline counterparts. On the other hand, glasses possess stress relaxation mechanisms that, through atomic or molecular mobility, mitigate crack formation and enhance mechanical resilience [17]. Given that electro-chemo-mechanical degradation is a dominant failure mode in SSBs, materials development strategies that leverage both the robustness of crystals and the compliance of glasses present a promising pathway.

Several representative studies highlight the multifaceted role of crystallinity. Cronau *et al.* systematically investigated argyrodites and demonstrated that while highly crystalline electrolytes provide intrinsically higher ionic conductivity, they require substantial stack pressure to maintain contact and reliable transport [18]. In contrast, glass-ceramic counterparts, with lower crystallinity, could sustain conductivity even under reduced stack pressure. Shuo *et al.* compared crystalline and glassy thiophosphates and revealed that crystalline electrolytes, due to higher electronic conductivity and accelerated decomposition, suffer from interfacial degradation, contact loss, and pronounced volume changes, whereas glassy electrolytes suppress electronic conduction, stabilize interfaces, and deliver improved cycling [19]. Maus *et al.* further demonstrated that post-synthetic processing affects crystallinity: moderate milling reduces particle size and enhances cathode composite performance, whereas excessive milling severely diminishes crystallinity, hinders ionic transport, and degrades cell behavior [20].

Taken together, these findings underscore the complexity of using “crystallinity” as a materials descriptor. Although methods, such as X-ray diffraction, total scattering with coherent length analysis, and SEM/TEM observations, as well as relative intensity ratio methods, allow partial quantification of

1 crystalline versus glassy fractions, the disentanglement of particle size, strain, and disorder effects  
2 remains unresolved. For practical implementation and sustained advancement, crystallinity must be  
3 addressed as a multifactorial parameter that resists simple computational prediction and still requires  
4 nuanced experimental investigation. As such, the systematic exploration of crystallinity, bridging  
5 atomic structure, processing, and electrochemical performance, remains an open frontier for the design  
6 of robust sulfide SEs.  
7

8  
9 Artificial intelligence (AI) has become a powerful tool for accelerating the discovery of SEs,  
10 particularly sulfide-based systems. By directly predicting key properties, such as ionic conductivity  
11 and migration barriers, AI enables high-throughput screening far beyond the reach of traditional  
12 methods. For example, Sendek *et al.* combined machine learning (ML) with density functional theory  
13 (DFT) to evaluate ~12,000 candidates, raising the likelihood of finding fast-ion conductors by 2.7-fold  
14 [21]. Zhao *et al.* introduced the hierarchical encoded crystal structure (HECS) descriptor to predict Li-  
15 argyrodite migration barriers [22], while Kahle *et al.* used high-throughput molecular dynamics to  
16 identify 130 promising lithium compounds [23]. Guo *et al.* expanded this scale dramatically, screening  
17 740,000 compounds with a universal ML interatomic potential [24]. Importantly, Cho *et al.*  
18 demonstrated experiment-driven active learning, which yielded a Li-argyrodite with a conductivity of  
19 13.02 mS cm<sup>-1</sup>, showing how AI can guide synthesis as well as design [25].  
20  
21

22 More focused studies illustrate AI's potential in sulfide electrolytes. Kong *et al.* employed a  
23 semi-supervised framework with local structural order parameters to screen 3,800 compounds,  
24 identifying 19 and synthesizing Li<sub>3</sub>LaP<sub>2</sub>S<sub>8</sub> derivatives [26]. Conductivity was initially modest, but  
25 improved through Sr substitution, demonstrating the value of semi-supervised approaches under data  
26 scarcity. Han *et al.* applied a variational autoencoder with multi-anion topological design, selecting  
27 Li<sub>7</sub>Si<sub>2</sub>S<sub>7</sub>I from 300 phase diagrams [27]. Despite being metastable, this compound achieved ~10<sup>-2</sup> S  
28 cm<sup>-1</sup> conductivity through multi-channel transport, challenging conventional assumptions of single-  
29 pathway ion mobility.  
30

31 Beyond property screening, large language models (LLMs) are emerging as a new tool. Wang *et al.*  
32 integrated LLMs with metadynamics simulations to clarify ion migration in hydride electrolytes  
33 [28], while Li *et al.* introduced a coevolutionary LLM-physics framework to combine literature mining  
34 with real-time physical modeling [29]. The Chameleon model further showed that cross-modal  
35 contrastive learning can couple textual descriptions with structural data to generate stable phases in the  
36 Li–P–S–Cl space [30]. Such advances suggest that LLMs can overcome traditional ML's limitations in  
37 mapping structure-property relations, opening new avenues for electrolyte design.  
38  
39

40 Despite these successes, critical challenges remain in bridging prediction and experiment.  
41 Current models often assume idealized stoichiometries, while real sulfide SEs display substantial  
42 compositional freedom. Substitutions and defect engineering, as in Sr-doped Li<sub>3</sub>LaP<sub>2</sub>S<sub>8</sub>, can  
43 significantly enhance conductivity, but such effects are rarely built into AI models. Reliance on  
44 convex-hull thermodynamics also limits realism: many high-performance SEs, such as Li<sub>7</sub>Si<sub>2</sub>S<sub>7</sub>I, are  
45 metastable and require careful kinetic control during synthesis. Furthermore, precursor chemistry plays  
46 a decisive role. In Li-argyrodite systems, different precursors alter phase purity and ionic transport;  
47 however, the choice of precursors remains underexplored in AI frameworks.  
48  
49

50 Looking forward, progress will depend on integrated, feedback-driven approaches that link  
51 modeling with experiment. Combining reaction energy network analysis, interfacial barrier modeling,  
52 and ML-accelerated molecular dynamics with high-throughput experimental feedback could enable  
53 predictive synthesis planning. The success of Cho's active-learning Li-argyrodite highlights the  
54 promise of such frameworks. By incorporating compositional variability, metastability, kinetics, and  
55 precursor effects, AI can evolve from identifying initial targets to guiding the full design-to-synthesis  
56 pipeline. This will be crucial for realizing optimized sulfide SEs and advancing their deployment in  
57 next-generation SSBs.  
58

59 High-entropy sulfide SEs (HE-SSEs) exploit configurational entropy to overcome the intrinsic  
60 limitations of conventional SEs [31]. Increasing configurational entropy in sulfide SEs can introduce

beneficial structural disorder, which broadens ion migration pathways and lowers transport barriers. Such entropy-driven stabilization fosters highly conductive frameworks, demonstrating that high-entropy design serves as a powerful strategy for enhancing ionic transport in SEs beyond the limits of conventional compositions [32]. Mechanistic studies, particularly by Ceder's group, reveal that multi-element substitution introduces a broad distribution of site energies, enabling percolative ion transport via multiple low-barrier pathways rather than a single high-energy route [33]. Synergistic effects, including overlapping site energy distributions, interstitial site occupation, lattice softening, and the "cocktail effect", create an optimized energy landscape for charge transport [31]. Such insights form a foundation for the rational design of next-generation HE-SSEs with superior ionic transport and stability.

Experimental evidence supports these benefits. In high-entropy argyrodites, such as  $\text{Li}_{6.5}(\text{Ge}_{0.5}\text{P}_{0.5})(\text{S}_{2.5}\text{Se}_{2.5})(\text{Cl}_{0.33}\text{Br}_{0.33}\text{I}_{0.33})$ , multi-anion and cation substitution reduced activation energies to  $\sim 0.22$  eV, though conductivity gains over optimized analogues were limited [34]. In the argyrodite structure, the cationic substitution effect has also been explored in  $\text{Li}_{6.5}[\text{P}_{0.25}\text{Si}_{0.25}\text{Ge}_{0.25}\text{Sb}_{0.25}]\text{S}_5\text{I}$ , realizing the ionic conductivity of  $\sim 13$  mS  $\text{cm}^{-1}$  with a very low activation energy ( $\sim 0.2$  eV), attributed to local lattice distortions and sublattice softening [35]. High ionic conductivity has also been demonstrated in LGPS-type electrolyte  $\text{Li}_{9.54}[\text{Si}_{1-\delta}\text{M}_\delta]_{1.74}\text{P}_{1.44}\text{S}_{11.1}\text{Br}_{0.3}\text{O}_{0.6}$  ( $\text{M} = \text{Ge}, \text{Sn}$ ), achieving 32 mS  $\text{cm}^{-1}$  [16].

HE-SSEs show markedly improved ionic conductivities, often linked to reduced activation energies. However, key questions remain unresolved. The relationship between configurational entropy and the Arrhenius prefactor is unclear, limiting predictive control of transport. The proposed "frustrated energy landscape" has not been clearly distinguished from disorder effects in glassy phases. Moreover, disentangling configurational and vibrational entropy contributions remains challenging, as lattice softening and phonon broadening may also lower barriers [31]. Finally, systematic design rules for selecting elemental combinations are lacking. Clarifying these aspects is essential for rational HE-SSE design.

From both material development and device application perspectives, reproducibility is a critical factor for commercialization. However, this has not yet been sufficiently ensured, as standardized protocols for conductivity measurements and systematic discussions on the reproducibility of material functionality across synthesis batches are still lacking. For research aimed at advancing material performance, a uniform comparison of transport properties is indispensable. Yet, a round-robin test conducted in 2020 revealed that, even when identical sulfide powder samples were distributed, the measured conductivities showed a standard deviation exceeding 50% [36]. This indicates the possibility of significant discrepancies between reported literature values and laboratory-scale measurements. Factors, such as crystallinity, fabrication pressure, stack pressure during measurement [18], as well as sample history (e.g., storage environment) and analysis methodology [37], have been suggested as contributing variables.

Even for nominally identical materials, transport reproducibility remains a critical challenge. Variations in conductivity often persist across different synthesis batches, even when synthesis methods and measurement environments are standardized. Using  $\text{Na}_3\text{SbS}_4$ , a representative Na-ion conducting sulfide electrolyte, as a model system, it has been suggested that such discrepancies stem from differences in defect concentrations caused by variations in the thermodynamic state of the material. In this context, while single-phase purity has been widely pursued, the potential benefits of deliberately utilizing co-existing phases have been highlighted [38]. Furthermore, the influence of trace oxygen impurities on the ionic transport properties of  $\text{Na}_3\text{PS}_4$  has also been discussed [39], underscoring the need to balance industrial demands for high purity with the functional requirements of electrochemical performance.

Realizing battery devices requires the intimate integration of multiple functional materials, inevitably leading to the formation of complex and diverse interfaces. Thus, reproducibility at the interface level directly translates into the reproducibility of overall cell performance. Indeed, a cell-

1 level round-robin test conducted in 2024, despite employing identical materials, revealed surprisingly  
2 significant variations in battery performance [40]. Considering the combined effects of thermodynamic  
3 states, crystallinity, and interfacial diversity, the importance of more standardized testing is reinforced.  
4 At the same time, these results raise concerns about the prevailing expectation for high battery  
5 performance even in fundamental materials research, suggesting that deepening fundamental  
6 understanding should not be conflated with demonstration of optimized device-level output.  
7  
8

9 Interfacial phenomena at the anode and cathode|sulfide-based SE interfaces critically govern the  
10 practical deployment of SSBs. In particular, contact with highly reducing Li(Na) metal or alloy-type  
11 electrodes, such as Li(Na) alloys [41, 42], and within composite cathodes [43–45] often triggers SE  
12 decomposition, uncontrolled interphase formation, and loss of interface contact, which collectively  
13 limit cell cyclability [46]. Interfacial engineering, therefore, emerges as a unifying theme across  
14 materials, processing, and, cell-design strategies. Stabilized interphases formed through chemical  
15 additives, such as  $\text{Li}_3\text{N}$ ,  $\text{LiX}$  (Cl, Br, I),  $\text{LiBH}_4$ , or irreducible SE [47] derivatives, can mitigate  
16 reduction reactions at the Li or C/Ag anode while retaining fast Li-ion transport. Surface coatings,  
17 gradient layers, and optimized composite architectures can significantly improve compatibility at both  
18 anode and cathode interfaces [48]. For quantitative analysis of interfacial reactions occurring at Li/SE  
19 contacts, coulometric titration time analysis (CTTA) provides a particularly powerful method to assess  
20 interfacial competitiveness and stability [49]. In chapter 3, (electro)chemical compatibility at various  
21 interfaces is also discussed.  
22  
23

24 SSBs are often touted as intrinsically safe, largely because they do not rely on flammable organic,  
25 liquid electrolytes. This assumption may hold true when oxide electrolytes are employed, but the  
26 situation is more complex for sulfide-based systems. Can a battery that generates toxic hydrogen  
27 sulfide gas upon exposure to air truly be considered safe? How, should safety be assessed? While this  
28 may appear to go beyond laboratory-scale concerns, a critical evaluation of safety is indispensable for  
29 SSBs, especially as they are promoted as both high-performance and inherently safe.  
30  
31

32 It is well established that conventional lithium-ion batteries undergo thermal runaway initiated  
33 by parasitic reactions at the anode, but reports also demonstrate that sulfide-based SSBs are not  
34 immune to combustion [50]. When argyrodite electrolytes are combined with charged Ni-rich cathodes  
35 (e.g.,  $\text{LiNi}_{0.8}\text{Co}_{0.1}\text{Mn}_{0.1}\text{O}_2$ , NCM811) and subjected to heating, explosive combustion occurs at around  
36  $150\text{ }^\circ\text{C}$ , triggered by oxygen release from the cathode [51]. Subsequent studies revealed that crystalline  
37 sulfide electrolytes are relatively more stable, whereas glassy sulfides react strongly with released  
38 oxygen, generating substantial heat and  $\text{SO}_2$  gas [52]. This has introduced crystallinity as a new  
39 dimension in the safety debate. In sulfide-based systems, oxygen and sulfur vapors reacting with  
40 lithium metal are considered the primary hazard [53], and although interfacial gas consumption can  
41 mitigate risk, it remains a major concern. Additional risks stem from  $\text{H}_2\text{S}$  release upon moisture  
42 exposure [54]. Strategies, such as oxygen substitution, incorporation of softer acid species, and surface  
43 treatments of SEs have been proposed, yet gas evolution in confined environments can still lead to  
44 catastrophic failure.  
45  
46

47 Looking ahead, mitigating these risks will require integrated strategies across materials, cell  
48 design, and system levels. On the materials side, designing hybrid electrolytes that combine the high  
49 conductivity of sulfides with the chemical robustness of oxides or halides, as well as applying  
50 protective coatings, may suppress oxygen and moisture-driven decomposition. At the cell level,  
51 architectures that allow early gas adsorption and efficient heat dissipation, combined with packaging  
52 tailored for thermal management, hold promise. At the system level, incorporating gas and thermal  
53 sensors, active cooling, and AI-based early-warning diagnostics can provide additional safeguards.  
54 Crucially, *operando* characterization and multiscale modeling must be leveraged to quantify  
55 degradation pathways and define standardized metrics for safety evaluation under realistic stresses.  
56 Ultimately, bridging fundamental materials chemistry with engineering-scale safety design will be  
57 essential to ensure the reliability of sulfide-based SSBs and accelerate their deployment in practical  
58 applications.  
59  
60

## Conclusion and Future Perspectives

In this section, we have discussed the progress and future outlook of sulfide-based SEs from both materials design and device application viewpoints. Several directions can be highlighted for the coming years. High-entropy effects have so far been mainly interpreted as averaged anion disorder, but a more constructive approach lies in multi-anion and complex-anion compounds, where different anions form the structural framework. The exploration that began with oxyhalides is now expanding towards sulfur halogen systems. From both glass and crystal viewpoints, further refinement of design principles is needed. While many recent discoveries have emerged from glass systems, taking advantage of unique local structures to enhance crystallinity represents another promising strategy. The enormous chemical space still to be explored presents a significant challenge in identifying metastable but functional structures, yet AI-driven prediction may offer a practical route. Such compositional design could also help suppress interfacial decomposition by employing graded compositional modulation to improve stability near interfaces.

From the safety viewpoint, as demonstrated in verification studies, low-voltage cathodes, such as  $\text{LiFePO}_4$ , are highly promising [51]. Sulfur cathodes, with their very high capacity, low operating potential, and absence of oxygen release, may ultimately provide a foundation for truly safe batteries [55]. On the industrial side, progress is accelerating: Mitsui Kinzoku has begun moving towards mass production of argyrodites (Sep. 2024), while Idemitsu has started developing cost-efficient synthesis routes for  $\text{Li}_2\text{S}$  (Feb. 2025). As for Na-ion conductors, although  $\text{Na}_3\text{SbS}_4$  is available in small quantities from chemical vendors, sulfide-based electrolytes are not yet ready for mass production, and worldwide efforts to identify viable candidate materials are still ongoing. From a broader perspective, the commercial viability of Na-based systems remains uncertain, and continued materials innovation must be coupled with clear evidence that solid-state sodium batteries can offer competitive advantages in terms of cost, safety, and performance. Insights gained from scaling up will be crucial not only for established compounds, but also for newly emerging materials [56]. With these advances, it is reasonable to expect that sulfide-based SEs will soon find their way into commercial vehicles and portable devices.

## Acknowledgment

This work was supported by the Toyota Physical and Chemical Research Institute through the Rising Fellow Program, by JSPS KAKENHI (grant number JP23K26762), and by the Japan Science and Technology Agency (JST) under the Adopting Sustainable Partnerships for Innovative Research Ecosystem (ASPIRE) program (grant number JPMJAP2419).

## Conflict of Interest

The authors declare no conflict of interest.

### 3. Perspectives on halide-based solid electrolytes

Xabier Martinez de Irujo-Labelde<sup>1</sup> and Wolfgang G. Zeier<sup>1,2,\*</sup>

<sup>1</sup> Institute of Inorganic and Analytical Chemistry, University of Münster, Corrensstr. 28/30, 48149 Münster, Germany.

<sup>2</sup> Institute of Energy Materials and Devices (IMD), IMD-4: Helmholtz Institute Münster, Forschungszentrum Jülich GmbH, 48149 Münster, Germany.

\*E-mail: [wzeier@uni-muenster.de](mailto:wzeier@uni-muenster.de)

#### Status

One of the major bottlenecks in the development of solid-state batteries is the design of an optimal solid electrolyte [1, 57, 58]. Various classes of materials are under extensive investigation at present. Beyond sulfide- and oxide-based solid ionic conductors, halide-based materials have stood out due to their facile synthesis and processability in combination with their enhanced (electro)chemical stability in contact with cathode materials at high voltages (**Figure 3**) [59–62]. However, the understanding of these materials is currently limited and aspects such as ionic conductivity and chemical stability against the anode counterpart are still open questions.

This section of the roadmap plans to bring up for discussion the current challenges to improve ionic transport and chemical stability of halide-based materials as well as offering tools for the design of future electrolytes based on this chemistry.

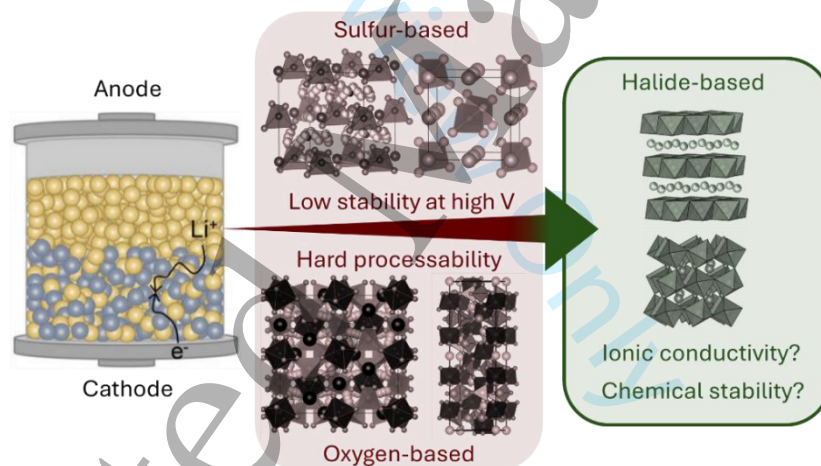


**Figure 3.** Halide-based materials as alternative to sulfide- or oxygen-based electrolytes.

#### Current and Future Challenges

Improving the ionic conductivity and chemical stability remains a key challenge for the practical implementation of halide-based materials as electrolytes in solid-state batteries (**Figure 4**). On the one hand, the ionic conductivity of these materials has lately experienced a great leap. For  $\text{Li}^+$  based chlorides, it has been found that many of the most promising materials show nominal compositions of  $\text{Li}_3\text{MCl}_6$  ( $M = \text{Sc}^{3+}, \text{Y}^{3+}, \text{In}^{3+}, \text{Ho}^{3+} \dots$ ), crystallize in a rock-salt related crystal structure, and the final structure is really dependent on the synthetic conditions. This framework offers low-energy ionic diffusion pathways facilitating ion migration [63–67]. Ionic conductivity can be further enhanced through aliovalent cation substitution in these systems (e.g.,  $\text{Li}_{3-x}\text{M}_{1-x}\text{Zr}_x\text{Cl}_6$ ) by the introduction of  $\text{Li}^+$  vacancies [68–72]. These vacancies facilitate ion transport, as the dominant diffusion mechanism in this system is vacancy-driven. In turn, ionic conductivity boosting can be achieved through isovalent

1 anion substitution from  $\text{Cl}^-$  to  $\text{Br}^-$  or  $\text{I}^-$  although the origin is still unclear. Some of the hypotheses  
2 being considered range from lattice polarizability [73], lattice expansion [71], to the depression of  
3 superionic transition [74]. However, one of the most accepted ones is the introduction of disorder  
4 within the metal center arrangement [75]. In a similar way, mechanochemical approaches can induce  
5 lattice disorder boosting the ionic conductivity [76].  
6

7  
8 In case of  $\text{Na}^+$  containing chlorides, the trend of ionic transport is hardly related to their  $\text{Li}^+$   
9 analogues.  $\text{Na}_x\text{MCl}_6$  ( $M = \text{Sc}^{3+}$ ,  $\text{Y}^{3+}$ ,  $\text{In}^{3+}$ ,  $\text{Zr}^{4+}$ ...) compositions offer very restricted  $\text{Na}^+$  mobility with  
10 ionic conductivities of approximately  $10^{-5}$   $\text{mS cm}^{-1}$  [77–79]. The larger size of  $\text{Na}^+$  with respect to  $\text{Li}^+$   
11 prevents the formation of layered structures, favoring other crystal structures, such as the ilmenite,  
12 cryolite, or caswellsilverite-related depending on the metal center size. These frameworks show less  
13 energetically favorable ionic migration pathways, explaining their low ionic transport. To enhance the  
14 ionic conductivity, the common approach of ion substitution has also been attempted in these systems.  
15 While isovalent anion substitution does not significantly impact on the ionic transport [80], aliovalent  
16 cation substitution enhances the ionic transport, albeit in a limited manner up to  $10^{-3}$   $\text{mS cm}^{-1}$  at  
17 optimal  $\text{Na}^+$  vacancy concentrations [81, 82]. Recently, it has been shown that  $\text{Na}^+$  transport can be  
18 largely increased when the materials are mechanochemically treated after the annealing or directly  
19 obtained by mechanochemical synthesis as in the case of  $\text{Li}^+$  containing materials. However, the  
20 increase of conductivity has not been associated in these cases to the introduction of disorder within  
21 the crystal lattice. In ball-milling prepared systems like  $\text{Na}_{3-x}\text{In}_{1-x}\text{Zr}_x\text{Cl}_6$ ,  $\text{Na}_{3-2x}\text{In}_{1-x}\text{Ta}_x\text{Cl}_6$ , and  
22  $\text{Na}_{2-x}\text{Zr}_{1-x}\text{Ta}_x\text{Cl}_6$ , reduced crystallite size has been linked to improved ionic conductivity [83–86].  
23 Additionally, prolonged ball milling of  $\text{NaTaCl}_6$  has been shown to enhance ionic conductivity, likely  
24 due to the increased amorphous content [87, 88].  
25

26  
27 In harmony with these findings, a new class of glassy superionic materials, either containing  $\text{Li}^+$   
28 [89–92] or  $\text{Na}^+$  [93–95] cations and based on mixed-anion chemistries has recently been found [96].  
29 Those materials generally exhibit  $\text{AMOC}_4$  compositions ( $A = \text{Li}^+$  or  $\text{Na}^+$ ,  $M = \text{Nb}^{5+}$  or  $\text{Ta}^{5+}$ ) coming  
30 from a partial replacement of  $\text{Cl}^-$  by  $\text{O}^{2-}$ , where  $\text{O}^{2-}$  anions are likely acting as glass former that help in  
31 the boosting of ionic conductivity to values over  $10$   $\text{mS cm}^{-1}$  and  $1$   $\text{mS cm}^{-1}$  in the case of  $\text{Li}^+$  [89–91]  
32 and  $\text{Na}^+$  [93–95] containing materials, respectively. Thus, the lower crystallinity associated with a  
33 lower crystallite size and larger amounts of amorphous fractions seems to be at the origin of the  
34 enhanced ionic transport in these materials, although the precise origin has yet to be determined.  
35 Therefore, although various tools have been developed to tune the ionic conductivity in halide-based  
36 materials, a deeper mechanistic understanding—both from structural and microstructural  
37 perspectives—is still needed.  
38

39  
40 On the other hand, huge efforts have recently been devoted to investigating the chemical  
41 compatibility of these materials against the anode counterpart. In particular, halide solid electrolytes  
42 often face challenges when interfaced with highly reducing anode materials, such as  $\text{LiIn}$  or  $\text{NaSn}$   
43 alloys [97, 98]. The primary concern lies in undesirable interfacial reactions, where the halide  
44 electrolytes may undergo ion intercalation and eventually reductive decomposition, forming resistive  
45 interphases that hinder ion transport. For instance,  $\text{Li}_3\text{InCl}_6$  and  $\text{Li}_3\text{YCl}_6$  in contact with anode  
46 materials form passivation layers composed of  $\text{LiCl}$ , indium metal, or other insulating species, which  
47 severely impede ion transport [71]. Additionally,  $\text{NaTaOCl}_4$  in contact with  $\text{Na}$  metal is reduced by  
48  $\text{Na}^+$  intercalation and decomposes to  $\text{Na}$  salts and/or  $\text{Nb/Ta}$  salts, or eventually to the metals [94].  
49 These detrimental reactions restrict the use of halide-based materials to catholyte configurations to  
50 prevent their contact with the anode counterparts [46, 98, 99]. Consequently, interfacial regulation  
51 strategies based on cell configuration, such as avoiding direct contact between halide electrolytes and  
52 metal anodes by employing more chemically stable separator layers (e.g., sulfide-based solid  
53 electrolytes, see chapter 2), have emerged as an effective and pragmatic approach [46]. In turn, some  
54 of these  $\text{Na}^+$  or  $\text{Li}^+$  containing halides have been demonstrated to take advantage from their redox  
55 activity, increasing the energy density and the areal discharge capacity of the battery in contact with a  
56 cathode material [100–102]. However, if the full potential of halide-based solid electrolyte as a “free-  
57  
58  
59  
60

standing” electrolyte in solid-state battery systems is to be unlocked, it is critical to understand and control the undesired interfacial chemical interactions.

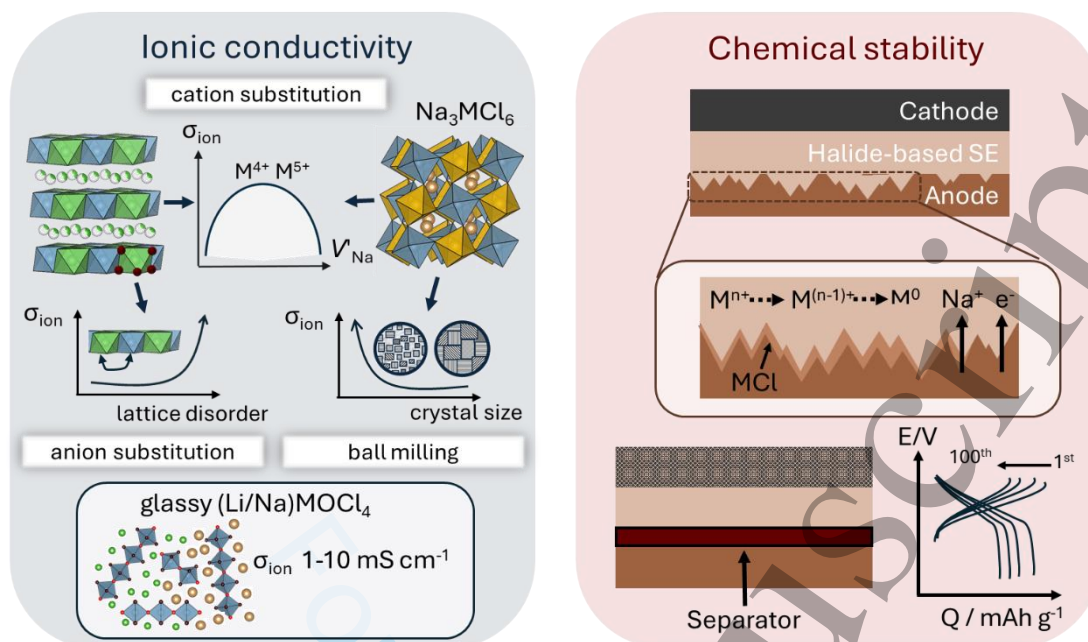


**Figure 4.** Ionic conductivity and chemical stability of halide-based materials represent major challenges nowadays and in the near future for their implementation in solid-state battery technologies.

## Conclusion and Future Perspectives

Halide- and oxyhalide-based compounds represent a promising class of materials in terms of their ease of synthesis, processability, and (electro)chemical stability at elevated potentials. In recent years, the ionic conductivity of  $\text{Li}^+$  and  $\text{Na}^+$  halide materials has significantly improved, reaching values comparable to those of superionic sulfide and oxide conductors, particularly the newly discovered glassy oxyhalides. Nevertheless, if halide-based materials are to be used as “free-standing” solid electrolytes, their chemical stability against the current anode materials should be improved. A promising approach to address this issue involves the careful selection of metal elements that are stable at low potentials, which could pave the way for designing the next generation of halide-based solid electrolytes. Furthermore, tailoring the approach by embedding these  $M$  centers within an amorphous mixed-anion matrix could offer a dual advantage: the already mentioned suppression of their direct interaction with the anode, thus enhancing chemical stability, while retaining the high ionic conductivities observed in disordered systems. Therefore, the development of halide-based materials with stabilized  $M$  centers in amorphous or glass-ceramic matrices presents a highly promising strategy. Such materials would not only overcome current stability limitations, but also maintain or even enhance ionic conductivity, making them strong candidates for next-generation solid electrolytes in solid-state batteries.

## Acknowledgment

This work was partially funded by Bundesministerium für Forschung, Technologie und Raumfahrt (BMFTR, 03XP0525B).

## Conflict of Interest

The authors declare no conflict of interest.

## 4. Post-Li/Na inorganic solid-state electrolytes

Jelena Popovic-Neuber<sup>1,\*</sup>

<sup>1</sup> Department of Energy and Petroleum Engineering, University of Stavanger, Stavanger, Norway.

\*E-mail: [jelena.popovic-neuber@uis.no](mailto:jelena.popovic-neuber@uis.no)

### Status

Post-Li and Na solid-state batteries, similarly to their liquid electrolyte counterparts, address issues revolving around materials resourcing and diversification, sustainability, and energy density [103]. Generally, the electrochemical performance and properties of solid-state electrolytes are dependent on the quality of the multiscale ion transport in the bulk related to structural factors, linked with suppression of electron conductivity, and its reactivity/ion transport at the interphases, caused by dynamic degradation when in contact with high-energy anodes and suitable cathodes (**Figure 5**) [104]. In the focus are typically materials exhibiting high room-temperature ionic conductivities,  $\sigma_{\text{ion,RT}}$ , suitable small migration barriers or activation energies,  $E_A$ , measured by electrochemical impedance spectroscopy (EIS), and high effective transference number for the moving ion,  $t_{i,\text{eff}}$ , measured by polarization techniques, as most relevant bulk performance factors for further investigations related to battery application. Additional important bulk transport factors include the ability to achieve high concentration of charge carriers, most commonly vacancies, and high values of prefactor,  $\sigma_0$ , also available from EIS measurements, linked with the attempt frequency and migration entropy [105]. The fact that the materials in focus are chemically reactive and are to be ultimately used in battery cells, and will thus form buried and evolving interphases upon galvanostatic cycling, calls for use and development of advanced *in situ* and *operando* characterization techniques, linked with modeling, which will consider the complex electro-chemo-mechanics, an interconnected influence of electrical, chemical, and mechanical behavior of the materials.

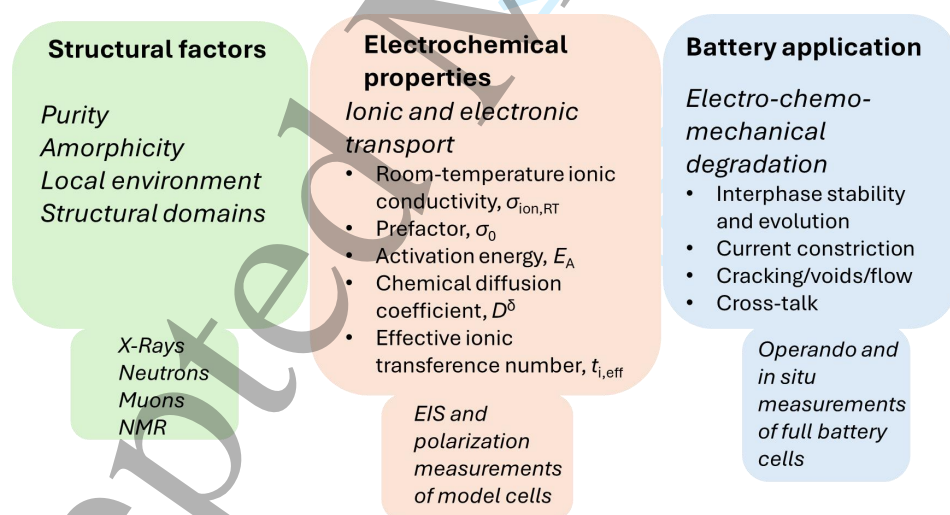


**Figure 5.** Triade of factors influencing the suitability of post-Li and Na solid-state battery electrolytes, including different structural ones, electrochemical properties and their final battery application. The boxes below state suitable characterization techniques for investigation of the specific factors.

In the case of K, several inorganic materials proved to be suitable for high performance at room temperature, including rhombohedral  $\beta''$ -alumina (e.g.,  $\text{K-}\beta''\text{-Al}_2\text{O}_3$ ), orthorhombic thioantimonates (e.g.,  $\text{K}_3\text{SbS}_4$ ), borohydrates (e.g.,  $\text{KB}_3\text{H}_8 \cdot \text{NH}_3\text{B}_3\text{H}_7$ ,  $\text{KCB}_9\text{H}_{10} \cdot 2\text{C}_3\text{H}_4\text{N}_2$ ), and tetragonal phosphidosilicates (e.g.,  $\text{KSi}_2\text{P}_3$ ) [106, 107]. The fact that the first three materials' classes are

successful analogues of known  $\text{Li}^+$  and  $\text{Na}^+$  ionic conductors indicates similar satisfactory conduction mechanisms for alkali metal ions. Fine tuning of  $\sigma_{\text{ion,RT}}$  and  $E_A$  in thioantimonates can be achieved through increase of concentration of charge carriers by W and Cl-doping and heat treatment in the electrochemical cell [108, 109]. First instances of electrochemical cells in which K metal was used as an anode in full cells or electrode to study interphase evolution show that borohydrates and thioantimonates may offer kinetic stability, either in the form of low overpotentials or isolation of electronically conducting phases in highly blocking interphases, while long-term cycling in full cells leaves room for additional improvement through materials engineering [107–109].

The high charge density due to divalency resulting in the stronger electrostatic interaction, as well as large ion radius for  $\text{Ca}^{2+}$  due to one additional electron shell compared to  $\text{Mg}^{2+}$ , reduce the number of appropriate materials classes, even more so in the Ca case. The behavior can be compared to  $\text{O}^{2-}$  inorganic conducting materials (e.g.,  $\text{CeO}_2$ ,  $\text{Zr}_{1-x}\text{Y}_x\text{O}_{2-y}$ ,  $\text{La}_{1-x}\text{Sr}_x\text{Ga}_{1-y}\text{Mg}_y\text{O}_{3-\delta}$ ) applied in high-temperature oxide fuel cells, with the difference of the larger and less charge dense  $\text{O}^{2-}$  ion, where most important structural factors for ionic conduction remain polarizability, flexibility, bottleneck size, disorder, and coordination environment [105]. In the Mg case, NASICON-type oxides [e.g.,  $\text{Mg}_{0.5}\text{Zr}_2(\text{PO}_4)_3$ ], sulfide glasses (e.g.,  $\text{MgS-P}_2\text{S}_5\text{-MgI}_2$ ), halides (e.g.,  $\text{MgAl}_2\text{Cl}_{8-x}\text{Br}_x$ ), chalcogenide spinels ( $\text{MgX}_2\text{Se}_4$ ,  $\text{X} = \text{Sc, B, Yb}$ ), and borohydride derivatives [e.g.,  $\beta\text{-Mg}(\text{BH}_4)\cdot\text{CH}_3\text{NH}_2$ ,  $\text{Mg}(\text{BH}_4)_2(\text{NH}_3\text{BH}_3)_2$ ] have been investigated [110–113]. The chalcogenide spinels and borohydrates are currently most promising, offering a suitable large distance between the mobile  $\text{Mg}^{2+}$  and neighboring ions with somewhat stabilizing covalent character of the bonds and distortion of the lattice allowing for increased number of ionic pathways [112, 113]. However, both of the mentioned electrolytes are not stable with the Mg electrode. Additional complexity in studying these materials arises from considerable electronic conductivity of the chalcogenide spinel phase, yielding a necessity of using ionogel interlayers for EIS measurements [113]. Borohydride derivatives (e.g.,  $\text{Ca}(\text{CB}_{11}\text{H}_{12})_2$ ,  $\text{Ca}(\text{BH}_4)_2\cdot 2\text{NH}_2\text{CH}_3$ ,  $\text{Ca}(\text{BH}_4)_2\cdot 3.30\text{CO}(\text{NH}_2)_2$ ) are also most promising  $\text{Ca}^{2+}$  conductors offering open space and exclusively ionic conduction pathways [114–116]. Unfortunately, only monocarboranes were tested in contact with  $\text{CaSn}_3$  alloy electrodes with promising results, while other electrolytes were not employed in relevant battery cells [114].

Main crystal structures that are currently investigated for F-conductivity include cubic fluorite (e.g.,  $\text{BaSnF}_4$ ) with high disordering of the mobile ion species and flattening of the mobile ion potential energy surface, and metastable alkaline-earth metal fluorides (e.g.,  $(\text{CaF}_2)_x(\text{BaF}_2)_{1-x}$ ) where mixing of Ca and Ba atoms allows for F-anion fluctuation, generating Frenkel pairs and low  $E_A$  [117, 118]. Although current focus is on the understanding of the bulk behavior, some of the older publications reported full battery cell performance, which was in particular promising with Zn anode ( $\text{Zn}/\text{BiSnF}_4/\text{BiF}_3$  at 60 °C) and thus initiated the wider interest in F-based solid-state batteries [119].

In the recent years, with the rise of metal organic framework synthesis and application in batteries, several such materials were suggested as suitable electrolytes for post-Li technologies. These are not covered here, as they are, in its essence quasi-solid-state conductors, exhibiting solvent-assisted hopping conduction mechanisms, allowing for higher  $\sigma_{\text{ion,RT}}$  and lower  $E_A$  [120]. As such, their performance and conduction mechanism must be compared to other composites, such as solid-liquid, gel, and hybrid polymer electrolytes. Unfortunately, in this community, which also sometimes has a hard time navigating the electrochemical methodology suitable for performance estimation of these specific materials, it is not fully uncommon to show comparison with true solid-state electrolytes.

## Current and Future Challenges

Similarly as in the Li and Na case, the variety of chemical structures investigated does not allow for comprehensive approaches for  $\sigma_{\text{ion,RT}}$  and  $E_A$  improvement. However, a deeper understanding of the relevance of Meyer-Neldel rule or other considerations linking the two most relevant parameters are necessary for specific chemistries. In terms of EIS as a technique to track the long-range ion movement (e.g., chemical diffusion), detailed information on the processing of the powder material into pellet,

1 including its density and fabrication or measurement pressures, are necessary to understand if the  
2 observed differences are materials or process related, but are often missing from the experimental part  
3 of relevant publications. If materials are mixed conductors, exhibit contact problems, or contain/form  
4 interphases, development of more extensive and complex equivalent circuits or transmission line  
5 models for treating EIS data is also necessary.  
6

7 The closer this field approaches the possible application domain, environmental sustainability  
8 aspects related to resourcing and recyclability, as well as materials' processability, which are currently  
9 not in the focus, will become more relevant. In fact, for materials optimization in battery cells, it is  
10 typically advised to perform it synergistically and simultaneously, and not one material at a time, as it  
11 is typically the case in the initial stages of these sub-technologies.  
12

13 Finally, ideas such as integration of automation and digitalization through high-throughput  
14 experiments/simulation and big data/artificial intelligence/machine learning approaches in a closed  
15 loop, with the hope that this will reduce cost and time-to-market, are also expected to rise in this field  
16 of materials research.  
17  
18  
19

## 20 **Concluding Remarks**

21 General understanding and development of post-Li and Na solid-state electrolytes for K, Mg, Ca  
22 and F-based solid-state batteries are currently in its cradle phase and is largely driven by the demands  
23 of specific chemistries in the field of battery technology, or the necessity to understand the complex  
24 interplay of structure and ion movement in the fields of materials chemistry and physics, inorganic  
25 chemistry, and solid state ionics. Ongoing research holds significant promise, both in terms of  
26 fundamental scientific discoveries related to movement of ions in solids and battery applications, in  
27 particular for their necessary diversification and technological advancement. The high level of the  
28 interdisciplinarity of the specific field calls for varied educational backgrounds of involved scientists  
29 and a truly collaborative approach.  
30  
31  
32  
33

## 34 **Acknowledgment**

35 Funding from FME BATTERY, a Norwegian Center for Environment-friendly Energy Research  
36 (FME), sponsored by the Research Council of Norway (project number 350373) is greatly appreciated.  
37  
38  
39

## 40 **Conflict of Interest**

41 The author declares no conflict of interest.  
42  
43  
44  
45  
46  
47  
48  
49  
50  
51  
52  
53  
54  
55  
56  
57  
58  
59  
60

## 5. Hydroborate solid electrolytes

Hugo Braun<sup>1,2</sup>, Arndt Remhof<sup>1,2</sup> and Corsin Battaglia<sup>1,3,4,\*</sup>

<sup>1</sup> Empa - Swiss Federal Laboratories for Materials Science and Technology, Duebendorf, Switzerland.

<sup>2</sup> Institute for Inorganic and Analytical Chemistry, University of Freiburg, Freiburg, Germany.

<sup>3</sup> Department of Information Technology and Electrical Engineering, ETH Zurich, Zurich, Switzerland.

<sup>4</sup> Institute of Materials, School of Engineering, EPFL, Lausanne, Switzerland.

\*E-mail: [corsin.battaglia@empa.ch](mailto:corsin.battaglia@empa.ch)

### Status

Hydroborates are salts with complex anions consisting of boron and hydrogen atoms (**Figure 6**). The most stable anion is the divalent  $B_{12}H_{12}^{2-}$  closo-hydroborate anion consisting of twelve equivalent boron atoms forming a closed icosahedral cage, where each vertex boron is terminated by a hydrogen atom. The room-temperature cation conductivity of  $Li_2B_{12}H_{12}$  and  $Na_2B_{12}H_{12}$  is  $<10^{-6} S cm^{-1}$ . However,  $Li_2B_{12}H_{12}$  and  $Na_2B_{12}H_{12}$  undergo a first-order phase transition at 350 °C [121] and 250 °C [122], respectively, from an ordered monoclinic low-temperature phase to a dynamically disordered cubic high-temperature phase, in which the  $B_{12}H_{12}^{2-}$  anions form a body-centered cubic lattice, exhibiting cation conductivities on the order of  $10^{-1} S cm^{-1}$ . The high-temperature cubic structure can be stabilized at room-temperature by anion mixing, combining, e.g.,  $Na_2B_{12}H_{12}$  with  $Na_2B_{10}H_{10}$  to form  $Na_4B_{12}H_{12}B_{10}H_{10}$  [123], in which anions form a dynamically disordered face-centered cubic lattice resulting in a room-temperature sodium-ion conductivity of several  $10^{-3} S cm^{-1}$ . The role of librational anion motion and geometric frustration to reach high cation conductivity was studied in detail [124, 125]. Even higher cation conductivity of up to several  $10^{-2} S cm^{-1}$  can be achieved by replacing one boron atom in each anion by a carbon atom, e.g.,  $Na_2CB_{11}H_{12}CB_9H_{10}$  [126]. These closo-hydrocarbaborates possess monovalent anions, reducing the cation occupancy and the electrostatic interaction between ions in the lattice.

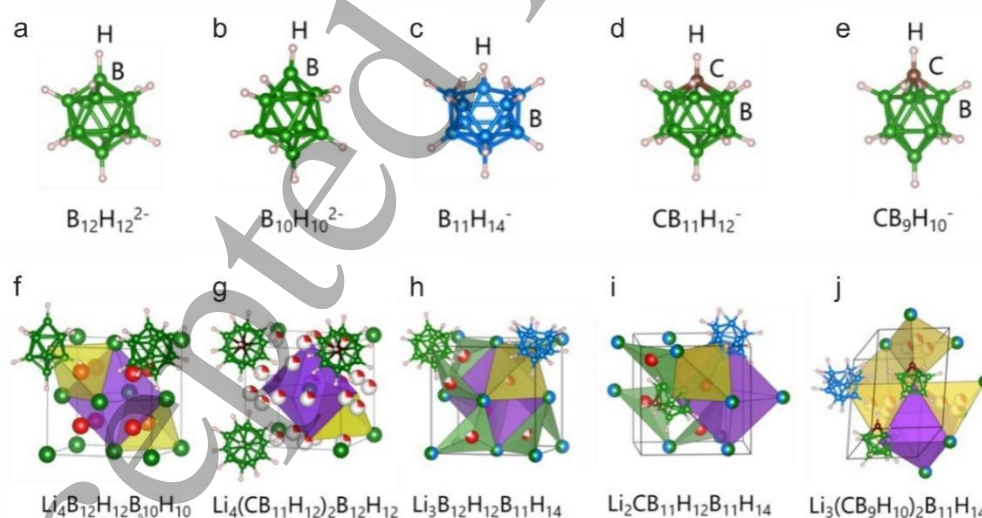


**Figure 6.** Examples of closo-hydroborate (a, b), nido-hydroborate (c), and closo-hydrocarbaborate anions (d, e), and examples of mixed-anion crystal structures (f–j).

Integration of these mixed-anion hydroborates into solid-state batteries was first demonstrated using relatively low-voltage cathodes, including  $TiS_2$  [127–130],  $LiFePO_4$  [130], and  $NaCrO_3$  [131].

More recently, stable galvanostatic cycling over several hundred cycles was also achieved for high-voltage cathodes, including  $\text{LiNi}_{0.8}\text{Mn}_{0.1}\text{Co}_{0.1}\text{O}_2$  (NMC811) [132] and  $\text{Na}_3(\text{VOPO}_4)_2\text{F}$  (Figure 7) [133], where sufficient oxidative stability was achieved by increasing the ratio of  $\text{CB}_{11}\text{H}_{12}^-:\text{CB}_9\text{H}_{10}^-$  and  $\text{CB}_{11}\text{H}_{12}^-:\text{B}_{12}\text{H}_{12}^{2-}$  from 1:1 to 2:1. While the closo-hydroborates also exhibit excellent reductive stability and are compatible with lithium and sodium metal anodes [123], closo-hydrocarbaborates and the open-cage nido-hydroborates show lower reductive stability [127]. Despite excellent anodic and cathodic stability, dendrite formation remains a critical bottleneck, limiting current density and areal capacity in solid-state batteries with hydroborate electrolytes.

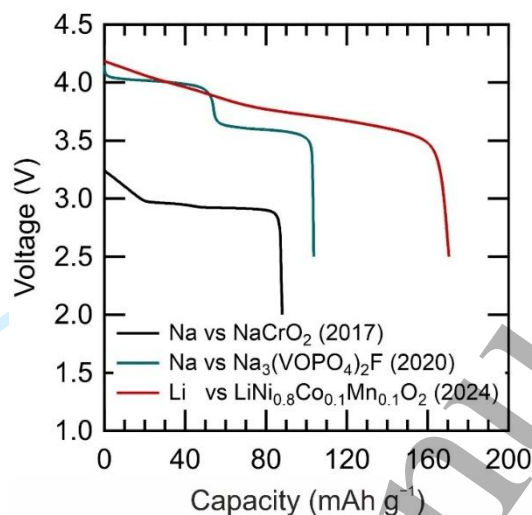


**Figure 7.** Evolution of cell voltage vs. discharge capacity of hydroborate solid-state battery cells fabricated in our laboratory.

Hydroborates offer a number of additional advantages over alternative solid electrolyte materials. Because boron and hydrogen are both very light elements, the density of these materials is typically very low ( $1.0\text{--}1.2\text{ g cm}^{-3}$ ), thus comparable or even slightly lower than for carbonate-based liquid electrolytes ( $1.2\text{--}1.3\text{ g cm}^{-3}$ ) and significantly lower than for argyrodite  $\text{Li}_6\text{PS}_5\text{Cl}$  ( $1.6\text{ g cm}^{-3}$ ) and garnet  $\text{Li}_7\text{La}_3\text{Zr}_2\text{O}_{12}$  ( $5.0\text{ g cm}^{-3}$ ). Mixed-anion crystal structures are most often synthesized from the precursor single-anion salts using chemo-mechanical synthesis. While the mixed-anion crystal structures may dissolve in a number of solvents, the hydroborate anions remain stable in air, water, and a number of solvents. Crystallization of the highly conducting mixed-anion hydroborate crystal structures from solution was demonstrated for several hydroborates and solvents, enabling solution-based infiltration of pre-fabricated porous electrode sheets with hydroborate electrolytes [134]. However, most cells in literature are fabricated employing cold pressing, benefitting from the ductile mechanical properties of hydroborates. Stack pressure during galvanostatic cycling is not a strict requirement with electrode materials with low volume expansion and contraction during cycling, such as  $\text{Na}_3(\text{VOPO}_4)_2\text{F}$  [133], but is required for electrode materials with considerable volume expansion, such as NMC811 [132]. Hydroborate electrolytes typically also exhibit high thermal stability of  $\sim 400\text{ }^\circ\text{C}$  and low toxicity (e.g., comparable toxicity for  $\text{Na}_2\text{B}_{12}\text{H}_{12}$  as for  $\text{NaCl}$ ) [135].

### Current and Future Challenges

While the community researching and developing hydroborate electrolytes has been limited to a handful of groups globally, hydroborates have surprisingly been able to keep up with the pace set by more intensively studied electrolyte materials, such as argyrodite  $\text{Li}_6\text{PS}_5\text{Cl}$  and garnet  $\text{Li}_7\text{La}_3\text{Zr}_2\text{O}_{12}$ . So far, almost all cells demonstrated in literature made use of lithium and sodium metal anodes, but struggle with lithium and sodium metal dendrite formation, which consequently limits the achievable current density and areal capacity of the cells. A recent study compared the cycling stability of

1 NMC811 cathodes vs. Li, InLi, and graphite electrodes, concluding that challenges with dendrites on  
2 the negative electrode mask the excellent performance and stability of the positive electrode [132].  
3 Consequently, hydroborate cells with higher positive electrode areal capacity  $> 1 \text{ mAh cm}^{-2}$  reported  
4 so far made use of either InLi [132] or NaSn anodes [134] with a redox potential above the onset for  
5 dendrite formation, compromising in exchange the energy density of these cells. Cathode electrolyte  
6 interphase formation at the interface between hydroborates and high-voltage cathodes, such as  
7  $\text{Na}_3(\text{VOPO}_4)_2\text{F}$  [133] and NMC811 [132], has been observed indirectly using electrochemical  
8 impedance spectroscopy, but remains very difficult to study in more detail with X-ray or electron beam  
9 based techniques because both boron and hydrogen are light elements. A recent study concluded that  
10 the electrochemical oxidation of  $\text{LiB}_{12}\text{H}_{12}$  proceeds successively through the formation of hydrogen-  
11 interconnected larger closo-clusters, e.g., the dimerization of two  $\text{B}_{12}\text{H}_{12}^{2-}$  anions into  $\text{B}_{24}\text{H}_{23}^{3-}$  [136].  
12 These clusters are expected to have even higher oxidative stability, thereby passivating the  
13 electrolyte/electrode interface. Analogous studies should also be conducted on the reductive stability of  
14 hydroborate electrolytes to better understand interface stability to lithium and sodium metal anodes and  
15 ultimately mitigate dendrite formation. Some attempts have also been made in integrating hydroborates  
16 with other solid electrolytes to benefit from the best of both worlds [79, 137] while mitigating  
17 shortcomings, a strategy that may be worth pursuing in more detail in the future.

21 A major handicap of hydroborate electrolytes is the high cost of hydroborate salts due to their  
22 applications in medicine. Currently, the cost per kg is on the order of USD 10,000 for  $\text{Li}_2\text{B}_{12}\text{H}_{12}$  and  
23  $\text{Na}_2\text{B}_{12}\text{H}_{12}$ , USD 100,000 for  $\text{Li}_2\text{B}_{10}\text{H}_{10}$  and  $\text{Na}_2\text{B}_{10}\text{H}_{10}$ , and even USD 500,000 for  $\text{LiCB}_{11}\text{H}_{12}$ .  
24 However, there are multiple efforts to develop cost-effective synthesis of closo-hydroborate and closo-  
25 hydrocarbaborate salts [138–140]. While closo-hydroborate anions can be synthesized via low-  
26 temperature solvothermal synthesis [138], the synthesis of closo-hydrocarbaborate anions proceeds via  
27 nido-hydroborate intermediates and is more complex [127, 139, 140]. Most hydroborate salts can be  
28 synthesized from the precursor  $\text{NaBH}_4$ , which is cheap and widely available. Lithium salts can be  
29 easily obtained via ion exchange from the corresponding sodium salts [130]. However, so far, we are  
30 not aware of any successful scale-up of hydroborate salt synthesis to the kg or multi-kg scale, although  
31 there are no apparent conceptual barriers. Achieving this level of scale-up is a prerequisite to  
32 demonstrate cell fabrication on MWh/y pilot line level. While boron chemistry has reputation of being  
33 relatively difficult, NASA studied the synthesis of boranes ( $\text{BH}_3$ ,  $\text{B}_2\text{H}_6$ ,  $\text{B}_5\text{H}_9$ ,  $\text{B}_{10}\text{H}_{14}$ ) as rocket fuel in  
34 detail in the 1960s, so competences from this period may be beneficial.

## 39 Conclusion and Future Perspectives

41 Hydroborate solid electrolytes have emerged as promising candidates for next-generation solid-  
42 state batteries due to their unique combination of high ionic conductivity, wide electrochemical  
43 stability windows, low density, excellent thermal stability, and low toxicity. The development of  
44 mixed-anion hydroborates and hydrocarbaborates has demonstrated that cation conductivities  
45 comparable to or exceeding state-of-the-art solid electrolytes can be achieved, while demonstrating  
46 compatibility with lithium and sodium metal anodes and high-voltage cathodes. Their ductile  
47 mechanical properties and solution processability are further advantages in view of solid-state battery  
48 manufacturing. Despite these advantages, several challenges, including solid electrolyte interphase  
49 formation and dendrite formation, must be addressed before solid-state batteries based on hydroborates  
50 can be commercialized.

53 Looking ahead, the most immediate bottleneck towards commercialization lies in scalable and  
54 cost-effective synthesis of hydroborate salts. While current production remains restricted to laboratory-  
55 scale quantities at high cost, routes based on inexpensive precursors, such as  $\text{NaBH}_4$ , and knowledge  
56 from historical boron chemistry research may offer promising opportunities for scale-up. The  
57 successful reduction of synthesis cost could unlock hydroborates as competitive solid electrolytes for  
58 both lithium and sodium solid-state batteries.

1 In perspective, hydroborates represent a relatively underexplored but highly versatile class of  
2 electrolyte materials with untapped potential. Their continuous progress, despite limited global  
3 research activity, underscores the strong potential of hydroborate electrolytes. With coordinated efforts  
4 in synthesis, interfacial characterization, and cell engineering, hydroborates may evolve from a niche  
5 research topic into a cornerstone electrolyte class for competitive high-performance, safe, and  
6 sustainable solid-state batteries.  
7  
8  
9

### 10 **Acknowledgment**

11 This work was supported by the Swiss National Science Foundation (SNSF) under contracts  
12 CRSII2\_160749/1 and 200021L\_192191 and by Innosuisse – Swiss Innovation Agency under contract  
13 number 49729.1 IP-EE.  
14  
15  
16

### 17 **Conflict of Interest**

18 The authors declare no conflict of interest.  
19  
20  
21  
22  
23  
24  
25  
26  
27  
28  
29  
30  
31  
32  
33  
34  
35  
36  
37  
38  
39  
40  
41  
42  
43  
44  
45  
46  
47  
48  
49  
50  
51  
52  
53  
54  
55  
56  
57  
58  
59  
60

## 6. Fully reduced (irreducible) solid electrolytes

Theodosios Famprakis<sup>1,a,\*</sup> and Marnix Wagemaker<sup>1,\*</sup>

<sup>1</sup> Radiation Science and Technology, Faculty of Applied Sciences, Delft University of Technology, Delft, The Netherlands.

<sup>a</sup> Current address: Inorganic Chemistry Laboratory, Department of Chemistry, University of Oxford, Oxford, United Kingdom.

\*E-mail: [t.famprakis@tudelft.nl](mailto:t.famprakis@tudelft.nl), [m.wagemaker@tudelft.nl](mailto:m.wagemaker@tudelft.nl)

### Status

In contrast to most known high-performance electrolytes, irreducible electrolytes are defined as inert to reduction by the corresponding metal, i.e., thermodynamically stable against lithium metal or down to 0 V vs. Li/Li<sup>+</sup> in the context of lithium-ion conductors. The key idea is that such electrolytes would not undergo decomposition in contact with low-voltage electrodes and could enable the practical application of high-performance anodes, such as lithium metal and silicon. This approach is an alternative to relying on the kinetically stabilized decomposition of the solid electrolyte into a favorable —ionically conducting and electronically insulating—solid-electrolyte interphase (SEI) [104], as exemplified, e.g., in the case of lithium phosphorus oxynitride (LiPON) [141, 142].

Irreducibility is a stringent constraint that in practice limits the chemical composition of the electrolytes in most cases to a combination of the mobile cation (e.g., Li<sup>+</sup>) and anions in their lowest oxidation state (i.e., fully-reduced; e.g., O<sup>2-</sup>, Cl<sup>-</sup>, etc.) while precluding reducible framework cations. Many such irreducible compounds are known (**Table 1**) and are often identified as components of the SEI formed by reductive decomposition of high-performance electrolytes, e.g., in contact with lithium metal the argyrodite Li<sub>6</sub>PS<sub>5</sub>Cl is reduced to the irreducible binaries Li<sub>2</sub>S, Li<sub>3</sub>P, and LiCl [143], and the aforementioned LiPON is reduced to Li<sub>3</sub>N, Li<sub>2</sub>O, and Li<sub>3</sub>P [141, 142]. The issue is that these binary irreducible compounds are usually ionic insulators.

An exception to this rule is the binary pnictides Li<sub>3</sub>P (~10<sup>-4</sup> S cm<sup>-1</sup> [144]) and particularly Li<sub>3</sub>N which has long been studied as a solid electrolyte exactly because of its high ionic conductivity [145] and stability against reduction. A mechanochemically prepared β-Li<sub>3</sub>N electrolyte has recently been reported to reach 2×10<sup>-3</sup> S cm<sup>-1</sup> and has shown promising results as an anolyte in lithium-metal solid-state batteries [146].

Recent work has focused on the (re)exploration of the mixed-anion phase space bounded by irreducible binaries with the goal of identifying new materials with enhanced ion conduction while maintaining irreducibility. In this vein, many lithium and sodium mixed-anion antiperovskites have been identified, with general formula A<sub>3</sub>XY (A = Li/Na; X = O<sup>2-</sup>/H<sup>-</sup>; Y = Cl<sup>-</sup>/Br<sup>-</sup>/I<sup>-</sup>/S<sup>2-</sup>/Se<sup>2-</sup>/Te<sup>2-</sup>) [147]. These typically suffer from low-to-modest ionic conductivities and/or reproducibility issues and will not be discussed further here. The previously identified Li<sub>7</sub>N<sub>2</sub>I has recently been demonstrated as an anolyte in a solid-state battery [148]. Li<sub>7</sub>N<sub>2</sub>I crystallizes in its own structure type (related to argyrodite via their similar MgCu<sub>2</sub>-type anion arrangement) and exhibits a modest ionic conductivity of 3×10<sup>-4</sup> S cm<sup>-1</sup>.

Significant promise has been demonstrated in the identification of anion-disordered antifluorite-like materials in the pseudo-tie lines LiCl-Li<sub>3</sub>N [149–151], Li<sub>2</sub>S-Li<sub>3</sub>P [152], Li<sub>2</sub>S-Li<sub>3</sub>N [153, 154], and Li<sub>2</sub>Se-Li<sub>3</sub>As [155]. The anion disorder is achieved by mechanochemical synthesis and most of these materials contain more than two Li per anion; they can thus be described as intermediates between the antifluorite and Li<sub>3</sub>Bi structure types. Their structure is based on an FCC arrangement of anions forming a network of tetrahedral and octahedral sites for Li, where the tetrahedral sites are preferentially occupied (i.e., antifluorite-like), while the octahedral sites act as reservoir for extra Li

and interstitial sites for ion migration. Furthermore, it has been recently demonstrated that ternary and quaternary mixed-anion compositions are accessible (e.g.,  $\text{Li}_{2.65}\text{S}_{0.35}\text{N}_{0.15}\text{P}_{0.5}$  [156];  $\text{Li}_{2.31}\text{S}_{0.41}\text{Br}_{0.14}\text{N}_{0.45}$  [151]), showing high ionic conductivities along with tunable anodic stability, and thus opening up a vast space for exploration and property optimization. As such, we focus the following discussion on antiperovskite-like materials.

**Table 1.** Key properties of irreducible electrolytes. Experimentally data are preferentially reported where available (n/a: not available).

Phase/Class	Ionic Conductivity ( $\text{S cm}^{-1}$ , RT)	Anodic Stability Limit (vs. $\text{Li}^+/\text{Li}$ )	Ref.
$\text{Li}_3\text{N}$	$\sim 10^{-3}$	$\sim 0.5$ V	[145, 146]
$\text{Li}_3\text{P}$	$\sim 10^{-4}$	$\sim 1$ V <sup>a</sup>	[144]
$\text{Li}_3\text{As}$	$< 10^{-7}$	n/a	[155]
$\text{Li}_2\text{O}$	$\sim 10^{-12}$	$\sim 3$ V <sup>a</sup>	[157]
$\text{Li}_2\text{S}$	$< 10^{-8}$	$\sim 2.2$ V	[153, 158]
$\text{Li}_2\text{Se}$	$< 10^{-7}$	n/a	[155]
$\text{LiH}$	n/a	$\sim 1$ V <sup>a</sup>	-
$\text{LiF}$	$< 10^{-14}$	$\sim 6.3$ V <sup>a</sup>	[159]
$\text{LiCl}$	$< 10^{-10}$	$\sim 4.2$ V <sup>a</sup>	[160]
$\text{LiBr}$	n/a	$\sim 3.6$ V <sup>a</sup>	-
$\text{LiI}$	$\sim 10^{-7}$	$\sim 2.8$ V <sup>a</sup>	[161]
$\text{Li}_7\text{N}_2\text{I}$	$\sim 3 \times 10^{-4}$	$\sim 1.1$ V	[148]
<b>Antiperovskites</b>			
$\text{Li}_3\text{OX}$ (X: Cl, Br)	$\sim 10^{-4}$ <sup>b</sup>	$\sim 3$ V <sup>a</sup>	[147]
$\text{Li}_3\text{HCh}$ (Ch: S, Se, Te)	$\sim 10^{-9}$ – $10^{-7}$	n/a	[162]
<b>Antifluorite-like</b>			
$\text{Li}_{1+2x}\text{Cl}_{1-x}\text{N}_x$	$\sim 10^{-5}$	$\sim 0.7$ – $1.4$ V	[149–151]
$\text{Li}_{2+x}\text{S}_{1-x}\text{N}_x$	up to $2 \times 10^{-4}$	$\sim 1.2$ – $2.2$ V	[151, 153, 154]
$\text{Li}_{2+x}\text{S}_{1-x}\text{P}_x$	up to $2 \times 10^{-4}$	n/a	[152]
$\text{Li}_{2+x}\text{Se}_{1-x}\text{As}_x$	$\sim 10^{-5}$ – $10^{-4}$	n/a	[155]
$\text{Li}_{2.65}\text{S}_{0.35}\text{N}_x\text{P}_{0.65-x}$	$\sim 10^{-3}$	$\sim 1.1$ V	[156]

<sup>a</sup>Experimental data not available, calculated stability limit from Richards *et al.* [163].

<sup>b</sup>It is debated whether these compositions are synthesizable in bulk form; the initial reports could not be reproduced, see discussion in [147].

## Current and Future Challenges

Irreducible electrolytes show potential for application as anolytes in multi-electrolyte battery designs. Irreducible solid electrolytes are intrinsically stable at low potentials, but their typically low anodic stability ( $< 2$  V vs.  $\text{Li}^+/\text{Li}$ ) precludes their application as the sole electrolyte in a battery, as they would decompose at the operating voltage of any typical battery cathode ( $> 3$  V vs.  $\text{Li}^+/\text{Li}$ ). Multi-electrolyte battery architectures leverage multiple electrolytes to ensure interfacial stability. In its simplest form, a dual-electrolyte architecture is demonstrated in **Figure 8**. An irreducible solid electrolyte could be used as anolyte, inert to reduction by the anode active material and protected from oxidation by the catholyte. The catholyte in turn would be selected to be resistant to oxidation by the cathode active material and protected from reduction by the anolyte. The concept can easily be extended to triple- (or generally multi-)electrolyte designs and such prototypes leveraging irreducible anolytes and low-potential anodes have already shown promising results in terms of cycling stability and power capability [146, 148, 149, 153, 154, 156].

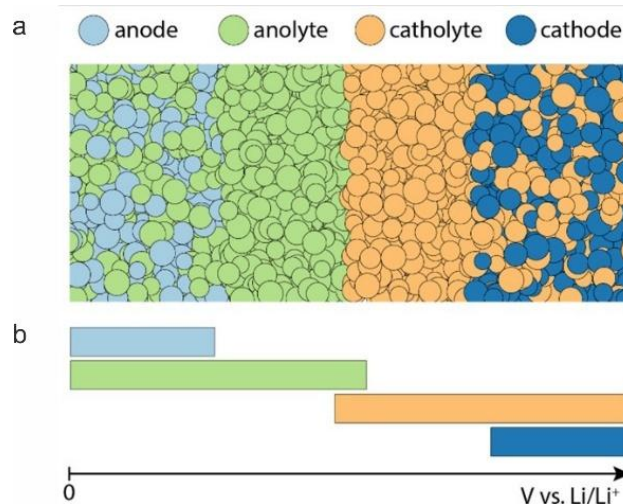


**Figure 8.** (a) Schematic of a dual-electrolyte solid-state battery. (b) Schematic of the working potentials (for anode, cathode) and electrochemical stability windows (anolyte, catholyte). The anolyte is inert to reduction by the anode and is protected from oxidation by the catholyte. The catholyte is inert to oxidation by the cathode and is protected from reduction by the anolyte.

In the context of multi-electrolyte architectures, the key properties of irreducible electrolytes become their ionic conductivity and stability to oxidation, as listed in **Table 1**. Though  $\text{Li}_3\text{N}$  with its high room-temperature ionic conductivity ( $\sim 10^{-3} \text{ S cm}^{-1}$ ) might seem like the obvious anolyte choice, its extremely limited stability window ( $\sim 0\text{--}0.5 \text{ V vs. Li}^+/\text{Li}$ ) makes it questionable whether it can form stable interfaces with other solid electrolytes. Electrochemical compatibility between different electrolytes has not been systematically investigated and represents a clear direction for future work; still preliminary calculations indicate that antifluorite-like irreducible electrolytes would be less prone to reaction with various potential catholytes, compared to  $\text{Li}_3\text{N}$  [150]. It has recently been shown that antifluorite-like materials can effectively show higher anodic stability than  $\text{Li}_3\text{N}$  (**Table 1**) while maintaining high ionic conductivity ( $\sim 10^{-3} \text{ S cm}^{-1}$  for  $\text{Li}_{2.65}\text{S}_{0.35}\text{N}_{0.15}\text{P}_{0.5}$  [156]).

Another area in which the extended anodic stability of antifluorites could prove critically advantageous is the application of next-generation silicon anodes. Reversible (de)lithiation of silicon proceeds through various phases and in a wide potential window ( $\sim 0$  to  $1 \text{ V vs. Li}^+/\text{Li}$ ), meaning  $\text{Li}_3\text{N}$  would be prone to oxidation against the anode above  $\sim 0.5 \text{ V vs. Li}^+/\text{Li}$ . In contrast, antifluorites are able to encompass the silicon operational potential window within their electrochemical stability window and could as such be key in enabling silicon-anode solid-state batteries.

Structural disorder could be leveraged as a rational design knob in irreducible solid electrolytes. Mechanochemical treatment of mixtures of irreducible binaries has been shown to favor formation of single-phase antifluorite-like materials with anion-disorder as a key structural feature. These anion-disordered materials are likely metastable: it has been shown (for some [153, 155] and assumed for others) that they would decompose upon high-temperature treatment to the corresponding binaries. Their kinetic stabilization is predicated on the configurational (and/or vibrational) entropy associated with anion disorder, and the high activation barrier for anion rearrangement (ordering) near room temperature. In practice, they are accessible through the high local-instantaneous effective temperature (and pressure) afforded by mechanochemistry [155], which effectively emulates quenching and successfully stabilizes the metastable disordered configurations of anions at room temperature. Further advancements will be facilitated by better understanding of the formation thermodynamics (balance between entropy and enthalpy) as well as optimization of out-of-equilibrium mechanochemical (and/or high-pressure [155, 162]) synthesis protocols. It would also be necessary to quantify the thermal stability of irreducible antifluorite-like solid electrolytes against decomposition (exsolution [155]) in the context of practical battery device fabrication and operation temperatures.

Beyond its critical effect on synthesis, anion-disorder intimately influences the ionic conductivity of antifluorite-like irreducible electrolytes. We have recently developed a computational protocol based on molecular dynamics simulations and percolation analysis to quantify this effect of local anion environments on ionic diffusivity in disordered antifluorite [153] (and argyrodite [164]) solid electrolytes. For irreducible antifluorites, we have shown that lithium ions preferentially hop through pnictide-rich regions [153, 156], explaining the trend of higher ionic conductivity with higher pnictide content,  $x$ , in  $\text{Li}_{2+x}\text{S}_{1-x}\text{N}_x$  [153],  $\text{Li}_{2+x}\text{S}_{1-x}\text{P}_x$  [152], and  $\text{Li}_{2+x}\text{Se}_{1-x}\text{As}_x$  [155]. We have preliminarily interpreted this correlation based on steric arguments, though our latest results on ternary mixed-pnictide compositions  $\text{Li}_{2.65}\text{S}_{0.35}\text{N}_x\text{P}_{0.65-x}$  indicate that chemical rationale (i.e., bonding nature, electronegativity, etc.) needs to be included for a full mechanistic picture. Our analysis clearly shows that the disordered anion arrangements produce interconnected percolation pathways, critically facilitating long-range ion diffusion compared to ordered variants of the same compositions (**Figure 9**) [153, 164]. Further refinements should aim to derive transferable descriptors linking composition to ionic conductivity via local-hopping-environment analysis and percolation arguments. It also remains unclear whether the anion disorder in these phases is in fact random or correlated [165]; and in the latter case whether there is scope for chemical tuning of the anion distribution and thus properties, e.g., through composition or synthetic optimization.

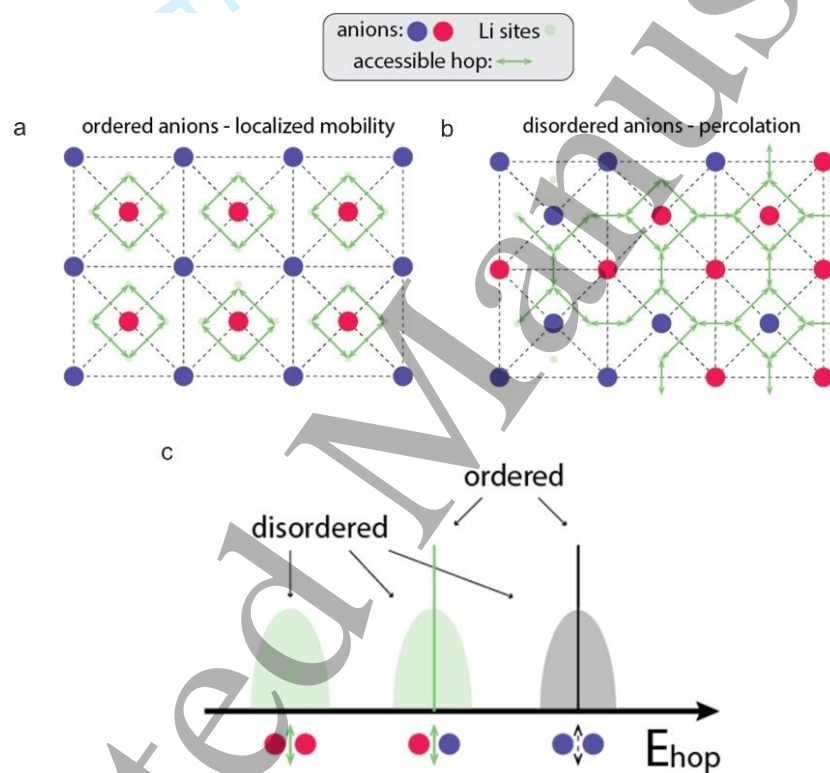


**Figure 9.** Effects of anion-disorder on lithium diffusivity. It is assumed in this schematic example that lithium hops are only allowed in the vicinity of a red anion. (a) Lithium mobility is localized in anion-ordered frameworks, (b) anion-disorder creates interconnected percolation pathways by (c) breaking the degeneracy of ion-hopping energies ( $E_{\text{hop}}$ ) and creating new local environments conducive to ion hopping.

## Conclusion and Future Perspectives

Irreducible electrolytes offer a direct route to eliminate anode-side electrolyte decomposition and associated performance losses in solid-state batteries. Recent discoveries have established design rules that now enable purposeful materials discovery:

- (1) Enforce irreducibility for thermodynamic stability to Li metal.

- 1 (2) Use out-of-equilibrium synthesis to stabilize otherwise inaccessible disordered structural  
2 frameworks.
- 3
- 4 (3) Exploit mixed-anion disorder to reach high ionic conductivity, upwards of  $10^{-3}$  S cm<sup>-1</sup> at room  
5 temperature.
- 6
- 7 (4) Deploy multi-electrolyte architectures that combine irreducible anolytes with oxidation-stable  
8 catholytes to enable high energy- and high power-density solid-state batteries.
- 9

10 Further work will focus on (i) consolidating phase maps and processing windows for irreducible  
11 electrolytes, (ii) benchmarking anodic limits and interfacial stability against leading sulfide/halide  
12 catholytes, and (iii) investigating lithium-plating-related properties, such as lithiophilicity, electronic  
13 conductivity, and mechanical properties of irreducible solid electrolytes. In parallel, multi-electrolyte  
14 prototypes leveraging irreducible anolytes with silicon and lithium-metal anodes at practical areal  
15 capacities will be validated. With these directions in mind, irreducible solid electrolytes can provide  
16 the missing anolyte link in practical multi-electrolyte solid-state batteries, unlocking the full promise  
17 of silicon and lithium-metal anodes without sacrificing cycle life, rate capability, or safety.

18  
19 Finally, it is not unlikely that the mixed-anion fully reduced electrolytes presently being identified  
20 and studied in the bulk, actually form *in situ* upon reductive decomposition of other (reducible)  
21 electrolytes, such as the Li<sub>6</sub>PS<sub>5</sub>Cl and LiPON examples discussed in the introduction, i.e., forming  
22 components of their respective SEIs. Thus, the exploration of the irreducible electrolyte phase space  
23 outlined above could also effectively contribute to the better fundamental understanding of SEI  
24 composition and behavior, leading to transferable insight for the development of solid-state batteries in  
25 general, regardless of the choice of electrolyte.

## 26 27 28 29 30 **Acknowledgment**

31 T.F. acknowledges funding provided by the European Union's HORIZON EUROPE program in  
32 the form of a Marie Skłodowska-Curie individual postdoctoral fellowship (project number 101066486),  
33 and by the Dutch Research Council (NWO) in the form of an open-competition XS grant  
34 (OCENW.XS22.4.210). M.W. acknowledges the financial support from the 'BatteryNL – Next  
35 Generation Batteries based on Understanding Materials Interfaces' project NWA.1389.20.089 of the  
36 NWA research program 'Research on Routes by Consortia (ORC)' funded by the Dutch Research  
37 Council (NWO).  
38  
39

## 40 41 42 **Conflict of Interest**

43 The authors declare no conflict of interest.  
44  
45  
46  
47  
48  
49  
50  
51  
52  
53  
54  
55  
56  
57  
58  
59  
60

## 7. Amorphous solid electrolytes: ionic conductivity and conduction mechanisms

Ke Huang<sup>1</sup>, Yan Zeng<sup>1</sup> and Bin Ouyang<sup>1,\*</sup>

<sup>1</sup> Department of Chemistry & Biochemistry, Florida State University, Tallahassee, FL 32306, USA.

\*E-mail: bouyang@fsu.edu

### Status

The growing demand for large-scale energy storage drives the search for safer, high-energy-density batteries. Solid-state electrolytes (SEs) hold the potential to replace flammable liquid solvents and can pair with the lithium metal anode, improving both safety and energy density in all-solid-state batteries [104, 166–168]. Unlike crystalline SEs, amorphous SEs allow ionic conductivity to be tuned through structural disorder, while also suppressing dendrite growth [169, 170] and eliminating grain-boundary resistance [141, 171, 172]. Certain metal halide-based amorphous electrolytes have been shown to exhibit remarkable mechanical flexibility [173, 174], facilitating battery processing during manufacturing. A widely used amorphous SE is LiPON [175], which has been extensively employed to demonstrate stable solid-state batteries [141, 176–179]. Beyond LiPON, amorphous electrolytes have been explored across oxides [180–183], sulfides [184–187], halides [87, 173, 174, 188], as well as several mixed-anion systems [91, 170, 189–191]. The best reported ionic conductivities reach up to  $\sim 10^{-2}$  S cm<sup>-1</sup> [188, 192–194], comparable to those of commercial liquid electrolytes. Despite this rapid progress, rational design principles for optimizing the accessible chemical space and maximizing ionic conductivity remain underdeveloped. In the following sections, we provide a comprehensive overview of the reported chemical spaces for amorphous battery electrolytes and discuss the proposed mechanisms of ion conduction.

The reported amorphous electrolytes can be classified depending on anion chemistry to be sulfides, oxides, halides, and mixed anions. Reported conductivities for Li, Na, K, and Mg electrolytes obtained from experimental measurements and various simulation approaches have been summarized in **Figure 10**. Among all amorphous electrolytes, sulfide-based amorphous electrolytes have attracted most attention in the past decades [12, 184, 195], particularly attributed to the possibility of approaching the ionic conductivity of liquid-electrolytes [36, 193]. The extracted ionic conductivity of this group can be represented by S-G1, S-G2, and S-G3, respectively. The chemical formula in general follows  $xM_2S-(1-x)P_2S_5$  (M = Li or Na), which allows tuning by changing the M<sub>2</sub>S to P<sub>2</sub>S ratio [196, 197]. Glass-ceramic thiophosphates (S-G1) are often argued to conduct better than glassy counterparts (S-G2) due to the fast crystalline pathways precipitating inside the amorphous matrix [185, 198, 199]. A notable example is glass-ceramic Li<sub>7</sub>P<sub>3</sub>S<sub>11</sub>, which reaches 17 mS cm<sup>-1</sup> at room temperature after melt quench and heat treatment [193], exceeding the  $\sim 10$  mS cm<sup>-1</sup> of conventional liquid electrolytes [200]. In other cases, amorphization of LGPS generally has reduced conductivity relative to the crystal [6, 201]. Simulations sometimes report very high conductivities for sulfide glasses, such as gc-Li<sub>42</sub>P<sub>16</sub>S<sub>61</sub> (33.1 mS cm<sup>-1</sup>) [196] and Li<sub>3</sub>PS<sub>4</sub> (19 mS cm<sup>-1</sup>) [202], but these values are extrapolated from high temperature and may be overestimated [203].

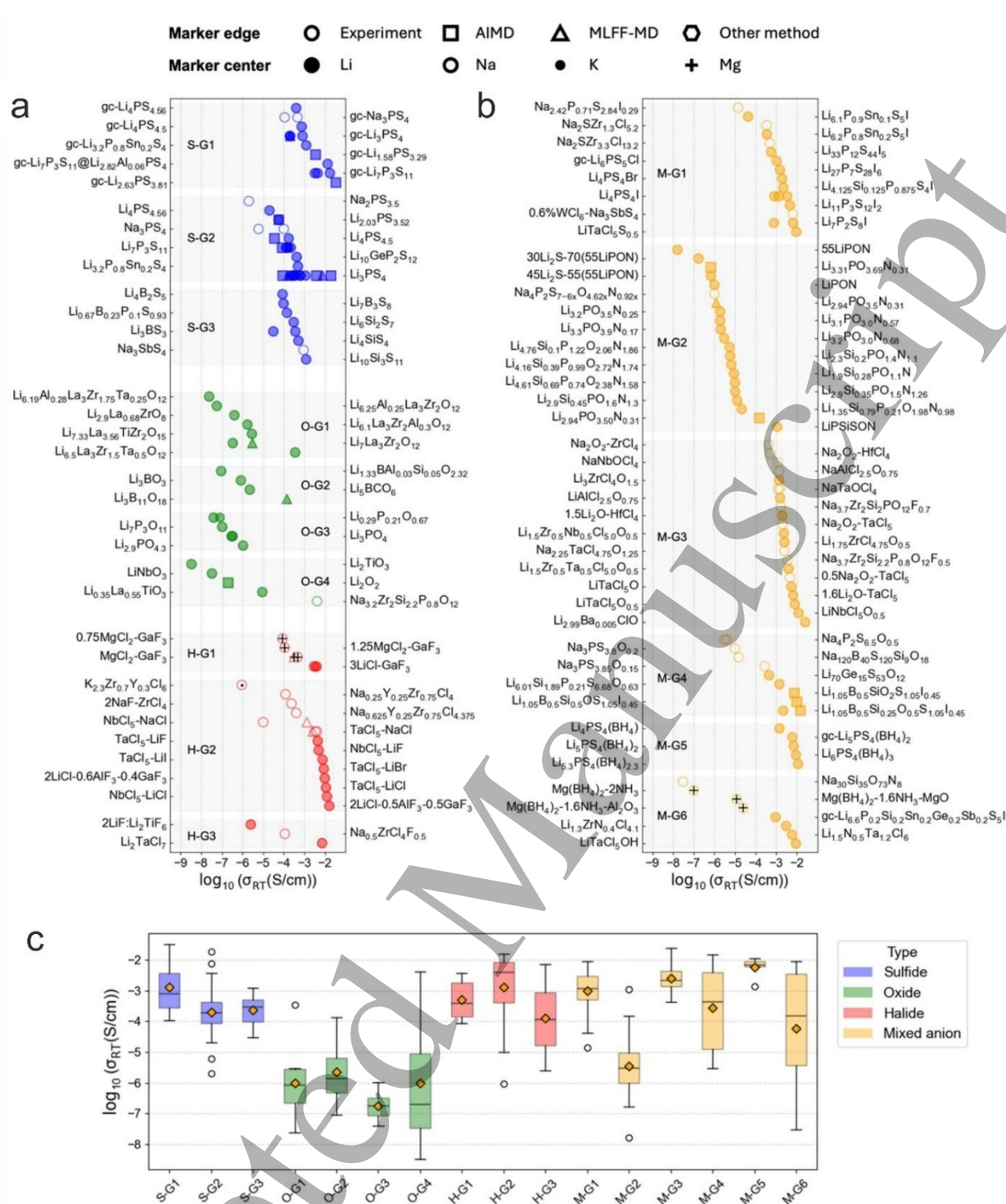


**Figure 10.** Room-temperature ionic conductivities of amorphous SEs. (a) Single-anion systems: sulfides (blue), oxides (green), and halides (red). Sulfides: S-G1, glass-ceramic thiophosphates; S-G2, glassy thiophosphates; S-G3, other sulfides. Oxides: O-G1, amorphous garnets; O-G2, borates; O-G3, phosphates; O-G4, other oxides. Halides: H-G1, clay-like binary halide mixtures; H-G2, non-clay-like binary or ternary halides; H-G3, other halides. (b) Mixed-anion system (orange), grouped as M-G1, chalcogenides; M-G2, LIPON and analogs; M-G3, oxyhalides; M-G4, oxysulfides; M-G5, thiophosphate-boron hydrides; M-G6, other mixed-anion compositions. (c) The corresponding box plot of ionic conductivities. The black line and orange diamond inside the box represent the median and mean value, respectively. Totals of reported amorphous SEs by type: sulfide  $n = 52$ , oxide  $n = 23$ , halide  $n = 26$ , and mixed anion  $n = 85$ . For detailed data on the ionic conductivity of all reported amorphous SEs, see **Table S1** in the Supporting Information.

Oxide amorphous SEs, including garnet-based (O-G1), borate (O-G2), phosphate (O-G3), and other families (O-G4), are much less developed in contrast to sulfide-based amorphous conductors. Moreover, they are always developed through doping and tuning of synthesis conditions taking a well-known crystalline phase, e.g., LISICON, NASICON, garnet, etc. As a contrast to the sulfide-based systems, there is significantly less work towards oxide amorphous SEs. The intention to more systematic exploration of oxide-based systems is likely to be discouraged by the fact that the amorphous phase shows lower or similar ionic conductivity compared to the crystalline reference in many situations [204–210]. Moreover, most oxide amorphous SEs tend to show much lower ionic conductivity than the best of the oxides. Nevertheless, there are some notable exceptions for such statement. For instance, a NASICON-based amorphous SE is reported to reach  $4.1 \text{ mS cm}^{-1}$  ionic conductivity, which is formed during the electrochemical process [211]. Moreover, the chemical space of oxides extends far beyond what has been explored and warrants more thorough investigation.

Halide amorphous SEs are another high-conductivity family. Ball milling mixtures of halide glass formers (such as  $\text{TaCl}_5$ ,  $\text{NbCl}_5$ ,  $\text{AlF}_3$ ,  $\text{GaF}_3$ ) with alkali or alkaline-earth salts can produce amorphous halides [173, 174, 188, 194, 212]. Some pairings, such as  $3\text{LiCl-GaF}_3$  or  $\text{MgCl}_2\text{-GaF}_3$ , form soft clay-like mixtures (H-G1) through partial anion exchange [173, 174, 213]. These show good conductivities,  $10^{-4}\text{--}10^{-2} \text{ S cm}^{-1}$ , and make intimate electrode contact during cycling [173]. Non-clay binary or ternary halide glasses (H-G2) can be even more conductive.  $\text{TaCl}_5$  or  $\text{NbCl}_5$ -based Li conductors are notable, benefiting from larger free volume and polyanion rotation than lower migration barriers [194, 212, 214]. The  $2\text{LiCl-0.5AlF}_3\text{-0.5GaF}_3$  composition reaches  $16 \text{ mS cm}^{-1}$  at room temperature, attributed to a deep eutectic phase that enhances Li transport [188]. Li electrolytes generally outperform Na, Mg, and K analogs because larger ionic radii raise barriers [215] and  $\text{Mg}^{2+}$  can be strongly bound to the anion framework [216].

We further group mixed-anion systems into chalcogenides (M-G1), LiPON and analogs (M-G2), oxyhalide (M-G3), oxysulfide (M-G4), thiophosphate-boron hydride (M-G5), and other variants (M-G6). As can be well expected, any mixed-anion system with sulfur and halogen being anion tends to show higher ionic conductivity, which is inherited from the single anion systems. As a contrast, oxide-based systems, in general show lower ionic conductivity, which can be represented by the LiPON family. A typical motivation for creating mixed anion is the hope of trade-off for phase and electrochemical stability, as well as the hope of potential synergistic effect for further enhanced ionic conductivity. For example, chalcogenides (M-G1), oxysulfides (M-G4), oxyhalides (M-G3) attract increasing attention recently as such design can lead to a reasonable balance among good moisture stability, broad electrochemical window, easier processability, and high ionic conductivity [91, 92, 170, 190, 217–220].

Understanding ion conduction in amorphous SEs is challenging due to structural disorder and the lack of unified descriptors, even within a single class. Strategies to enhance conductivity mainly focus on lowering the activation barrier for ion hopping, increasing carrier concentration, or both, to form continuous percolation pathways. We classify mechanisms discussed in 132 studies into seven categories (**Figure 11**): local structure [220–223], density/free volume [186, 224–226], stoichiometry [192, 217, 227, 228], crystallinity [193, 195, 198], polyanion rotation [202, 229–231], correlated motion [174, 182, 202], and space charges [198, 232, 233]. Among these, crystallinity is dominant in glass-ceramic SEs, where percolating crystalline motifs within the amorphous matrix are believed to boost conductivity. Stoichiometry and space charges primarily affect carrier concentration, while the other four factors mainly reduce activation barriers. Notably, polyanion rotation represents a dynamic coupling between polyanion motion and ion diffusion, constituting a distinct type of local structural effect. We highlight it separately to emphasize its emerging importance, which has also led to occasional conflicting reports [202, 231, 234–237] that warrant further case-by-case theoretical and experimental investigation.

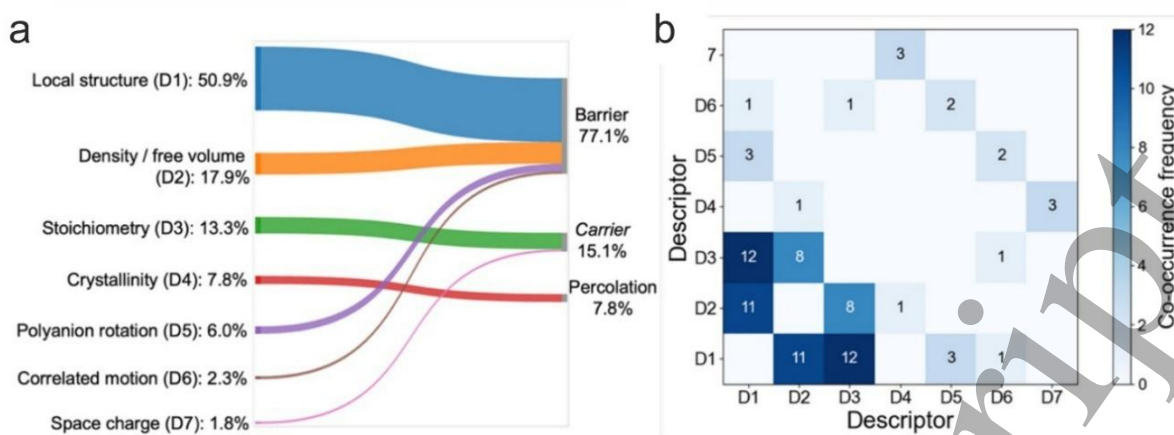


**Figure 11.** Descriptor landscape for ionic conductivity mechanisms in amorphous SEs. (a) Use frequency of each descriptor across the reported amorphous SEs, defined as each descriptor's occurrence count divided by the total occurrences of all descriptors. The descriptors are grouped according to the contribution to  $\sigma$  from migration barrier  $E_a$  (77.1%), charge-carrier concentration  $n$  (15.1%), or both (7.8%). (b) Descriptor co-occurrence matrix. Each cell ( $D_i, D_j$ ) counts pairs that appear together in the same SE; the diagonal ( $D_i, D_j$ ) is excluded. For detailed data on the descriptors of all reported amorphous SEs, see **Table S1** in the Supporting Information.

**Figure 11a** exhibits the use frequency of the above descriptors across all amorphous SEs. For crystalline ionic conductors, recent studies suggest that high conductivity arises from three factors: (i) crystalline frameworks that minimize the fluctuation of coordination environments, thereby lowering diffusion barriers [238], (ii) compositional disorder that promotes ion percolation [33, 239, 240], and (iii) framework-stoichiometries [241] interplay that influences both carrier concentration and activation barriers. In contrast, amorphous SEs urgently require tools to probe local structures, as over half of the literature attributes high conductivity to this factor. Ion percolation is further complicated by the absence of symmetry, demanding careful statistical treatment from both experiments and simulations. More accessible descriptors include density and composition, both shown in 17.9% and 13.3% cases to strongly affect conductivity. Building systematic datasets correlating these variables with conductivity would provide an efficient entry point for understanding amorphous SEs. Finally, these descriptors are often interdependent. As illustrated in **Figure 11b**, multiple descriptors, particularly local structure, density, and stoichiometry, frequently coexist. This overlap suggests that, in practice, one may substitute difficult-to-measure descriptors with more accessible ones to advance design rules for amorphous SEs.

### Current and Future Challenges

As a contrast to crystalline electrolytes, it is somewhat surprising that there is much less systematic work for expanding the chemical space of amorphous electrolytes, while many crystalline electrolyte systems have been well explored with the aid of high-throughput computational screening [242–246]. Moreover, the compositional design of amorphous electrolytes is largely driven by heuristic hypotheses from experienced experimentalists, while in many cases, people tend to start from some crystalline analog when designing amorphous electrolytes. There could be broader spaces for further extending the viable chemical spaces of amorphous materials if the state-of-the-art high-throughput virtual screen, machine learning, as well as automated synthesis approaches can be adapted into the discovery of amorphous electrolytes [247, 248].

Meanwhile, extending the length and time scale for molecular statistical simulation of SEs through MD, MC, or other methods is always a challenge. For amorphous SEs, such a challenge is more severe, particularly considering two factors: (i) The melt and quench process typically requires a

1 much longer time to equilibrate and (ii) there is a possibility for amorphous materials to evolve at  
2 different temperatures [249–251], which further brings the evolvement of ionic conductivity.  
3  
4

## 5 **Conclusion and Future Perspectives**

6 To summarize, we have compiled a curated dataset of amorphous solid electrolytes from 132  
7 published studies. This dataset captures the reported distributions of ionic conductivity and the  
8 proposed ion-conduction mechanisms. Our analysis highlights that amorphous solid electrolytes hold  
9 significant promise, not only for achieving high ionic conductivity, but also for enabling flexible  
10 synthesis and processing strategies in solid-state batteries. At the same time, the relatively limited  
11 exploration and understanding of ion transport in amorphous systems underscores a major opportunity  
12 to expand the viable chemical space.  
13  
14  
15

## 16 **Acknowledgment**

17 All authors acknowledge the startup funding from Florida State University to support this work.  
18  
19

## 20 **Conflict of Interest**

21 The authors declare no conflict of interest.  
22  
23  
24  
25  
26  
27  
28  
29  
30  
31  
32  
33  
34  
35  
36  
37  
38  
39  
40  
41  
42  
43  
44  
45  
46  
47  
48  
49  
50  
51  
52  
53  
54  
55  
56  
57  
58  
59  
60

## 8. Glass-ceramic solid electrolytes: halides

Juhyoun Park<sup>1</sup> and Yoon Seok Jung<sup>1,2,\*</sup>

<sup>1</sup> Department of Chemical and Biomolecular Engineering, Yonsei University, Seoul 03722, South Korea.

<sup>2</sup> Department of Battery Engineering, Yonsei University, Seoul 03722, South Korea.

\*E-mail: yoonsjung@yonsei.ac.kr

### Status

Glass-ceramics are metastable phases positioned between amorphous and crystalline materials; they comprise an amorphous matrix with embedded crystalline domains formed through partial nucleation (**Figure 12a**). The field emerged in 1953, when  $\text{Li}_2\text{O}-2\text{SiO}_2$  synthesized at high temperatures was unexpectedly found to exhibit superior mechanical strength compared to conventional glass [252]. This discovery established the concept of “controlled crystallization,” which became the foundation for glass-ceramic manufacturing, and was later extended to solid electrolyte (SE) applications [253].

Glass/glass-ceramic SEs offer distinct advantages. For example, the structural disorder in glass provides compositional flexibility, which can enhance the ionic conductivity, chemical and interfacial stability, and mechanical ductility [254]. Additionally, the absence of grain boundaries allows for the densification of cold-pressed pellets [254, 255]. A representative example is the  $\text{Li}_2\text{S}-\text{P}_2\text{S}_5$  system, in which crystallinity plays a decisive role in ionic conductivity (**Figure 12b, c**). For example,  $70\text{Li}_2\text{S}-30\text{P}_2\text{S}_5$  ( $\text{Li}_7\text{P}_3\text{S}_{11}$ ) exhibits an ionic conductivity of  $\sim 0.05 \text{ mS cm}^{-1}$  in the ball-milled glass state,  $\sim 10^{-8} \text{ S cm}^{-1}$  in the fully crystalline state, and  $\sim 3 \text{ mS cm}^{-1}$  in the glass-ceramic state [256].

Halide SEs have attracted increasing attention owing to their superior oxidative stability ( $>4 \text{ V}$ ) compared to their sulfide counterparts [71, 257]. Notably, after the rediscovery of  $\text{Li}_3\text{YCl}_6$ , it was confirmed that mechanochemically synthesized materials exhibit higher ionic conductivity than those obtained by simple annealing, as ball milling often yields distinct structural motifs that enhance transport [71, 258]. Although sulfide SEs can deliver  $\text{Li}^+$  conductivities exceeding  $10 \text{ mS cm}^{-1}$  [6], no crystalline halide SEs have yet achieved comparable levels. Recently, however, the emergence of glass/glass-ceramic halide SEs has renewed interest in the subject, as glassy phases offer opportunities to improve both their ionic conductivity and mechanical properties.

Most crystalline halide SEs exhibit hexagonal close-packing (trigonal  $P\bar{3}m1$  and orthorhombic  $Pnma$   $\text{Li}_3\text{YCl}_6$ -structure) or cubic close-packing (monoclinic  $C2/m$   $\text{Li}_3\text{InCl}_6$ -structure) [257]. Compared to sulfides, these frameworks provide narrower  $\text{Li}^+$  migration channels, thereby imposing intrinsic upper limits on ionic conductivity [257]. Consequently, despite extensive compositional screening, no crystalline halide SEs have surpassed  $5 \text{ mS cm}^{-1}$ . By contrast, glassy halide SEs lack long-range periodicity and are free from such structural constraints, spurring a growing interest in their development as highly conductive electrolytes.

Glass/glass-ceramic halide SEs are typically synthesized from a combination of glass formers and network modifiers [259]. Glass formers include low-melting or sublimable metal chlorides, such as  $\text{AlCl}_3$ ,  $\text{ZrCl}_4$ , and  $\text{TaCl}_5$ , whereas network modifiers include Li-based salts, such as  $\text{Li}_2\text{O}$ ,  $\text{Li}_2\text{O}_2$ ,  $\text{Li}_3\text{PO}_4$ , and  $\text{LiCl}$  (or analogous Na salts). Upon ball milling or annealing, these precursors undergo anion rearrangement, generating diverse structural motifs with varying coordination environments. In this short review, we highlight the compositional design, structural characteristics, synthesis methods, and potential applications of glassy halide SEs and outline the key problems that must be addressed for their future commercialization.

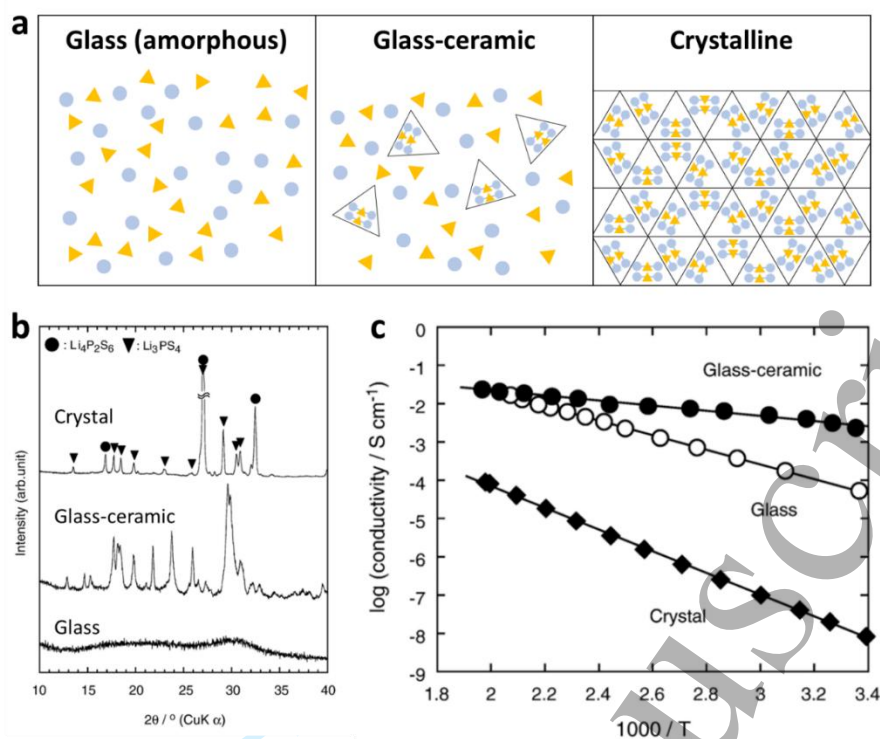


**Figure 12.** Structural and ionic transport characteristics of glass, glass-ceramic, and crystalline solid electrolytes (SEs). (a) Schematic illustrating the glass, glass-ceramic, and crystalline materials; blue circles and yellow triangles represent the anionic and cationic constituents, and black-outlined triangles indicate the crystalline domains. (b) X-ray diffraction (XRD) patterns and (c) Arrhenius plots of 70Li<sub>2</sub>S-30P<sub>2</sub>S<sub>5</sub> SEs. Reprinted from [256], Copyright (2006), with permission from Elsevier.

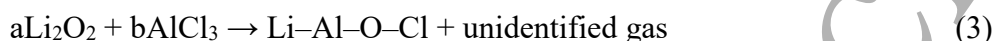
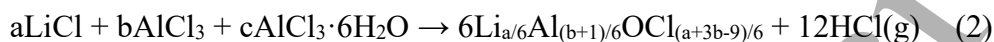
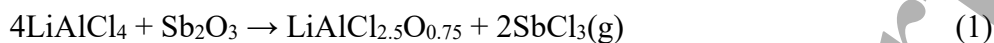
Jung *et al.* reported that mechanochemically prepared  $n\text{LiCl-GaF}_3$  ( $n = 2, 3$ ) exhibits a clay-like behavior with a modulus below 1 MPa [173]. Nuclear magnetic resonance and X-ray absorption spectroscopy analyses revealed an amorphous phase containing  $\text{GaCl}_m\text{F}_{n-m}$  complex anions [260], which Gupta *et al.* linked to the observed ductility [213]. Specific Al-based compositions were subsequently identified with similar mechanical softness and ionic conductivities of up to 1–16 mS  $\text{cm}^{-1}$  [261]; even  $\text{Mg}^{2+}$ -conducting analogs have been demonstrated [174]. Although this ductility enables intimate interfacial contact with active materials, some compositions suffer from compatibility problems with other SEs, necessitating careful consideration in the all-solid-state battery (ASSB) design [173].

ZrCl<sub>4</sub> and TaCl<sub>5</sub> are inorganic, molecular solids that can act as glass formers [259], enabling the synthesis of both crystalline and amorphous SEs. The heat treatment of Li<sub>n</sub>MCl<sub>6</sub> ( $M = \text{Zr, Ta}$ ) yields low-conductivity crystalline phases, whereas oxygen incorporation or prolonged ball milling produces highly conductive glassy halide SEs [262]. For example, crystalline LiTaCl<sub>6</sub> exhibits a low ionic conductivity of  $\sim 10^{-8}$  S  $\text{cm}^{-1}$  [263], whereas glass-ceramic LiMOCl<sub>4</sub> ( $M = \text{Nb, Ta}$ ) forms glass-ceramic phases with conductivities over 10 mS  $\text{cm}^{-1}$  [89]. Similarly, annealed Li<sub>2</sub>ZrCl<sub>6</sub> crystallizes in a monoclinic phase with an ionic conductivity of 0.006 mS  $\text{cm}^{-1}$  [258], whereas mechanochemically prepared Li<sub>2</sub>ZrCl<sub>6</sub> or ZrO<sub>2</sub>-2Li<sub>2</sub>ZrCl<sub>6</sub> achieves an ionic conductivity of 0.4 or 1.3 mS  $\text{cm}^{-1}$ , respectively (Figure 13a, b) [258, 264]. These findings highlight the growing trend of re-synthesizing crystalline halide compositions into glass/glass-ceramic phases containing amorphous domains to markedly improve their ionic conductivity.

Structurally, the crystalline Zr/Ta-based halide SEs contain isolated MCl<sub>6</sub> octahedra without corners or edge-sharing linkages [258, 263]. By contrast, glassy halides feature disordered arrangements of multiple coordination units, such as trigonal bipyramids and tetrahedra [91]. Zhang *et al.* demonstrated that oxygen atoms could bridge TaCl<sub>5-a</sub>O<sub>a</sub> units in 1.6Li<sub>2</sub>O-TaCl<sub>5</sub> [91], reminiscent of

conductivity enhancements in oxysulfide glass-ceramic SEs [195]. However, owing to the inherent disorder of glass structures, current characterizations have been largely limited to identifying the building-unit types. Quantitative insights into the degree and connectivity of these units are scarce, highlighting the need for more advanced structural investigations.

Li–Al–O–Cl (LAOC) systems have recently garnered attention owing to their cost-effectiveness, soft mechanical properties, and high ionic conductivities ( $>1 \text{ mS cm}^{-1}$ ), which are likely related to the low melting point ( $<200 \text{ }^\circ\text{C}$ ) of  $\text{AlCl}_3$ . Dai *et al.* synthesized oxychloride SEs with polymer-like mechanical properties by oxidizing  $\text{LiAlCl}_4$  using  $\text{Sb}_2\text{O}_3$  (**Eq. 1**) [261]. Alternative oxygen sources, such as  $\text{AlCl}_3 \cdot 6\text{H}_2\text{O}$  or  $\text{Li}_2\text{O}_2$ , can also be employed (**Eqs. 2 and 3**) [265–267], although these reactions are invariably accompanied by gas evolution.



Cyclic voltammetry indicated that the oxidation stability of LAOC was limited to below 4 V, and long-term cycling with layered oxide cathodes (cutoff at 4.8 or 4.3 V) was enabled by passivation through  $\text{LiAlO}_2$  formation at the cathode interface [261, 262, 267]. On the anode side, a comparable passivation mechanism derived from oxygen-rich Al environments allowed stable cycling with Li-In anodes [262]. Additionally, the low melting point allowed interfacial wetting and infiltration into cathode interparticle voids, thereby forming integrated  $\text{Li}^+$  transport channels within the electrode (**Figure 13c, d**) [268].

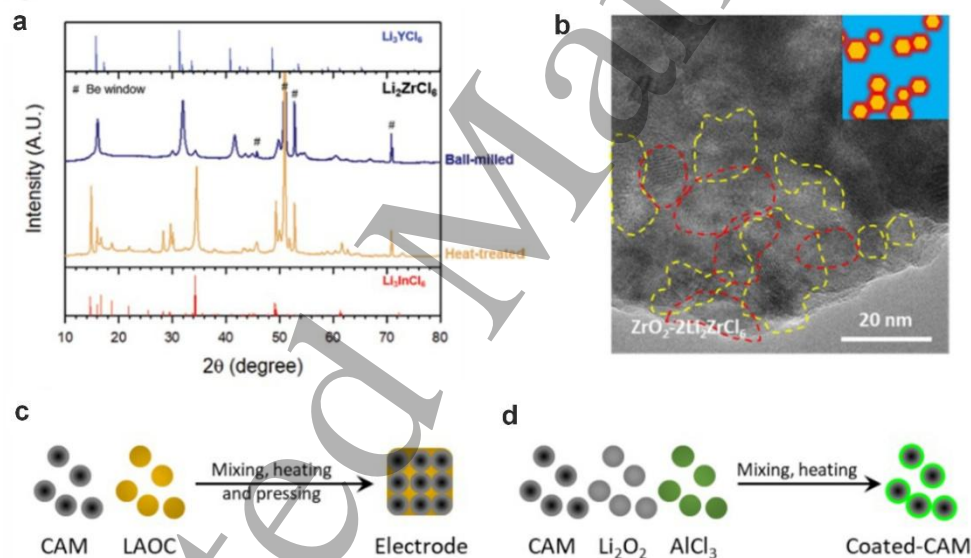


**Figure 13.** Glassy halide SEs with structural characteristics and electrode-level applications. (a) XRD patterns of the heat-treated  $\text{Li}_2\text{ZrCl}_6$  and mechanochemically prepared samples of  $\text{Li}_2\text{ZrCl}_6$ . Reprinted from [258], Copyright (2021), with permission from Wiley-VCH GmbH, John Wiley & Sons. (b) Transmission electron microscopy (TEM) image of  $\text{ZrO}_2\text{-}2\text{Li}_2\text{ZrCl}_6$ . Reproduced from [264]. CC BY 4.0. Schematic of the electrode-level application of LAOC via thermal infiltration using (c) preformed LAOC and (d) precursors.

### Current and Future Challenges

The particle size of the SEs strongly influences the effective ionic conductivity of the composite electrodes [269]. Even with comparable intrinsic conductivities, smaller particles generally exhibit higher effective conductivities. However, controlling the particle sizes of glassy halide SEs can be challenging. The particle sizes of sulfide SEs can be readily tuned by wet milling or synthesis [270,

271]. By contrast, halide SEs are highly solvent-sensitive and remain unstable even in nonpolar solvents, with  $\text{Li}_3\text{InCl}_6$  being a rare exception [257]. According to the hard and soft acid-base (HSAB) theory, this instability arises from structural units, such as  $\text{AlCl}_3$ ,  $\text{ZrCl}_4$ , and  $\text{TaCl}_5$ , which not only serve as precursors, but can also persist in the products. As harder acids than  $\text{InCl}_3$ , they react more readily with solvents, thereby imparting pronounced solvent sensitivity to glassy halide SEs. Consequently, solution-based methods to control the particle size are impractical. Instead, dry processes, such as jet milling, which have proven to be effective for sulfide SEs [272], may also be applicable to halide SEs.

The air stability of amorphous halide SEs can be expected to be lower than that of conventional crystalline halides. According to the HSAB theory,  $\text{Al}^{3+}$ ,  $\text{Zr}^{4+}$ ,  $\text{Ta}^{5+}$ , and  $\text{Ga}^{3+}$  are harder metal cations than  $\text{Y}^{3+}$  and  $\text{In}^{3+}$  [273] and thus exhibit higher reactivity towards moisture. For example, in  $\text{Li}_2\text{ZrCl}_6$ ,  $\text{Zn}^{2+}$  substitution improves the air stability [274], suggesting that incorporating softer metal elements can be effective, albeit with inherent compositional limitations. Alternatively, surface modifications that impede moisture exposure, such as vapor-phase coatings with hydrophobic polymers—for example, fluorinated poly(dimethylsiloxane)—provide a promising approach [275].

Owing to their poor intrinsic reductive stability and limited passivation ability, the direct application of halide SEs to anodes is inherently restricted [257], which can necessitate hybrid configurations with anolytes such as sulfides, oxides, or nitrides. This makes interfacial compatibility a critical consideration in cell design. Kwak *et al.* first reported side reactions at the  $\text{Li}_2\text{ZrCl}_6|\text{LPSCl}$  interface and proposed mitigation through the incorporation of F or O [264]. Rosenbach *et al.* revealed the formation of a resistive  $\text{InS}^-$ -containing layer at the  $\text{Li}_3\text{InCl}_6|\text{LPSCl}$  interface [46], whereas Samanta *et al.* correlated the resistance evolution with the electronegativity of the metal element in halide SEs [276]. Because  $\text{Al}^{3+}$ ,  $\text{Zr}^{4+}$ ,  $\text{Ta}^{5+}$ , and  $\text{Ga}^{3+}$  are more electronegative than  $\text{In}^{3+}$ , amorphous halide SEs are likely to exhibit more pronounced incompatibility with sulfides than with  $\text{Li}_3\text{InCl}_6$ .

Beyond sulfides, attention has recently been extended to “irreducible” SEs with ionic conductivities of approximately  $1 \text{ mS cm}^{-1}$ , which can be paired with halides to enable stable cycling with Li metal anodes [277, 278]. As the name suggests, these materials are composed of anions such as  $\text{F}^-$ ,  $\text{O}^{2-}$ ,  $\text{OH}^-$ , and  $\text{N}^{3-}$ , which cannot be further reduced. Shen *et al.* reported that at the  $\text{Li}_3\text{OCl}|\text{Li}_3\text{InCl}_6$  interface, a  $\text{LiInO}_2$ -containing passivation layer forms [279], enabling the stable operation of full cells with Li metal anodes. More recently, the concept of “dynamic” reductive stability has been proposed for  $\text{Li}_3\text{YCl}_6$  and  $\text{Li}_3\text{YCl}_3\text{Br}_3$ , with stability extending down to 0.2 V (vs.  $\text{Li}^+/\text{Li}$ ) [100]. Although still insufficient for the direct use of Li metal, this finding demonstrates the feasibility of pairing halide SEs with alternative high-capacity phosphorus anodes, thereby highlighting potential paths towards high-energy all-halide ASSBs.

## Conclusion and Future Perspectives

In summary, glass/glass-ceramic SEs represent a unique class of materials exhibiting higher ionic conductivities than their crystalline counterparts. Among these, halide-based systems are promising candidates because of their superior conductivity and ductility, which are enabled by their compositional, structural, and processing flexibility. Nevertheless, several problems must be addressed for their practical implementation:

- (1) Severe solvent incompatibility necessitates solvent-free particle size control, via jet milling for example, to enhance effective ionic transport in composite electrodes.
- (2) Poor air stability requires compositional tuning or surface modifications to ensure compatibility with dry-room processing.
- (3) Cell-level strategies—including hybrid stacking with different SEs and the adoption of alternative anodes—must be further developed.

1 In the long term, establishing fundamental correlations between the building-unit  
2 distribution/connectivity and ionic, mechanical, and chemical properties could transform the structure-  
3 property relationships into predictive design tools, accelerating rational compositional screening. With  
4 these advances, glassy halide SEs could emerge as key enablers of high-energy and high-power ASSBs.  
5  
6  
7

### 8 **Acknowledgment**

9 This work was supported by the National Research Foundation of Korea (NRF) grant funded by  
10 the Korea government (MSIT) (No. RS-2024-00343349) and by the Human Resources Development  
11 Program (No. 20214000000320) of the Korea Institute of Energy Technology Evaluation and Planning  
12 (KETEP), funded by the Ministry of Trade, Industry, and Energy of the Korean government.  
13  
14  
15

### 16 **Conflict of Interest**

17 The authors declare no conflict of interest.  
18  
19  
20  
21  
22  
23  
24  
25  
26  
27  
28  
29  
30  
31  
32  
33  
34  
35  
36  
37  
38  
39  
40  
41  
42  
43  
44  
45  
46  
47  
48  
49  
50  
51  
52  
53  
54  
55  
56  
57  
58  
59  
60

## 9. Redox-active solid electrolytes

Jingui Yang<sup>1</sup>, Siyuan Guo<sup>1</sup>, Torsten Brezesinski<sup>1</sup> and Florian Strauss<sup>1,\*</sup>

<sup>1</sup> Institute of Nanotechnology, Karlsruhe Institute of Technology (KIT), Kaiserstr. 12, 76131 Karlsruhe, Germany.

\*E-mail: [florian.strauss@kit.edu](mailto:florian.strauss@kit.edu)

### Status

Solid electrolytes (SEs) are indispensable components of solid-state batteries (SSBs) because they determine ion transport and play an important role in interfacial stability. Ideally, SEs should combine superionic conductivity with high (electro)chemical stability towards both cathode and anode across the entire operating voltage range. However, modern SEs, including sulfide-, halide-, and polymer-based materials, are not electrochemically inert. Instead, they often exhibit intrinsic redox activity that triggers parasitic reactions at the interface between electrolyte and the other electrode components. These interfacial processes are usually only partially reversible and often lead to the formation of resistive interphases that block charge transfer and ultimately limit long-term cycling stability [280].

Previous research efforts have largely focused on mitigating such adverse side reactions. Common strategies include applying protective surface coatings to electrode materials, substituting elements in the SEs to expand their (electro)chemical stability window, or developing dual-electrolyte architectures to decouple cathode and anode chemistry [281–283]. These approaches are based on the long-standing paradigm of the necessity of having an inert SE, viewing it as a passive cell component whose only function is to enable fast ion transport between the active materials. However, this paradigm has recently been called into question. In fact, there is growing evidence that redox activity in SEs may not necessarily be detrimental. Under some circumstances, the intrinsic redox processes can be exploited in a reversible manner, thereby providing additional capacity for the battery. This paradigm shift defines SEs no longer as passive components, but as functional materials that directly contribute to the cell performance.

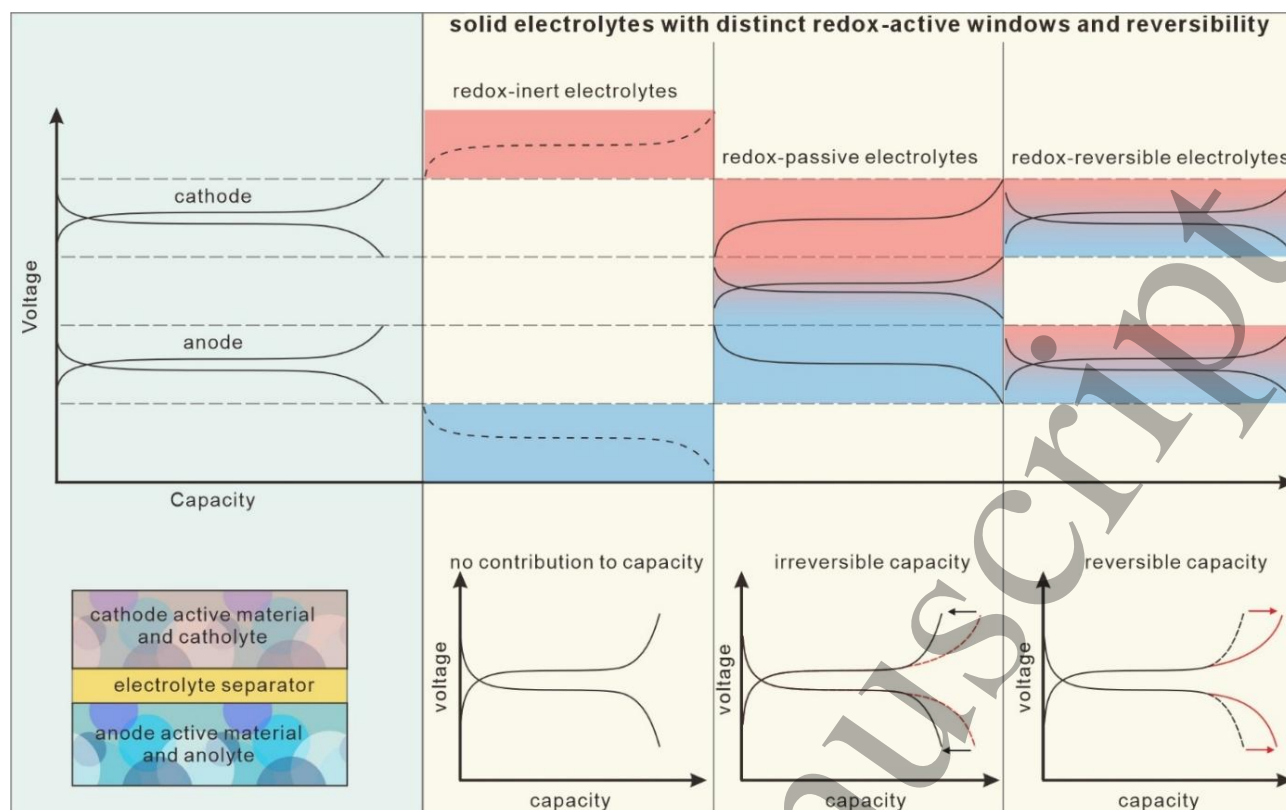


**Figure 14.** Classification of SEs for SSBs: redox-inert materials only provide ion conduction; redox-passive materials decompose irreversibly and only contribute to capacity over the first few cycles; and redox-reversible materials align reversible redox reactions with electrode potentials, adding reversible capacity and increasing the specific energy.

As illustrated in **Figure 14**, SEs can be classified according to their redox behavior. Redox-inert SEs have a wide electrochemical stability window, with the anodic and cathodic limits lying beyond the working potential of the active materials and thus contributing no additional capacity. Redox-passive SEs undergo redox processes within the operating voltage range. However, these reactions are either irreversible or, if reversible in nature, occur at potentials that do not overlap with those of the active materials. In contrast, redox-reversible SEs exhibit redox activity in the working potential ranges of the active materials, enabling them to participate in reversible charge storage. Such materials not only provide ion conduction, but also contribute to additional capacity, thereby increasing the specific energy on a cell level. This classification invites a more comprehensive rethinking of the functionality of SEs.

In the following sections, we highlight recent advances in sulfide- and halide-based redox-active SEs for lithium-sulfur and lithium-ion batteries. However, the general design strategies are also promising for extension to post-Li systems.

### Current and Future Challenges

Sulfide SEs have attracted great attention due to their exceptionally high ionic conductivities at room temperature. However, their electrochemical stability windows are relatively narrow [6]. On the cathode side, oxidative stability is limited by the sulfur chemistry:  $S^{2-}$  anions are prone to oxidation at relatively low potentials. On the anode side, reductive stability is defined by the reduction of framework cations, such as  $P^{5+}$ ,  $Ge^{4+}$  or  $Si^{4+}$ , depending on the specific composition. In combination with high-voltage (intercalation) cathodes, sulfide SEs often behave as redox passive. They undergo irreversible decomposition into polysulfides and/or elemental sulfur and other poorly conductive

species that impede lithium transport and accelerate impedance growth [284]. Despite this apparent instability, recent studies have shown that sulfur redox can be reversible in sulfide SEs [285]. In solid-state lithium-sulfur batteries (SSLSBs), sulfide SEs are actively involved in redox processes and contribute significantly to reversible capacity. Interestingly, several systems were found to deliver capacities that exceed the theoretical limit of sulfur alone [286, 287]. This is because, in these cases, the sulfide SEs act not only as passive ion conductors but also as an additional electrochemically active phase. Building on this insight, the introduction of new redox-reversible chemistries offers a promising strategy for overcoming the sluggish sulfur conversion that limits SSLSBs. An effective approach is the incorporation of iodine species [288]. With a redox potential that is slightly higher than that of sulfur but overlaps strongly and with intrinsically faster kinetics, iodine can act as a redox mediator, thereby accelerating sulfur conversion, especially during charging, and enabling SSLSBs to compete with or even outperform liquid-electrolyte-based counterparts. Such a targeted design thus opens up new avenues for improving battery performance. However, the advantageous redox activity comes with tradeoffs. It inevitably involves structural and morphological changes which can negatively affect ionic conductivity and add to the overall volume changes in the composite electrode. These problems are particularly serious in lithium-sulfur battery systems, where sulfur undergoes a volume expansion of about 80% upon lithiation ( $\text{Li}_2\text{S}$  formation) and the different species suffer from inherently low electronic conductivities. Overall, these effects accelerate mechanical degradation, interfacial instability, and capacity loss, highlighting the delicate balance between exploiting redox activity and maintaining long-term cycling stability.

Halide SEs typically have a much higher anodic stability because their oxidation chemistry is determined by halide anions rather than  $\text{S}^{2-}$ . In general, the high oxidative stability makes halides particularly attractive as catholytes for high-voltage oxide cathodes. However, due to the presence of transition metal cations that tend to undergo reduction, they generally exhibit poor cathodic (reductive) stability [289]. Interestingly, unlike sulfide SEs, which undergo conversion reactions, halide SEs exhibit (de)lithiation behavior. The latter is expected to offer better reversibility and have fewer negative effects on ionic conductivity, as their structural framework remains intact [100, 290]. Fe-based halides, such as  $\text{Li}_{2.9}\text{Fe}_{0.9}\text{Zr}_{0.1}\text{Cl}_6$  and  $\text{Li}_{1.3}\text{Fe}_{1.2}\text{Cl}_4$ , utilize the  $\text{Fe}^{2+}/\text{Fe}^{3+}$  redox couple with an average potential of  $\sim 3.6$  V vs.  $\text{Li}^+/\text{Li}$  and can be combined with various cathode active materials, including  $\text{LiCoO}_2$  and layered Ni-rich oxides [291, 292]. Notably,  $\text{Li}_{1.3}\text{Fe}_{1.2}\text{Cl}_4$  was found to also show promising properties as an all-in-one material (catholyte and cathode active material) for SSBs [291]. Other transition metal halides further enrich the available redox chemistry.  $\text{Li}_3\text{VCl}_6$  operates with the  $\text{V}^{2+}/\text{V}^{3+}$  redox couple at  $\sim 3.06$  V, delivers an intrinsic specific capacity of  $\sim 80$  mAh  $\text{g}^{-1}$ , and shows good compatibility with  $\text{LiFePO}_4$  cathodes [290].  $\text{Li}_3\text{TiCl}_6$  stands out for its dual redox activity, combining  $\text{Ti}^{3+}/\text{Ti}^{4+}$  at 3.62 V and  $\text{Ti}^{2+}/\text{Ti}^{3+}$  at 1.86 V [293]. Halide SEs have also proven to be promising redox-reversible anolyte materials. For example,  $\text{Li}_3\text{YCl}_3\text{Br}_3$  (with  $\text{Y}^{3+}/\text{Y}^{2+}/\text{Y}^+$  redox) exhibits a dynamic stability window with a lower limit of about 0.2 V vs.  $\text{Li}^+/\text{Li}$  and is compatible with red phosphorus anodes [100]. Similar design strategies have also been extended to various sodium systems and show promising results [294, 295]. Despite this progress, and although it is assumed that the (de)lithiation behavior of halide SEs has less of an impact on their transport properties than conversion reactions, significant fluctuations in ionic conductivity were observed at different states of charge [100, 292]. Since halides already have lower conductivities than common liquid electrolytes, this dependence could become a major obstacle to practical SSB operation. In addition, they also undergo volume changes during battery operation, which compromises the electrode integrity over time.

## Conclusion and Future Perspectives

Redox activity in SEs, long considered a disadvantage, is increasingly recognized as an opportunity. With suitable anode/cathode combinations, redox-active SEs can directly contribute to electrode capacity and thus improve energy density. Due to their shared chemistry with lithium-sulfur battery systems, sulfides are natural candidates for redox-reversible catholytes. The incorporation of

iodine or other redox mediators offers a promising way to overcome sluggish sulfur kinetics and boost performance. In halides, the stable anion framework enables reversible redox activity of transition metal species, making them attractive for high-voltage cathode applications. However, to exploit the potential of redox-reversible SEs, several key challenges must be overcome:

- (1) The redox behavior of SEs is still poorly understood. In the case of sulfides, there is a considerable discrepancy between experimentally and theoretically determined stability windows [57]. While this has often been attributed to kinetic effects, a recent study suggests that sulfides degrade via indirect pathways involving initial (de)lithiation followed by thermodynamic decomposition [296]. *In situ* spectroscopic and electrochemical probes will be essential for elucidating these mechanisms and will enable the rational design of redox-reversible SEs.
- (2) The ionic conductivity in redox-reversible SEs is not stable but evolves with the state of charge, i.e., the redox behavior, and often decreases upon decomposition. This increases the internal resistance, reduces the utilization of active material, and limits rate capability. Future work should focus on the coupled transport of ions and electrons across complex electrode|electrolyte interfaces while optimizing the electrode's microstructure to maximize both the capacity contribution from the electrolyte and the ionic conduction.
- (3) Redox-active SEs are subjected to volume changes during battery operation. Together with the expansion/contraction of the active material, this increases mechanical stress and accelerates degradation. Mitigation strategies could include combining them with active materials exhibiting the opposite volume change behavior to compensate for dimensional fluctuations. Furthermore, current findings suggest that state-of-charge-dependent SE softening could enable self-healing mechanisms [291]. Exploiting this behavior may open up a new dimension in electrolyte design.

In summary, embracing rather than avoiding redox activity in SEs could reshape the future of SSBs. By combining mechanistic insights with strategic materials design, redox-reversible SEs promise higher energy density, improved cycling stability, and major advances in next-generation batteries.

### Acknowledgment

J.Y. and F.S. are grateful to the German Federal Ministry of Research, Technology and Space (BMFTR) for funding within the project MELLi (03XP0447). S.G. and F.S. acknowledge the financial support from the Innovation Pool Automat, a project within the Helmholtz Research Program "Materials and Technologies for the Energy Transition (MTET), Topic 2: "Electrochemical Energy Storage".

### Conflict of Interest

The authors declare no conflict of interest.

## 10. Processing/large-scale manufacturing

Shuo Wang<sup>1,\*</sup> and Shu-Bo Wang<sup>1</sup>

<sup>1</sup> School of Materials Science and Engineering, Wuhan University of Technology, Wuhan 430070, China.

\*E-mail: shuowang@whut.edu.cn

### Status

The preparation processes play a pivotal role in tailoring the crystal structure and ionic conductivity of solid electrolytes. In this chapter, the manufacturing methods for polymer, oxide, sulfide, and halide solid electrolytes, and composite electrolyte membranes are discussed (**Figure 15**), and their merits and drawbacks are analyzed. A roadmap for future advancements in the manufacturing processes is also provided.

### Current and Future Challenges

For polymer electrolytes, the typical processing technique is the solution-casting method. First of all, the lithium salt is dissolved in a polar solvent, followed by the dissolution of the polymer. Then, the homogeneous solution is cast onto a substrate and evaporated to yield a freestanding polymer solid electrolyte film [297]. This method is straightforward and amenable to large-scale continuous production. However, the utilization of toxic organic solvents raises environmental and safety concerns. Alternatively, for thermoplastic polymers, such as polyethylene oxide (PEO), a solvent-free approach has been employed. This method typically involves dry mixing of PEO and lithium salt powders—via ball milling or manual grinding—followed by hot-pressing into a dense composite electrolyte film. This dry-processing method eliminates the utilization of toxic solvents, making it more environmentally benign and time-efficient [298]. Nevertheless, it faces challenges in achieving continuous manufacturing compared to solution-casting processes.

For oxide solid electrolytes, the conventional solid-state reaction method is widely employed. A typical synthesis involves stoichiometric weighing of precursor powders, such as  $\text{Li}_2\text{O}$ ,  $\text{La}_2\text{O}_3$ ,  $\text{ZrO}_2$ , and  $\text{Ta}_2\text{O}_5$ , with excess lithium salt to compensate for volatilization during high-temperature treatment. Then, the mixture is thoroughly homogenized via manual grinding or wet ball milling, followed by calcination in an alumina crucible at approximately  $950\text{ }^\circ\text{C}$  for 8 h. The resulting product is then re-ground, pressed into pellets, and sintered at  $1150\text{--}1200\text{ }^\circ\text{C}$  to obtain dense  $\text{Li}_{6.8}\text{La}_3\text{Zr}_{1.8}\text{Ta}_{0.2}\text{O}_{12}$  (LLZTO) ceramics, which typically exhibit a high ionic conductivity of  $0.9\text{ mS cm}^{-1}$  [299]. Similar procedures could also be used for the preparation of  $\text{Na}_3\text{Zr}_2\text{Si}_2\text{PO}_{12}$  SEs.

Sulfide or halide solid electrolytes are highly sensitive to moisture, resulting in the degradation of ionic conductivity [300]. Therefore, they are typically synthesized and manufactured under an inert atmosphere. Based on their crystal structure, they can be broadly categorized into three primary types: glassy, glass-ceramic, and crystalline [19]. Glassy sulfides are primarily synthesized via melt-quenching or high-energy ball milling. The melt-quenching process involves the following steps: initially, the precursors, such as  $\text{Li}_2\text{S}$ ,  $\text{P}_2\text{S}_5$ , and  $\text{B}_2\text{S}_3$ , are dry mixed and then pressed into pellets. Subsequently, the pellets are put into a carbon-coated quartz tube and heated to the molten state, followed by rapid cooling in ice water or liquid nitrogen to obtain glassy sulfide electrolytes with room-temperature ionic conductivities of approximately  $0.1\text{--}1\text{ mS cm}^{-1}$  [301]. However, this method is complex, time-consuming, and energy-intensive. Notably, the successful preparation of purely glassy halide electrolytes via melt-quenching has not been reported to date.

High-energy ball milling is a popular technique for amorphizing sulfide or halide electrolytes through mechanical collisions at high rotational speeds, which produce substantial heat and facilitate the formation of glassy solid electrolytes. The rotational speed and duration of ball milling significantly influence the phase composition and crystallinity of the final product. Only higher speeds promote the formation of glassy phases [302]. For example, ball milling a mixture of  $\text{Li}_2\text{S}$  and  $\text{P}_2\text{S}_5$  in a 70:30 molar ratio at 500 rpm for 24 h yields the glassy  $70\text{Li}_2\text{S}\cdot 30\text{P}_2\text{S}_5$  sulfide electrolyte [19, 303]. Similarly, glassy  $\text{LiTaCl}_6$  halide electrolyte can also be obtained via high-energy ball milling [194]. Subsequent heat treatment of the glassy  $70\text{Li}_2\text{S}\cdot 30\text{P}_2\text{S}_5$  intermediates can produce glass-ceramic electrolytes containing  $\text{P}_2\text{S}_7^{4-}$  or  $\text{PS}_4^{3-}$  groups [303]. However, the ball milling method suffers from poor batch-to-batch consistency, material adherence to container walls, time consumption, and limited scalability due to equipment size constraints.

The solid-state reaction method is commonly used for preparing crystalline sulfide solid electrolytes. The precursors are typically dry-mixed, pressed into pellets, sealed in a vacuum tube, and then annealed at high temperature to obtain crystalline materials, such as  $\text{Li}_6\text{PS}_5\text{Cl}$  ( $3.4 \text{ mS cm}^{-1}$ ) [287],  $\text{Li}_{5.5}\text{PS}_{4.5}\text{Cl}_{1.5}$  ( $8.4 \text{ mS cm}^{-1}$ ) [304],  $\text{Li}_{5.5}\text{PS}_{4.5}\text{Cl}_{0.8}\text{Br}_{0.7}$  ( $9.6 \text{ mS cm}^{-1}$ ) [305], and  $\text{Li}_2\text{In}_{1/3}\text{Sc}_{1/3}\text{Cl}_4$  ( $2 \text{ mS cm}^{-1}$ ) [306]. However, the high cost and the size of quartz tubes impede large-scale production. Recently, Wang *et al.* reported a scalable synthesis strategy for sulfide solid electrolytes, specifically LPSCB with a high ionic conductivity of  $13 \text{ mS cm}^{-1}$ , based on rapid mixing followed by heat treatment. This process enables the reproducible production of kg-scale batches and offers notable advantages in simplicity, making it suitable for mass production [56].

The liquid-phase method is also widely used for synthesizing sulfide/halide electrolytes. Preparation details are as follows. To begin with, the precursors are dissolved in a solvent. Then, the solvent is heated, stirred to facilitate reaction, followed by evaporation to yield an intermediate product. Finally, this intermediate is annealed to obtain the final solid electrolyte [307]. Notably, this method enables the synthesis of some solid electrolytes that are challenging to be prepared via traditional solid-state reaction routes, such as  $\text{Li}_7\text{P}_2\text{S}_8\text{I}$  and  $0.6\text{LiI}\cdot 0.4\text{Li}_4\text{SnS}_4$  [308]. Similarly, halide electrolytes like  $\text{Li}_3\text{InCl}_6$  can be prepared by reacting  $\text{LiCl}$  and  $\text{InCl}_3$  in water, followed by heat treatment at  $200 \text{ }^\circ\text{C}$  for 4 h under vacuum [66]. Additionally, using  $\text{NH}_4\text{Cl}$  solutions, intermediates such as  $(\text{NH}_4)_3[\text{MCl}_6]$  ( $\text{M} = \text{Y}, \text{Sc}, \text{Er}$ ) can be obtained, which are subsequently converted to  $\text{Li}_3\text{MCl}_6$  halide electrolytes [309].

Composite solid electrolytes are generally classified into two main categories: polymer-based composites incorporating inorganic fillers and inorganic-based composites with polymer additives. For polymer-based composite electrolytes, lithium salts and polymers are typically dissolved in a solvent. Then, a small amount of inorganic ceramic powder, such as inert  $\text{Al}_2\text{O}_3$  or ion-conductive oxide, sulfide, or halide electrolytes, is added to the solvent and stirred to achieve uniform dispersion. Finally, the slurry is tape-cast and dried to produce a polymer-based composite electrolyte membrane. Currently, the ionic conductivity is relatively low, typically ranging from  $0.1$  to  $1 \text{ mS cm}^{-1}$  [310]. For inorganic-based composite electrolyte membranes, the binder is first dissolved in a solvent, followed by the addition of a high fraction ( $\geq 80 \text{ wt}\%$ ) of inorganic solid electrolyte. The mixture is then tape-cast and dried to obtain the inorganic-based composite electrolyte films [311]. However, sulfide electrolytes are particularly sensitive to polar solvents and often undergo deleterious decompositions, significantly degrading ionic conductivity. Even in weakly polar or non-polar solvents, the ionic conductivity of  $\text{Li}_{5.5}\text{PS}_{4.5}\text{Cl}_{1.5}$  decreases from  $10$  to  $6 \text{ mS cm}^{-1}$ . Based on the  $\text{Li}_{5.5}\text{PS}_{4.5}\text{Cl}_{1.5}$  electrolyte, the ionic conductivity of the composite electrolyte film is typically around  $1\text{--}3 \text{ mS cm}^{-1}$  [311].

To mitigate the conductivity loss of sulfide electrolytes during wet-film processing, dry-film processing techniques have attracted increasing attention. This method typically involves dry-mixing inorganic solid electrolytes with polytetrafluoroethylene (PTFE) binder, followed by thermal rolling to fibrillate the PTFE, thereby forming a composite electrolyte membrane [312]. For example,  $\text{Li}_{5.4}\text{PS}_{4.4}\text{Cl}_{1.6}$  was dry mixed with PTFE to obtain a composite film with a high ionic conductivity of  $8.4 \text{ mS cm}^{-1}$  [312]. Owing to the instability of halide electrolytes in solvents, even in non-polar solvents such as p-xylene, they will decompose, resulting in very low conductivity. Hence, halide-based composite membranes are also commonly fabricated using PTFE as binder via a dry process,

such as  $\text{Li}_3\text{InCl}_6$ -PTFE composite electrolyte membrane ( $1 \text{ mS cm}^{-1}$ ) [313]. However, PTFE-based composite membranes exhibit poor stability against lithium metal and are prone to decomposition that causes a sharp increase in electronic conductivity, leading to battery failure [312].

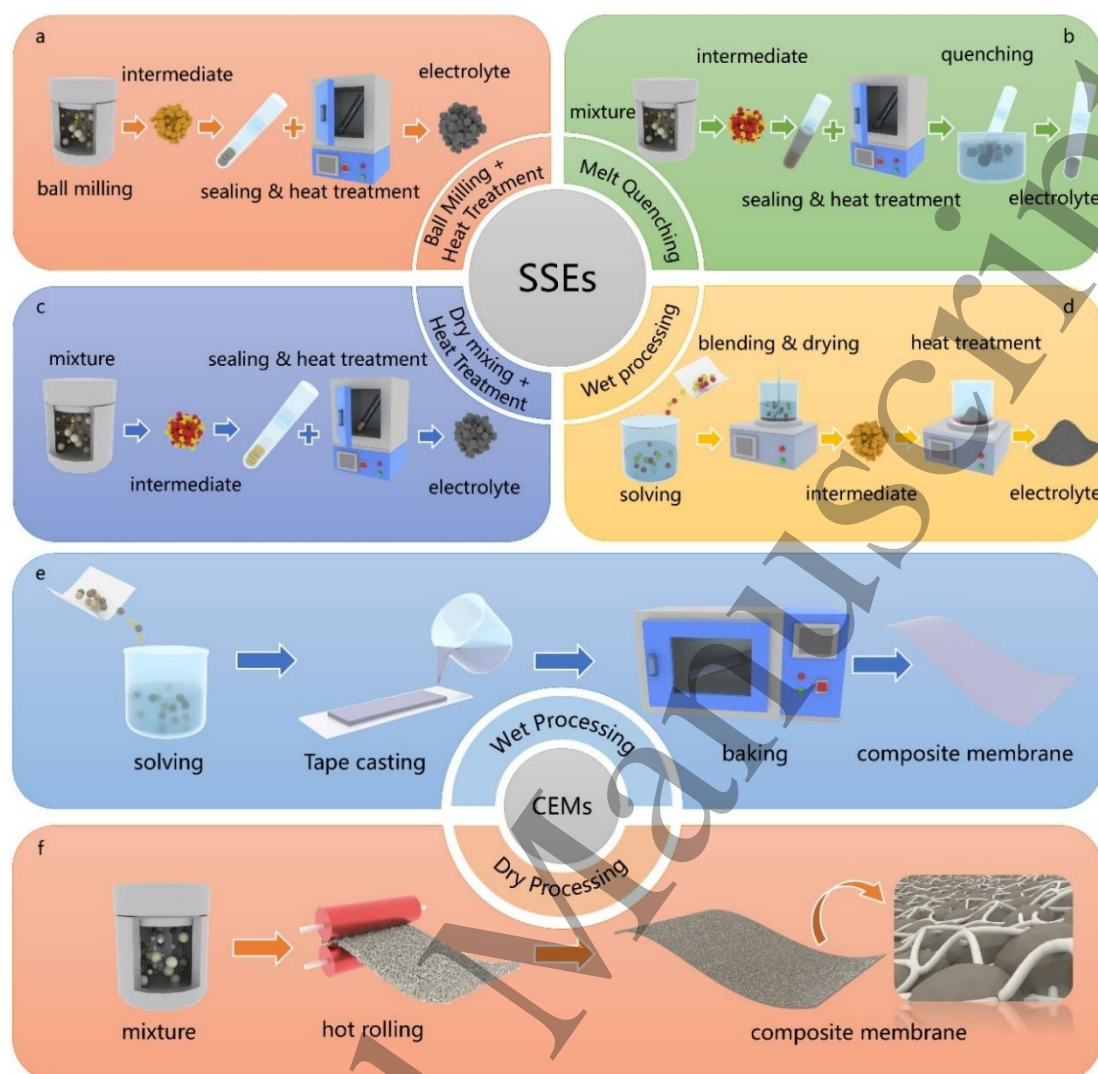


**Figure 15.** Preparation methods of solid electrolytes, including (a) ball milling followed by heat-treatment, (b) melt quenching, (c) dry mixing followed by heat-treatment, and (d) wet processing, and processing methods of composite electrolyte membranes, including (e) wet and (f) dry processing.

## Conclusion and Future Perspectives

For the manufacturing of inorganic ceramic solid electrolytes, the solid-state high-temperature reaction method is more suitable for large-scale industrial production. In the future, more efforts should focus on optimizing the particle size distribution of solid electrolytes. The synthesis of ultrafine powder with particle size distributions ranging from tens to hundreds of nanometers is of great significance for increasing the active material loading and effective ionic conductivity in the composite cathodes. Due to limitations in ball-milling capacity and the size of quartz tubes, developing new scalable production technologies for glass-type sulfide electrolytes is also essential. For sulfide-based composite electrolyte membranes, future work should prioritize optimizing the type and content of binders to enhance mechanical strength, reduce thickness, and maintain high room-temperature ionic conductivity. Regarding halide-based composite membranes, improving the solvent resistance of halides and selecting appropriate solvents are critical for enabling the large-scale, liquid-phase processing of halide-based composite films.

1  
2  
3 **Acknowledgment**

4 S.W. acknowledges the Natural Science Foundation of China (grant number 52302305) and  
5 Natural Science Foundation Exploration Program of Wuhan (Morning Light Plan) (grant number  
6 202401jc0089).  
7  
8  
9

10 **Conflict of Interest**

11 The authors declare no competing interests.  
12  
13  
14  
15  
16  
17  
18  
19  
20  
21  
22  
23  
24  
25  
26  
27  
28  
29  
30  
31  
32  
33  
34  
35  
36  
37  
38  
39  
40  
41  
42  
43  
44  
45  
46  
47  
48  
49  
50  
51  
52  
53  
54  
55  
56  
57  
58  
59  
60

# 11. Outlook for high-throughput and machine-learning guided synthesis of solid electrolytes

Eric McCalla<sup>1,\*</sup>

<sup>1</sup> Department of Chemistry, McGill University, Montreal, Canada

\*E-mail: eric.mccalla@mcgill.ca

## Status

High-throughput experiments have long been utilized to optimize various components in modern rechargeable batteries. Early efforts by the Dahn group, for example, focused on thin film anodes where combinatorial sputtering was used to synthesize a variety of materials at once and an electrochemical cell that could test 64 materials simultaneously was used for battery testing [314, 315]. The first efforts to use high-throughput experiments for solid electrolytes also involved thin film synthesis. Here, perovskites were tested as interlayers between the solid electrolyte and the cathode materials [316, 317]. These studies involved the mapping of ionic conductivity across varied compositions, but these were limited to compositions easily explored by thin film deposition techniques and did not consider other necessary properties for solid electrolytes.

The all-solid electrolytes discussed to date in this roadmap have undergone a significant amount of research & development primarily aimed at optimizing ionic conductivity. This has resulted in quite complex compositions (e.g., garnet oxide solid electrolytes are typically 4 metals or more plus oxygen) and thus reside in highly underexplored composition spaces. Furthermore, a very limited amount of research has aimed at systematically screening such materials while determining the multitude of properties required to make a viable solid electrolyte. Thus, it becomes imperative to have accelerated synthesis systems that can make samples by traditional synthesis routes (e.g., solid state, co-precipitation, sol-gel) to not be limited to compositions accessible by thin film deposition techniques. Beyond synthesis, the new workflows must be effective in determining not only ionic conductivity, but also electronic conductivity, electrochemical stability window, chemical stability with metallic anodes, mechanical compatibility with electrodes, etc. Thus, it is essential that all relevant characterization tools must keep up with the synthesis without bottleneck.

The current push towards accelerating solid electrolyte design revolves around a combination of automation and machine-learning (ML) to guide experiments. One finds some systems that are fully automated like the A-lab at Berkeley, but these systems are currently limited to X-ray diffraction [318]. To date, these workflows do not screen electrolyte properties and developing this aspect remains an important objective for fully automated battery material development. By contrast, some semi-automated systems that can screen electrolyte properties have been developed. **Figure 16** illustrates the workflow in the McCalla lab where a researcher is able to synthesize about 1,500 materials per year while determining structures and key electrolyte properties [319, 320]. The group has used this system to develop solid electrolytes for both Li and Na batteries including oxide ceramics, glasses, glass-ceramic composites, and ceramic-ionic liquid composites [320–322]. So far, the throughputs of both approaches (fully and semiautomated) is comparable for moderate group sizes (>10,000 samples/year) [323], though progress is certainly still being made in this regard. In both the fully automated and semiautomated cases, the use of machine-learning is proving highly effective in closing the design loop and reducing the number of samples that need to be made in any given composition space [324].

In this chapter, I focus on further progress required to address challenges encountered in accelerating solid electrolyte development by harnessing both high-throughput experiments and machine-learning to more efficiently explore complex compositions.

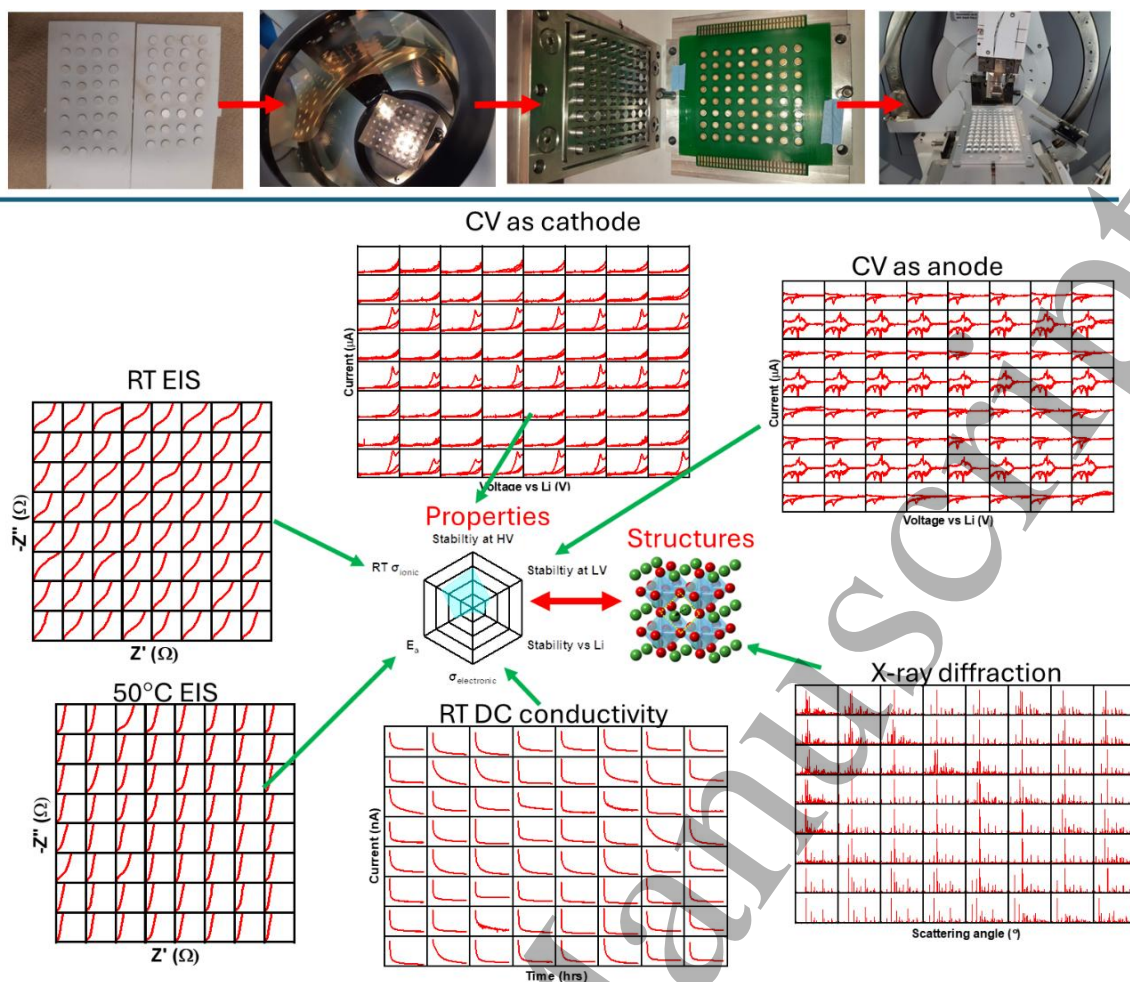


**Figure 16.** Top: pictures of key steps in the combinatorial screening of solid electrolytes showing pellets, gold coating, an EIS cell with spring mounted contacts, and automated X-ray diffraction. Bottom: resulting data used to generate high-throughput radar plots of key electrolyte properties. Adapted from [319], Copyright (2022), with permission from The Electrochemical Society.

## Current and Future Challenges

Both the fully and semi-automated systems discussed in the previous section are currently being used to effectively explore oxide materials. For example, the A-lab has been used to synthesize 41 materials that were previously only studied computationally out of a list of 58 attempted targets [318]. The McCalla lab, by contrast, optimizes previously known materials and has studied the impact of a huge list of dopants (>60) in promising oxide electrolytes [325]. This approach has yielded improvements in the key intrinsic properties needed for solid electrolytes (e.g., ref. [325]). There is also no obvious limit to the level of complexity of the material that can be screened. For example, hybrid ceramic oxide/liquid electrolyte composites are of high current interest in the literature and in industry to yield viable oxide-based electrolytes [326]. Such materials could easily be studied using the methods developed previously for the ceramic-IL composite [322].

Machine-learning algorithms certainly continue to develop, but current tools seem sufficient to dramatically reduce the number of samples that need to be made. Though for cathodes, we have recently been successful in screening triple doping (15 million combinations) with only about 1,000 samples when guided by ML pre-trained on the materials project [327]. This success is, in part, due to the fact that it is acceptable to have numerous failures when each batch of samples contains 64 materials; there is no need for the ML algorithms to be error-free. There is therefore no obstacle to ML being of immediate use to any accelerated experimental platforms. By contrast, when computation/ML are used on their own with only low-throughput experimentation, there is a tendency to narrow down

1 the candidate list extremely aggressively to match the low experimental throughput and the result can  
2 be over-screening (e.g., ref. [279] down selected the candidate list from >20,000 to 1 without  
3 experimental data). There is also a current lack of computational tools to calculate all intrinsic  
4 properties needed to make viable electrolytes.  
5

6 With regards to using the accelerated materials platforms for solid electrolyte development, there  
7 remains two important capabilities that need to be developed. The first is to be able to perform the  
8 syntheses under entirely inert atmospheres. A number of chapters in this roadmap focus on materials  
9 that are inherently unstable in air with even low moisture levels being sufficient to degrade them  
10 rapidly. In such cases, the experimental workflows utilized must be entirely under inert atmosphere.  
11 This is not trivial to implement in high-throughput, but a few groups are in the progress of doing this.  
12 The McCalla group, for example, has connected a tube furnace to a glovebox that has a gold-coater in  
13 it, and this now permits us to make competitive halide materials on the combinatorial scale, though the  
14 throughput is not as high as for the air-stable workflows [328, 329]. There are also efforts underway to  
15 establish an A-lab 2.0 to have an inert atmosphere workflow for fully automated synthesis/XRD  
16 without compromise on throughput [330].  
17

18 The second need for innovation is to be able to test full solid batteries in high-throughput. It is  
19 certainly useful to determine a variety of intrinsic properties, but at some point the electrolyte needs to  
20 be designed with particular cathodes and anodes in mind. Thus, preparation of electrolyte/cathode  
21 composites needs to be developed in high-throughput. Importantly, metallic anodes need to be  
22 deposited from the melt or vapor in such a way to overcome interfacial resistance. This would enable  
23 effective high-throughput critical current density testing (CCD), which to date has not occurred except  
24 on a down-selection of materials [321]. There is also a very important concern regarding  
25 reproducibility here. QuantumScape has recently published a combinatorial study for CCD where they  
26 measured the CCD many times on the same sample by depositing numerous Li contacts by vapor  
27 deposition. The results show a very large variation in the CCD values obtained such that at certain  
28 currents there was only a small fraction of cells that failed; this means that to ensure no failures at a  
29 certain current many measurements must be performed [331]. This raises serious concerns about the  
30 maximum throughput achievable in CCD measurements given that a single measurement on each  
31 sample might be insufficient. Presumably, similar variations would occur in full solid batteries, such  
32 that efforts must be made to develop approaches that either reduce the variability or obtain meaningful  
33 values despite the variability.  
34  
35  
36  
37  
38

## 39 **Conclusion and Future Perspectives**

40 Accelerated testing is enabling broader exploration of potential solid electrolytes, but the  
41 progression towards screening all necessary properties must continue. This will enable rapid  
42 developments in each of oxides, sulfides, halides, hybrids/composites, and other emerging candidates.  
43 Efficiently tuning the properties of promising materials will be enhanced by coupling experiments with  
44 machine-learning. Such workflows are not so costly, especially if automation is only used when  
45 required [323]. This will be especially true moving forward as the cost of automation continues to  
46 decrease. This will lead to a situation where it is no longer a few select labs that can do this, but the  
47 tools will become more widely accessible and enable a greater democratization of high-throughput  
48 research. ML-driven accelerated experimental approaches are poised to become game-changers in  
49 applications such as solid-state batteries where there is a high degree of device complexity.  
50  
51

## 52 **Acknowledgment**

53 The author acknowledges support from the Natural Sciences and Engineering Research Council  
54 of Canada under the auspices of a Discovery Grant.  
55  
56  
57

## 58 **Conflict of Interest**

59 The author declares no conflict of interest.  
60

## 12. Advanced *operando* investigation of solid-state batteries

Benjamin Mercier-Guyon<sup>1</sup>, Ove Korjus<sup>1</sup>, Patrice Perrenot<sup>1</sup> and Claire Villevieille<sup>1,\*</sup>

<sup>1</sup> Université Grenoble Alpes, Université Savoie Mont Blanc, CNRS, Grenoble INP, LEPMI, 38000 Grenoble, France.

\*E-mail: [claire.villevieille@grenoble-inp.fr](mailto:claire.villevieille@grenoble-inp.fr)

### Status

Solid-state batteries are widely regarded as one of the most promising candidates for the next generation of electrochemical energy storage systems. However, realizing this vision requires overcoming several critical challenges, particularly those associated with ionic and electronic transport properties within solid matrices. To accelerate progress in this field, *operando* techniques have emerged as a powerful approach, providing excellent insight into the fundamental processes that govern battery performance. Unlike *ex situ* approaches, which only offer snapshots before or after cycling, *operando*-based investigations allow real-time monitoring of structural, chemical, and mechanical changes occurring within the cell. This capability is essential to identify degradation pathways, interfacial instabilities, and failure mechanisms that ultimately determine device lifetime and efficiency [332, 333]. A wide range of experimental techniques is now available to probe reaction mechanisms in solid-state batteries. These techniques can be broadly classified into two categories. The first encompasses bulk-sensitive methods, such as X-ray and neutron scattering, which provide information on structural evolution, phase transitions, and lattice dynamics within the electrolyte and electrode materials. The second category focuses on microstructural investigations, often achieved through advanced imaging approaches (e.g., tomography, electron microscopy), which reveal morphological changes, grain connectivity, and interfacial degradation at different length scales. Together, these complementary methods enable a multi-scale understanding of transport phenomena and degradation processes, paving the way towards rational design strategies for improved solid-state systems.

*Operando* imaging has emerged as a transformative approach to probe electrochemical systems, enabling a real-time observation of morphological evolutions under realistic operating conditions. By minimizing artifacts typically introduced by sample preparation (mechanical fracture, air exposure) and *post-mortem* cell relaxation, this methodology provides a more accurate and faithful representation of the system's behavior.

*Operando* imaging was primarily confined to synchrotron X-ray facilities, whose high-brilliance sources allow rapid and non-invasive investigation of the majority of battery systems. Despite inherent challenges in detecting lithium with X-rays due to its low electron density, significant studies have successfully captured the formation and growth of lithium dendrites under *operando* conditions, unveiling the origin of short-circuiting in solid-state battery (**Figure 17a, b**) [334, 335]. In contrast, neutron imaging exhibits a remarkable sensitivity to <sup>6</sup>Li and recent advances in brighter neutron sources have enabled *operando* <sup>6</sup>Li tracking and the visualization of lithium concentration evolution. Studies have revealed the ionic network as critical bottlenecks both in separators and in thick solid-state composite electrodes, although the <sup>6</sup>Li spontaneous isotopic diffusion affecting quantification is often overlooked [336, 337]. However, the limited neutron flux currently available excludes 3D *operando* imaging without stopping the cycling and relaxing the system. However, due to the miniaturization of materials within new-generation battery systems, both large-scale facilities lack investigations at the nm range (X-ray synchrotron limited at 50 nm resolution and neutron source at a few μm).

Unlike organic liquid electrolytes, whose formulation had to be modified to the imaging techniques, SSBs enable a realistic and meaningful investigation by electron microscopy. *Operando*

scanning electron microscopy (SEM) [338, 339] and transmission electron microscopy (TEM) [340] have already provided critical insights into interfacial evolution and failure mechanisms. Although *operando* SEM has enabled substantial progress, a major limitation remains: the buried nature of critical electrochemically active interfaces, which are often inaccessible in conventional setups. In this context, *operando* FIB (focused ion beam)-SEM emerges as a promising technique. By uniting advanced electron-based imaging with site-specific milling, FIB-SEM offers the capability to reconstruct 3D morphologies with nanometer resolution while simultaneously probing electrochemically relevant interfaces (**Figure 17c, d**) [341].

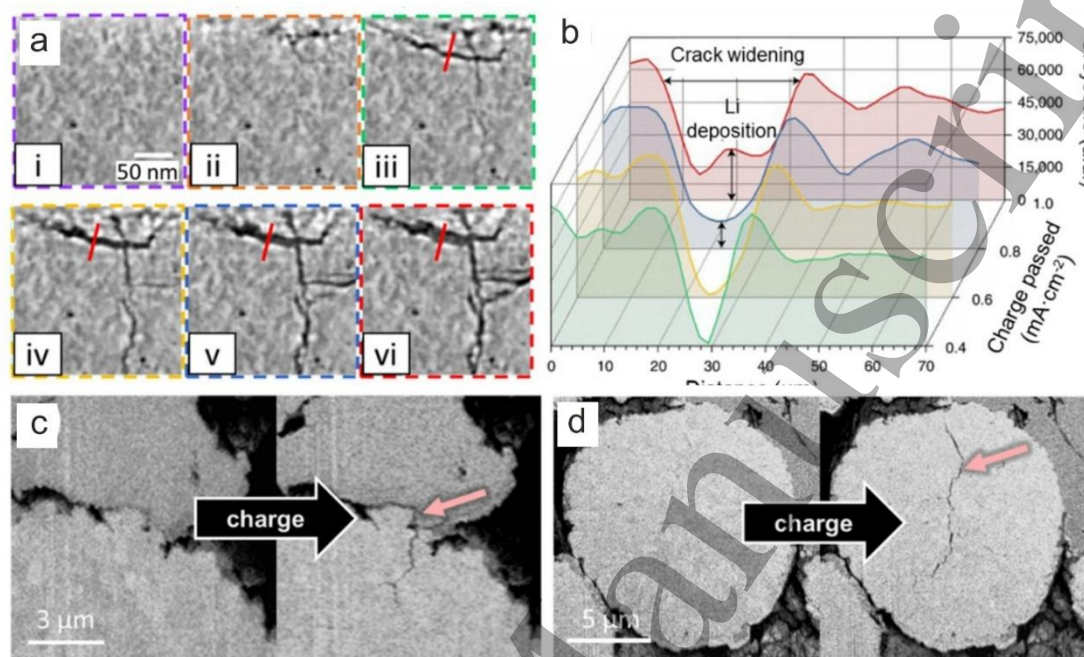


**Figure 17.** (a) *In situ* phase-contrast XCT of virtual cross-sections during a single plating of a Li|Li<sub>6</sub>PS<sub>5</sub>Cl|Li cell and (b) analysis of lithium deposition showing that cracks propagate ahead of Li. Adapted from [335], Copyright (2021), with permission from Springer Nature. *Operando* FIB-SEM cross-section of a composite with NMC622 and amorphous LPS highlighting (c) decohesion of the active material to the ionic network and (d) intergranular fracturing of polycrystalline active material. Adapted from [341], Copyright (2024), with permission from American Chemical Society.

Scattering measurements can help identifying crystalline phase evolution occurring during cycling at the electrolyte and composite electrode levels. Ideally, the measurement should be performed *operando* to ensure that the dynamic of the processes is maintained, giving a real vision of the degradation processes [342–344]. Neutron powder diffraction (NPD) is particularly valuable for studying Li-ion batteries, both *operando* and *ex situ*, because it enables the determination of the positions and site occupancies of light elements, such as lithium. It also allows for clear differentiation between transition metals (e.g., Fe, Ni, Co, Mn), which is often challenging with X-ray diffraction. Numerous *operando* cell designs have been developed for liquid electrolyte systems [345–347], but for solid-state batteries, the cell design is more complex, as it must maintain sufficient pressure to allow cycling of thick electrodes—necessary due to the high mass loading required for neutron measurements. Despite these challenges, this remains a rapidly expanding field, with new solid-state battery cell designs under active development (**Figure 18a**) [343].

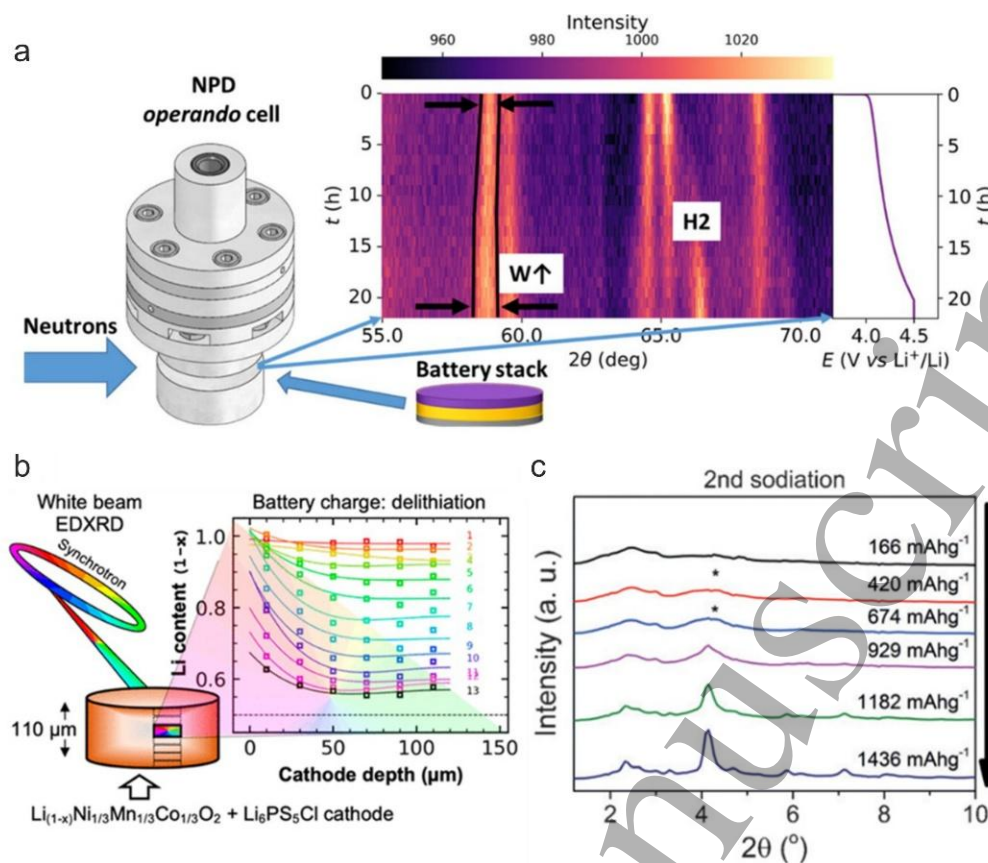


**Figure 18.** (a) *Operando* TiZr NPD during charging of NMC532, showing broadening of NMC reflections and the formation of the H<sub>2</sub> phase. Reproduced from [343], Copyright (2025), with permission from American Chemical Society. (b) Depth-resolved *operando* XRD of an NMC111 electrode at a synchrotron, revealing the development of a de-lithiation gradient. Reproduced from [348]. CC BY 4.0. (c) Reconstructed XRD-CT data from a single voxel (1.2×1.2 μm<sup>2</sup>) in a Na<sub>3</sub>P electrode during *operando* sodiation. The asterisk denotes P nanoparticles. Reproduced from [349], Copyright (2017), with permission from Wiley-VCH GmbH, John Wiley & Sons.

In contrast to neutrons, which have a weak interaction (neutrons/matter), synchrotron X-ray diffraction (s-XRD) offers several advantages for *operando* studies. First, due to its significantly higher flux (compared to neutrons), s-XRD enables measurements on samples with very low mass loading. Second, s-XRD allows for depth profiling, enabling the investigation of inhomogeneities across electrodes during cycling. Several research groups have used this technique to reveal non-uniform lithiation within electrodes and the formation of lithiation gradients during cycling (**Figure 18b**) [348, 350]. Li *et al.* [350] demonstrated that, in thick LiNi<sub>0.8</sub>Mn<sub>0.1</sub>Co<sub>0.1</sub>O<sub>2</sub> (NMC811) electrodes, localized charging can occur even during the electrode discharging process.

Combining techniques, such as three-dimensionally resolved X-ray diffraction computed tomography (XRD-CT) [349, 351, 352] and X-ray micro-diffraction imaging [353, 354], can shed light on novel processes. XRD-CT has already been widely applied, primarily for phase identification and quantification. Multiple *ex situ* XRD-CT studies have been used to investigate decomposition products formed during cycling. For example, Thompson *et al.* [355] demonstrated that LPSCl undergoes partial decomposition throughout the entire electrolyte during cycling, producing LiCl and Li<sub>2</sub>S. Similarly, Hu *et al.* [351] revealed the formation of local stress hotspots in LPSCl electrolytes during both cycling and cell fabrication. Despite these advances, XRD-CT is less frequently employed for full Rietveld refinement in solid-state battery studies due to technique-related artefacts. Furthermore, long measurement times limit its widespread application in *operando* investigations. Sottmann *et al.* [349]

1 conducted *operando* XRD-CT (**Figure 18c**) on liquid sodium-ion batteries, illustrating its potential for  
2 broader application, including future studies on solid-state batteries.  
3  
4

## 5 6 **Current and Future Challenges**

7 Several critical issues must still be addressed before the full potential of advanced  
8 characterization techniques can be exploited for solid-state battery research. The first challenge relates  
9 to the design of the electrochemical cells used in the literature. In the absence of standardized protocols,  
10 it is nearly impossible to make meaningful comparisons between studies [356]. One of the main  
11 sources of discrepancy lies in the applied pressure. Since the pressure applied on the different cell  
12 components is rarely controlled or reported, the observed decomposition pathways and interfacial  
13 reactions can vary drastically from one study to another.  
14  
15

16 Ohno *et al.* highlights this issue comparing ionic conductivities from different research groups  
17 working on the same standardized material [36]. This discrepancy is largely attributed to differences in  
18 measurement setups. Based on these considerations, several groups have proposed innovative  
19 configurations to better control the pressure applied to the stack during measurements and cycling tests.  
20 For example, the study by Chen *et al.* [357] suggests using a liquid medium to apply pressure to the  
21 stack, rather than a solid medium, as is generally the case in compression devices. Lee *et al.* [358] used  
22 a variable-height compression device employing springs. In this way, after the initial pressure is set,  
23 meaning the volume changes in the active material during lithiation and delithiation no longer affect  
24 the pressure on the stack.  
25  
26

27 A second limitation concerns the mass loading of the electrodes employed. In many reports, the  
28 loading is far from realistic values typically required for practical applications. This not only affects  
29 the electrochemical performance of the cell, but can also lead to misinterpretations, for instance,  
30 regarding the presence or absence of concentration gradients within the electrode. The third issue  
31 arises from beam-induced damage during *operando* or *in situ* experiments. High-intensity X-ray or  
32 neutron beams can trigger unwanted side reactions, alter interfacial chemistry, or modify  
33 microstructures, thereby biasing the conclusions drawn from the data. Addressing these limitations  
34 requires the development of new cell designs that combine several key features: controlled and  
35 reproducible pressure application, the use of electrodes with realistic (high) mass loadings, and  
36 mitigation strategies to minimize beam-induced artifacts. Establishing such standardized protocols will  
37 be essential to generate reliable, comparable, and application-relevant insights into the mechanisms  
38 that govern solid-state batteries.  
39  
40  
41  
42

## 43 **Acknowledgment**

44 ANR Grant OpInsolid is acknowledged for the financial support of this work, as well as the PEPR  
45 Batteries, France Relance 20230, Openstorm project.  
46  
47

## 48 **Conflict of Interest**

49 The author declares no conflict of interest.  
50  
51  
52  
53  
54  
55  
56  
57  
58  
59  
60

# 13. NMR as a key to unlocking defect structure and dynamics in emerging solid electrolytes

H. Martin R. Wilkening<sup>1</sup>

<sup>1</sup> Institute of Chemistry and Technology of Materials, Stremayrgasse 9, Graz University of Technology, 8010 Graz, Austria.

\*E-mail: [wilkening@tugraz.at](mailto:wilkening@tugraz.at)

## Status

The solid electrolyte, either as a ceramic or a hybrid material composed of ceramic and polymer, is a central component in all-solid-state and quasi-solid-state batteries, ensuring efficient transport of charge carriers between the two electrochemically active compartments. Nuclear magnetic resonance (NMR) spectroscopy [359, 360] is exceptionally well-suited to investigate local structural environments using high-resolution techniques, such as fast magic angle spinning (MAS). NMR has been employed not only to identify the structural motifs associated with spin-active charge carriers (e.g., <sup>6</sup>Li, <sup>7</sup>Li, <sup>23</sup>Na, <sup>19</sup>F, <sup>17</sup>O), but also to probe the local coordination geometry of framework elements in solid electrolytes (e.g., <sup>31</sup>P, <sup>19</sup>F, <sup>119</sup>Sn, <sup>11</sup>B, <sup>29</sup>Si, <sup>27</sup>Al). Such site-specific information, derived from chemical shifts, anisotropies, and coupling constants, is essential for elucidating both the average and defect structures of emerging (electrolyte) materials [359]. In addition, NMR can detect structural disorder, polymorphs, and local phase heterogeneity, providing insight into how these variations influence ionic mobility and overall electrolyte performance [361]. When combined with complementary methods, such as diffraction and scattering, NMR contributes to a comprehensive understanding of structure-dynamics relationships, which are critical for advancing electrolyte design [27, 362].

To investigate ion dynamics, NMR offers a uniquely versatile set of techniques capable of non-invasively probing ionic motion over an exceptionally broad timescale, spanning, in some cases, more than ten orders of magnitude. **Figure 19** provides an overview of the various NMR methods [363–366] available to quantify both microscopic jump rates and macroscopic diffusion coefficients.

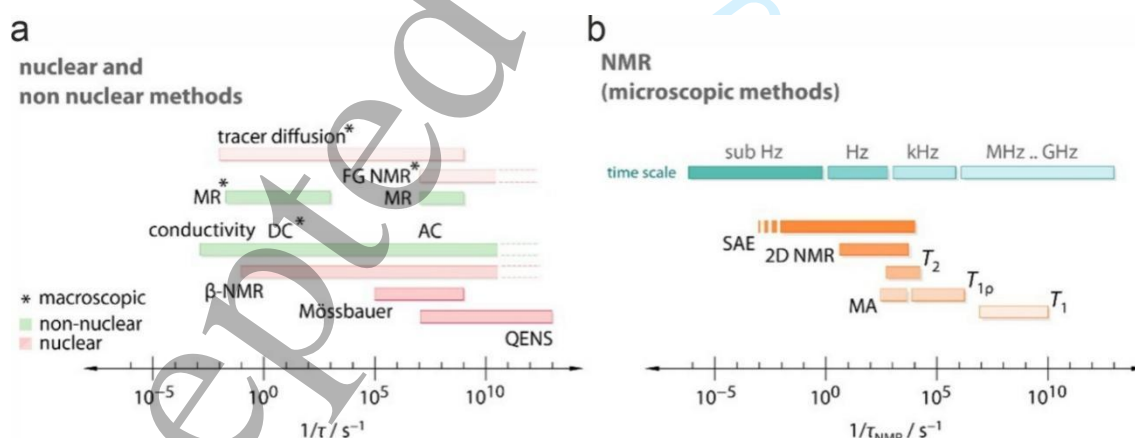


**Figure 19.** (a) Overview of nuclear and non-nuclear methods used to probe diffusion properties, along with the characteristic timescales to which they are sensitive (FG NMR: field-gradient NMR; QENS: quasi-elastic neutron scattering; MR: mechanical relaxation; DC, AC: direct-current and alternating-current measurements). Adapted from [365]. CC BY 4.0. (b) Selected NMR techniques (time-domain and high-resolution 2D NMR) and their respective timescales spanning a dynamic window from the sub-Hz to the GHz regime (SAE: spin-alignment echo NMR; MA: motional averaging of NMR lines;  $T_{1(\rho),2}$  relaxation NMR methods). Adapted from [365]. CC BY 4.0.

These results can be directly compared with dynamic parameters obtained from complementary nuclear and non-nuclear techniques, enabling a comprehensive understanding of ion transport processes. Furthermore, NMR-derived jump rates and site occupancies can serve as benchmarks for computational models and molecular dynamics simulations, providing a quantitative link between experiments and theory [367, 368].

In recent years, time-domain and high-resolution  $^7\text{Li}$  and  $^{23}\text{Na}$  NMR measurements have been employed to investigate sequentially activated diffusion processes in some of the most prominent solid electrolytes, including, e.g., LGPS-type compounds [368], argyrodite materials [362, 365, 369, 370], and LTPS [371]. The results from the latter are exemplarily shown in **Figure 20**. Future studies will aim to deepen our understanding of how local defect structures influence both short-range and long-range ionic dynamics, within the bulk and particularly at interfacial regions, i.e., at the contact zones between the solid electrolyte and the electrochemically active materials.

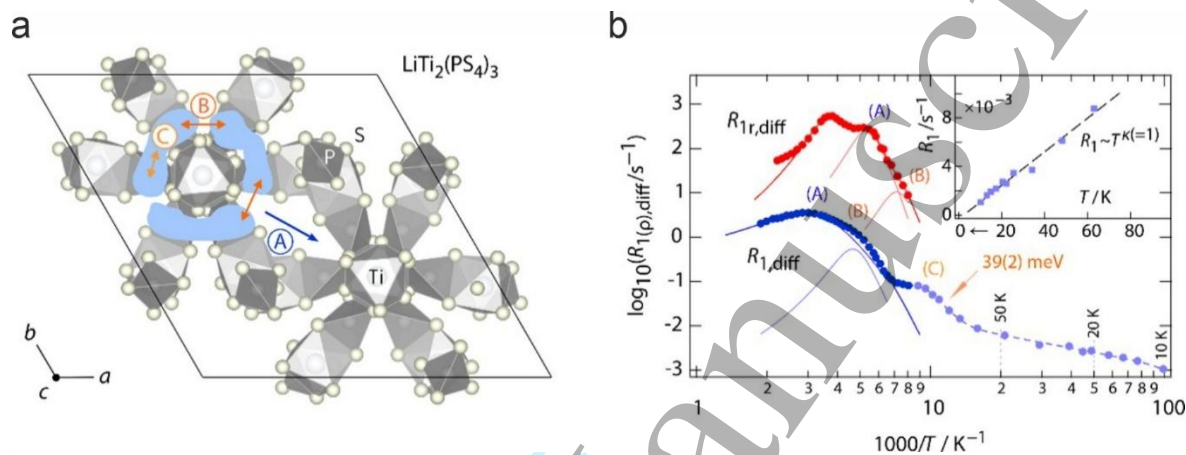


**Figure 20.** (a) Crystal structure of  $\text{LiTi}_2(\text{PS}_4)_3$ , a fast ionic conductor, showing several  $\text{Li}^+$  diffusion pathways: strictly localized motions within pocket-like regions (C), inter-pocket jumps (B), and inter-ring hopping (A). The latter is the rate-determining step that governs long-range ion transport. Adapted from [371]. CC BY 4.0. (b) Using  $^7\text{Li}$  NMR relaxation rate  $R_1 = 1/T_1(1/T)$  measurements, these processes can be studied separately, provided a sufficiently wide temperature range is accessible. For example, fast intra-pocket motions are characterized by an activation energy of only  $0.04 \text{ eV}$  and give rise to peak C, observed at temperatures as low as  $T \approx 100 \text{ K}$ . At even lower temperatures, the relaxation rate enters a regime  $R_1 \sim T^{\kappa=1}$ , where it is dominated by coupling to conduction electrons. Adapted from [371]. CC BY 4.0.

### Current and Future Challenges

The properties of solid electrolytes are highly sensitive to structural, compositional, and processing factors, which can strongly influence both short- and long-range ion transport [372]. Even slight variations in preparation conditions, such as small changes in composition, annealing, or calcination protocols, can strongly affect the transport parameters of a solid electrolyte. Even if long-range transport remains essentially unchanged, the elementary jump processes that govern ion dynamics on shorter length scales may be significantly altered. NMR, depending on the temperature and frequency window chosen for relaxation-rate measurements, can probe both regimes: short-range motions and long-range transport. This makes it a powerful tool to unravel the impact of defect structures that emerge from different preparation conditions [373]. The next step would be to benchmark such findings against commercially available electrolytes to assess their quality in terms of ionic transport properties [374].

In general, the strength of NMR lies in its ability to provide not only average transport parameters, but also site-specific information on dynamic processes [375]. Future studies may therefore apply high-resolution techniques, such as 2D exchange spectroscopy, to identify energetically favored

diffusion steps and exchange mechanisms. For very fast ion conductors, such methods must be carried out at sufficiently low temperatures, as 2D NMR is most sensitive to slow exchange processes. At higher temperatures, coalescence effects may obscure the off-diagonal cross-peaks that encode this site-specific information. A limitation arises from the narrow chemical shift range of  ${}^6\text{Li}$ , the preferred isotope for these experiments since second-order quadrupolar effects are largely suppressed. In diamagnetic materials, this range may be insufficient to resolve the relevant processes. By contrast, in materials containing moderate concentrations of paramagnetic centers [376], hyperfine (Fermi contact) interactions provide enhanced spectral separation, provided that longitudinal relaxation times remain long enough. Such studies require low magnetic fields and fast magic-angle spinning, a combination that has been available for many years. For diamagnetic electrolytes, extending both the frequency and temperature ranges [368] will be crucial to capture the various diffusion steps of charge carriers across different material classes, including oxides, sulfides, thiophosphates, halides, and hydrides [377].

As already noted, understanding degradation processes at macroscopic interfaces in all-solid-state batteries poses a further challenge for NMR spectroscopy. *Operando* and *in situ* studies are often limited by low spin densities in interfacial regions, leading to weak NMR signals. Polarization transfer methods are expected to help overcome this limitation [378]. An early approach is  $\beta$ -NMR, where the polarization of the  ${}^8\text{Li}$  isotope, generated for example after neutron capture, is independent of the Boltzmann factor [379]; other approaches benefit from ion-implanted methods [380, 381]. Similar sensitivity issues arise when studying microscopic interfacial dynamics in hybrid electrolytes [382, 383] that combine polymer and ceramic phases. In these cases, signal-enhanced NMR could provide key insights not only into ion dynamics, but also into the local environments of Li ions at interfaces. Nanocrystalline materials, with their high fraction of interfacial regions (thicknesses on the order of  $\sim 2$  nm), already provide sufficiently high spin densities to be probed by NMR [384–387]. Alternatively, ion dynamics in interfacial regions may be studied by suitable *ex situ* measurements, provided that larger samples can be prepared to mimic *operando* conditions [388].

Finally, care must be taken when interpreting *in situ* or *operando* NMR experiments carried out under strong external magnetic fields [389], as these fields can influence the formation of metallic Li phases compared with cells cycled in zero-field conditions. In such cases, *ex situ* high-resolution measurements, taking into account and overcoming NMR skin effects, remain an indispensable complement.

## Conclusion and Future Perspectives

NMR, widely used in medicine, life sciences, and materials research, is also an indispensable tool in battery science due to the excellent NMR receptivity of key charge carriers, such as  $\text{Li}^+$  and  $\text{Na}^+$ . Their nuclear spin interactions with local magnetic and electric fields enable detailed characterization of atomic-scale structures and dynamic processes. In the study of ion dynamics, future research should move beyond measuring average transport behavior towards probing individual ion hopping events [371]. In particular, the investigation of rotational-translational couplings remains an important research area for fundamentally understanding interrelation effects in electrolytes with polyanion host frameworks [390, 391].

In battery devices, *operando* and *in situ* NMR [378, 392, 393], even under MAS conditions [394], will be crucial for visualizing local structural changes, particularly those associated with degradation mechanisms, and for tracking the corresponding dynamics at interfaces. Importantly, NMR can directly detect the formation of Li metal, enabling monitoring of dendrite growth under operating conditions [395–397]. However, because interfacial regions often contain only a small number of NMR-active nuclei, achieving sufficient signal intensity remains a significant challenge. Advanced methods for enhancing spectral resolution and NMR sensitivity [378, 393] will therefore be essential for future studies aiming to understand the diverse interfacial phenomena in all-solid-state batteries. Emerging NMR approaches [359], such as ultra-fast MAS, multi-nuclear correlation experiments, and especially dynamic nuclear polarization (DNP [393, 397]), are not only expected to enable the study of

1 dilute nuclei at interfaces, but also in low-abundance phases. Combined with time-domain relaxation  
2 rate measurements across broad frequency and temperature ranges [371], these techniques will allow  
3 detailed mapping of ion dynamics over multiple timescales. Together, these advances promise to  
4 extend the reach of NMR, providing deeper insight into both bulk and interfacial transport processes in  
5 solid electrolytes.  
6  
7  
8

### 9 **Acknowledgment**

10 Financial support by the Deutsche Forschungsgemeinschaft (DFG) is highly appreciated [former  
11 research unit 1277 (molife)].  
12  
13  
14

### 15 **Conflict of Interest**

16 The author declares no conflict of interest.  
17  
18  
19  
20  
21  
22  
23  
24  
25  
26  
27  
28  
29  
30  
31  
32  
33  
34  
35  
36  
37  
38  
39  
40  
41  
42  
43  
44  
45  
46  
47  
48  
49  
50  
51  
52  
53  
54  
55  
56  
57  
58  
59  
60

# 14. Recycling of solid electrolytes in solid-state batteries

Kerstin Wissel<sup>1,\*</sup> and Oliver Clemens<sup>1,\*</sup>

<sup>1</sup> University of Stuttgart, Institute for Materials Science, Heisenbergstr. 3, 70569 Stuttgart, Germany

\*E-mail: oliver.clemens@imw.uni-stuttgart.de, kerstin.wissel@imw.unistuttgart.de

## Status

The recycling of solid-state batteries (SSBs) represents a more recent area of research compared to the recycling of conventional lithium-ion batteries (LIBs). Latest studies are beginning to address specific challenges associated with diverse cell formats and material combinations used. SSBs employ solid electrolytes, such as oxides, sulfides, halides, or polymers, and often incorporate lithium metal anodes, which is different from LIBs. These components improve performance; however, they also complicate end-of-life processing because of their reactivity and limited recyclability when applying procedures initially designed for conventional LIBs.

The recycling of conventional LIBs generally utilizes pyrometallurgical and hydrometallurgical methods to recover critical elements (e.g., lithium, cobalt, nickel) [398, 399]. Recovering these metals using pyrometallurgy requires high temperatures and reducing atmospheres. Hydrometallurgical recycling uses aqueous solution chemistry to dissolve battery materials, enabling the selective extraction of individual elements via solvent extraction and precipitation. These processes are effective; however, they are energy-intensive, require complete material decomposition, and involve complex re-synthesis. Direct recycling serves as an alternative approach for the recovery and regeneration of functional battery components; nevertheless, research in this area remains in earlier stages [400]. This approach preserves the structure and chemistry of the original materials, potentially reducing energy consumption and processing cost compared to other strategies. Recycling processes typically involve additional mechanical pretreatment steps for battery disassembly and the separation into recoverable fractions (e.g., black mass, current collectors, housing, etc.).

To adapt these methods for the recycling of SSBs, it is required to address material-specific challenges, specifically the handling of (partially) sensitive SEs and the safe recovery of lithium metal. Mechanical separation is challenging due to strong interfacial bonding (e.g., separation of adhesive lithium metal and (intermixed) SEs from other cell components is not easily possible). Moreover, electrolyte-specific strategies are necessary due to the diverse chemical and physical properties of different SE classes.

Thus far, most research on SSB recycling has been theoretical or conceptual. Experimental studies are scarce and often concentrate on simplified material systems with varying levels of compositional complexity instead of full cells. Consequently, extensive research and development remain necessary to establish scalable, economically viable recycling methods for SSBs.

## Current and Future Challenges

Despite recent progress in developing recycling strategies for SSBs, numerous significant challenges persist that hinder the implementation of these strategies. The next section addresses these challenges and introduces strategies related to different types of SEs. In addition, future challenges are discussed (Figure 21).

For oxidic SSBs based on, for example, garnet-type (e.g.,  $\text{Li}_7\text{La}_3\text{Zr}_2\text{O}_{12}$ ), NASICON-type (e.g.,  $\text{Li}_{1+x}\text{Al}_x\text{Ti}_{2-x}(\text{PO}_4)_3$ ), or perovskite-type (e.g.,  $\text{Li}_{3-x}\text{La}_{2/3-x}\text{TiO}_3$ ) SEs, pyrometallurgical processes are only partially suitable, as they may cause redistribution of chemical elements and formation of undesired, thermodynamically stable phases, particularly when dealing with complex material

1 mixtures of different electrolytes and electrode materials [401]. Hydrometallurgical approaches  
2 possess greater potential and are also essential for further processing of slags produced during  
3 pyrometallurgy. Materials can be either completely or selectively dissolved [402, 403]. Lithium can be  
4 recovered, for example, by supercritical CO<sub>2</sub> extraction [404]. Direct recycling methods for relithiation  
5 may be based on solid-state reactions or hydrothermal processes [405].

6  
7 The main challenge in recycling SSBs utilizing sulfides and thiophosphates as SEs is that they are  
8 instable upon exposure to air or humidity. To mitigate safety hazards and prevent electrolyte  
9 degradation, handling in dry rooms or under inert atmospheres is required. Consequently,  
10 pyrometallurgical and hydrometallurgical processes are unsuitable. However, due to their high  
11 solubility in organic solvents, solvent-based separation methods, including dissolution followed by  
12 recrystallization, are a promising alternative. This strategy has been investigated for separating  
13 argyrodite-type Li<sub>6</sub>PS<sub>5</sub>X (X = Cl, Br, I) [406, 407] and β-Li<sub>3</sub>PS<sub>4</sub> [408] from different transition metal  
14 oxide electrode materials using solvents such as ethanol and N-methylformamide. The dissolved  
15 electrolytes may chemically interact with other components of the battery, particularly electrode active  
16 materials [407, 408]. This suggests that the electrode materials may require further purification or  
17 treatment via hydrometallurgy. Further investigations are required to determine the compatibility of  
18 these solvent-based methods when using lithium metal. Solvent-based methods, as well as thermal and  
19 mechanochemical treatments provide approaches for the (direct) re-synthesis or reconditioning of  
20 deteriorated SEs through relithiation [409].

21  
22 For halide-based SSBs, the same concerns regarding moisture sensitivity apply, thus processing in  
23 a dry environment is as crucial. Halide and sulfide SEs share many similarities regarding recycling,  
24 re-synthesis, and reconditioning. For example, for Li<sub>3</sub>InCl<sub>6</sub>, the concept of a solvent-based separation  
25 technique using a solvent as simple as water can be applied. This is due to the SE's ability to reversibly  
26 convert between its hydrated and dehydrated forms after dissolution [66]. However, side reactions that  
27 degrade both the SE and active materials may occur [410].

28  
29 To process polymer SSBs, solvent-based dissolution can be also employed to effectively separate  
30 polymers and active materials [411]. As both the polymers and conducting lithium salts decompose at  
31 relatively low temperatures, conventional high-temperature approaches are unsuitable due to the  
32 formation of hazardous byproducts and significant material loss [412]. Hydrometallurgical recycling of  
33 other battery components can be significantly hindered by any polymer impurities [413]. Furthermore,  
34 the low cost of polymeric SEs is a major problem from an economic point of view when considering  
35 recycling, requiring processes to be cost-effective and energy-efficient.

36  
37 As SSBs approach commercial readiness, recycling strategies must significantly improve to  
38 address the increasing complexity and diversity of next-generation battery systems. Implementing  
39 techniques that perform well in optimal laboratory conditions is often inadequate when applied to  
40 "real-world" cell architectures, which typically contain various solid electrolytes, lithium metal anodes,  
41 and feature tightly integrated designs. Thus, the scaling-up of recycling requires solutions that meet  
42 higher demands for process robustness and safety. In this context, translating promising lab-scale  
43 techniques into industrially feasible processes remains a major hurdle. Several issues, including  
44 mechanical wear caused by shredding of hard materials, the necessity for an inert or moisture-free  
45 environment, and the requirement for high-purity separation, must be resolved. Systems must be  
46 scalable, flexible, and automated to effectively accommodate the wide array of cell chemistries and  
47 formats expected in future applications. Consequently, cell formats and treatment protocols must be  
48 standardized. However, recycling different types of electrolytes may require distinctly specialized  
49 methods. This differs from the recycling of conventional LIBs, for which typically a certain degree of  
50 compatibility between the materials is found, particularly for the recovery of metals from the active  
51 material. The integration of artificial intelligence and robotics may also facilitate the automation of  
52 disassembly, optimize sorting and separation procedures, and increase process adaptability.

53  
54 Design-for-recycling will be pivotal in enabling more efficient end-of-life management. Future  
55 battery modules should feature, for example, easy-to-disassemble housings, reversible bonding agents,  
56  
57  
58  
59  
60

and accessible current collectors. These design principles simplify disassembly, minimize cross-contamination, and enhance the value of recovered fractions. To do this, battery designers, materials scientists, process engineers, and recycling specialists must collaborate closely from the earliest stages of development.

Conducting comprehensive life cycle assessments is essential for evaluating the environmental and economic effects of SSB recycling. Beyond recovering critical elements, future strategies should aim to directly recycle individual functional battery materials. Such an approach would reduce emissions and the necessity for energy-intensive re-synthesis.

Finally, for large-scale industrial implementation, robust regulations must be established. Policies promoting circular designs could accelerate market adoption. Furthermore, recycling infrastructure must be developed, or existing infrastructure must be modified. Ultimately, only a concerted effort between academia, industry, and policymakers will enable the advancement of safe, economically viable, and scalable recycling solutions for solid-state batteries. This will ensure their long-term sustainability and contribution to the energy transition.



**Figure 21.** Future challenges for recycling of solid-state batteries.

## Conclusion and Future Perspectives

Significant progress has been made in the development of recycling strategies for SSBs; nonetheless, many challenges remain. Recent research has already demonstrated that effective separation processes can be defined, enabling the recovery of different battery components. These initial successes lay an important basis for future developments while also underscoring the necessity for continued research efforts as cell chemistries and designs diversify. Importantly, the field still offers the rare opportunity to shape an emerging battery technology from the ground up with circularity in mind. While early findings suggest that some material combinations are more difficult to process than others, it is not yet clear which configurations will ultimately prove most compatible with recycling. SSBs might even provide benefits over conventional LIBs in terms of recyclability and resource requirements during end-of-life processing.

Future research should include post-lithium technologies, such as lithium-sulfur or solid-state batteries based on other ions (e.g.,  $\text{Na}^+$ ,  $\text{K}^+$ ,  $\text{Mg}^{2+}$ ). These technologies may introduce new challenges, although they use analogous materials, indicating that insights gained from SSB recycling could be transferable. A coordinated effort to integrate recycling considerations into early-stage battery

1 development, combined with technological advancements and policy support, will be essential to  
2 realize a sustainable and economically viable circular battery economy.  
3  
4

### 5 **Acknowledgment**

6 K.W. is grateful to the Baden-Württemberg Stiftung for financial support through the  
7 Postdoctoral fellowship for leading early career researchers.  
8  
9

### 10 **Conflict of Interest**

11 The authors declare no conflict of interest.  
12  
13  
14  
15  
16  
17  
18  
19  
20  
21  
22  
23  
24  
25  
26  
27  
28  
29  
30  
31  
32  
33  
34  
35  
36  
37  
38  
39  
40  
41  
42  
43  
44  
45  
46  
47  
48  
49  
50  
51  
52  
53  
54  
55  
56  
57  
58  
59  
60

## References

- [1] Janek J and Zeier W G 2023 Challenges in speeding up solid-state battery development *Nat. Energy* **8** 230–40
- [2] Schmaltz T, Hartmann F, Wicke L, Weymann L, Neef C and Janek J 2023 A roadmap for solid-state batteries *Adv. Energy Mater.* **13** 2301886
- [3] Sung J, Heo J, Kim D-H, Jo S, Ha Y-C, Kim D, et al. 2024 Recent advances in all-solid-state batteries for commercialization *Mater. Chem. Front.* **8** 1861–87
- [4] Huang J, Wu K, Xu G, Wu M, Dou S and Wu C 2023 Recent progress and strategic perspectives of inorganic solid electrolytes: fundamentals, modifications, and applications in sodium metal batteries *Chem. Soc. Rev.* **52** 4933–95
- [5] Yu T, Haoyu L, Sun Y, Guo S and Zhou H 2025 Ductile inorganic solid electrolytes for all-solid-state lithium batteries *Chem. Rev.* **125** 3595–662
- [6] Kamaya N, Homma K, Yamakawa Y, Hirayama M, Kanno R, Yonemura M, et al. 2011 A lithium superionic conductor *Nat. Mater.* **10** 682–6
- [7] Weng W, Lan Y, Tang D, Fu L, Tan W and Zhong S 2025 Research Progress on Lithium Sulfide Synthesis: A Review *ACS Appl. Energy Mater.* **8** 13139–54
- [8] Ohno S, Banik A, Dewald G F, Kraft M A, Krauskopf T, Minafra N, et al. 2020 Materials design of ionic conductors for solid state batteries *Prog. Energy* **2** 022001
- [9] Kraft M A, Culver S P, Calderon M, Böcher F, Krauskopf T, Senyshyn A, et al. 2017 Influence of lattice polarizability on the ionic conductivity in the lithium superionic argyrodites  $\text{Li}_6\text{PS}_5\text{X}$  (X = Cl, Br, I) *J. Am. Chem. Soc.* **139** 10909–18
- [10] Robert G, Malugani J and Saida A 1981 Fast ionic silver and lithium conduction in glasses *Solid State Ion.* **3–4** 311–5
- [11] Kondo S, Takada K and Yamamura Y 1992 New lithium ion conductors based on  $\text{Li}_2\text{S-SiS}_2$  system *Solid State Ion.* **53–56** 1183–6
- [12] Mercier R, Malugani J-P, Fahys B and Robert G 1981 Superionic conduction in  $\text{Li}_2\text{S-P}_2\text{S}_5\text{-LiI}$ -glasses *Solid State Ion.* **5** 663–6
- [13] Deiseroth H J, Kong S T, Eckert H, Vannahme J, Reiner C, Zaiß T, et al. 2008  $\text{Li}_6\text{PS}_5\text{X}$ : A class of crystalline Li-rich solids with an unusually high  $\text{Li}^+$  mobility *Angew. Chem. Int. Ed.* **47** 755–8
- [14] Minami K, Hayashi A, Ujiie S and Tatsumisago M 2009 Structure and properties of  $\text{Li}_2\text{S-P}_2\text{S}_5\text{-P}_2\text{S}_3$  glass and glass-ceramic electrolytes *J. Power Sources* **189** 651–4
- [15] Kato Y, Hori S, Saito T, Suzuki K, Hirayama M, Mitsui A, et al. 2016 High-power all-solid-state batteries using sulfide superionic conductors *Nat. Energy* **1** 16030
- [16] Li Y, Song S, Kim H, Nomoto K, Kim H, Sun X, et al. 2023 A lithium superionic conductor for millimeter-thick battery electrode *Science* **381** 50–3
- [17] Saito M, Araki T, Onodera Y, Ohara K, Seto M, Yoda Y, et al. 2025 Discovery of collective nonjumping motions leading to Johari–Goldstein process of stress relaxation in model ionic glass *Acta Mater.* **284** 120536
- [18] Cronau M, Szabo M, König C, Wassermann T B and Roling B 2021 How to Measure a Reliable Ionic Conductivity? The Stack Pressure Dilemma of Microcrystalline Sulfide-Based Solid Electrolytes *ACS Energy Lett.* **6** 3072–7

- 1 [19] Wang S, Zhang W, Chen X, Das D, Ruess R, Gautam A, et al. 2021 Influence of Crystallinity  
2 of Lithium Thiophosphate Solid Electrolytes on the Performance of Solid-State Batteries *Adv.*  
3 *Energy Mater.* **11** 2100654
- 4 [20] Maus O, Lange M A, Frankenberg F, Stainer F, Faka V, Schlautmann E, et al. 2025 Influence  
5 of Post-Synthesis Processing on the Structure, Transport, and Performance of the Solid  
6 Electrolyte  $\text{Li}_{5.5}\text{PS}_{4.5}\text{Cl}_{1.5}$  in All-Solid-State Batteries *Adv. Energy Mater.* **15** 2403291
- 7 [21] Sendek A D, Cubuk E D, Antoniuk E R, Cheon G, Cui Y and Reed E J 2019 Machine  
8 Learning-Assisted Discovery of Solid Li-Ion Conducting Materials *Chem. Mater.* **31** 342–52
- 9 [22] Zhao Q, Avdeev M, Chen L and Shi S 2021 Machine learning prediction of activation energy  
10 in cubic Li-argyrodites with hierarchically encoding crystal structure-based (HECS) descriptors  
11 *Sci. Bull.* **66** 1401–8
- 12 [23] Kahle L, Marcolongo A and Marzari N 2020 High-throughput computational screening for  
13 solid-state Li-ion conductors *Energy Environ. Sci.* **13** 928–48
- 14 [24] Guo X, Wang Z, Yang J-H and Gong X-G 2024 Machine-learning assisted high-throughput  
15 discovery of solid-state electrolytes for Li-ion batteries *J. Mater. Chem. A* **12** 10124–36
- 16 [25] Cho M Y, Pyo K, Lee B D, Kim H, Shin J, Seo J Y, et al. 2025 Discovering  
17 Multi-Compositional Li-Argyrodite Solid-State Electrolytes via Experimental Active Learning  
18 *Small* **21** 2410008
- 19 [26] Kong S, Matsui N, Hori S, Hirayama M, Mori K, Saito T, et al. 2025 Exploration of Lithium-  
20 Ion Conductors Based on Local Coordination Environments Using Crystallographic Site  
21 Fingerprints *J. Am. Chem. Soc.* **147** 24336–46
- 22 [27] Han G, Vasylenko A, Daniels L M, Collins C M, Corti L, Chen R, et al. 2024 Superionic  
23 lithium transport via multiple coordination environments defined by two-anion packing *Science*  
24 **383** 739–45
- 25 [28] Wang Q, Yang F, Wang Y, Zhang D, Sato R, Zhang L, et al. 2025 Unraveling the Complexity  
26 of Divalent Hydride Electrolytes in Solid-State Batteries via a Data-Driven Framework with  
27 Large Language Model *Angew. Chemie Int. Ed.* **64** e202506573
- 28 [29] Li J, Hu Y, Xia G, Mo W, Li B, Jia Y, et al. 2025 Coevolution of large language models with  
29 physical models boosts advanced battery research *Cell Reports Phys. Sci.* **6** 102553
- 30 [30] Park H, Onwuli A and Walsh A 2025 Exploration of crystal chemical space using text-guided  
31 generative artificial intelligence *Nat. Commun.* **16** 4379
- 32 [31] Schweidler S, Botros M, Strauss F, Wang Q, Ma Y, Velasco L, et al. 2024 High-entropy  
33 materials for energy and electronic applications *Nat. Rev. Mater.* **9** 266–81
- 34 [32] Li S, Lin J, Schaller M, Indris S, Zhang X, Brezesinski T, et al. 2023 High-Entropy Lithium  
35 Argyrodite Solid Electrolytes Enabling Stable All-Solid-State Batteries *Angew. Chemie Int. Ed.*  
36 **62** e202314155
- 37 [33] Zeng Y, Ouyang B, Liu J, Byeon Y-W, Cai Z, Miara L J, et al. 2022 High-entropy mechanism  
38 to boost ionic conductivity *Science* **378** 1320–4
- 39 [34] Strauss F, Lin J, Duffiet M, Wang K, Zinkevich T, Hansen A-L, et al. 2022 High-Entropy  
40 Polyanionic Lithium Superionic Conductors *ACS Mater. Lett.* **4** 418–23
- 41 [35] Lin J, Cherkashinin G, Schäfer M, Melinte G, Indris S, Kondrakov A, et al. 2022 A High-  
42 Entropy Multicationic Substituted Lithium Argyrodite Superionic Solid Electrolyte *ACS Mater.*  
43 *Lett.* **4** 2187–94
- 44  
45  
46  
47  
48  
49  
50  
51  
52  
53  
54  
55  
56  
57  
58  
59  
60

- [36] Ohno S, Bernges T, Buchheim J, Duchardt M, Hatz A K, Kraft M A, et al. 2020 How Certain Are the Reported Ionic Conductivities of Thiophosphate-Based Solid Electrolytes? An Interlaboratory Study *ACS Energy Lett.* **5** 910–5
- [37] Kalyk F, Pescara L, Drüscher M and Vargas-Barbosa N M 2026 Toward Robust Ionic Conductivity Determination of Sulfide-Based Solid Electrolytes for Solid-State Batteries *Adv. Funct. Mater.* **36** e09479
- [38] Shimoda M, Maegawa M, Yoshida S, Akamatsu H, Hayashi K, Gorai P, et al. 2022 Controlling Defects to Achieve Reproducibly High Ionic Conductivity in Na<sub>3</sub>SbS<sub>4</sub> Solid Electrolytes *Chem. Mater.* **34** 5634–43
- [39] Schnaubelt F, Panda A, Wagner D, Ziegler M, Dang H A, Zeier W G, et al. 2025 Impurities in Na<sub>2</sub>S Precursor and Their Effect on the Synthesis of W-Substituted Na<sub>3</sub>PS<sub>4</sub>: Enabling 20 mS cm<sup>-1</sup> Thiophosphate Electrolytes for Sodium Solid-State Batteries *Adv. Energy Mater.* **15** e03047
- [40] Puls S, Nazmutdinova E, Kalyk F, Woolley H M, Thomsen J F, Cheng Z, et al. 2024 Benchmarking the reproducibility of all-solid-state battery cell performance *Nat. Energy* **9** 1310–20
- [41] Li J, Su H, Liu Y, Zhong Y, Wang X and Tu J 2024 Li alloys in all solid-state lithium batteries: a review of fundamentals and applications *EER* **7** 18
- [42] Lee Y G, Fujiki S, Jung C, Suzuki N, Yashiro N, Omoda R, et al. 2020 High-energy long-cycling all-solid-state lithium metal batteries enabled by silver–carbon composite anodes *Nat. Energy* **5** 299–308
- [43] Lei Y J, Liu H W, Yang Z, Zhao L F, Lai W H, Chen M, et al. 2023 A review on the status and challenges of cathodes in room-temperature Na-S batteries *Adv. Funct. Mater.* **33** 2212600
- [44] Koerver R, Zhang W, de Biasi L, Schweidler S, Kondrakov A O, Kolling S, et al. 2018 Chemo-mechanical expansion of lithium electrode materials—on the route to mechanically optimized all-solid-state batteries *Energy Environ. Sci.* **11** 2142–58
- [45] Walther F, Koerver R, Fuchs T, Ohno S, Sann J, Rohnke M, et al. 2019 Visualization of the interfacial decomposition of composite cathodes in argyrodite-based all-solid-state batteries using time-of-flight secondary-ion mass spectrometry *Chem. Mater.* **31** 3745–55
- [46] Rosenbach C, Walther F, Ruhl J, Hartmann M, Hendriks T A, Ohno S, et al. 2023 Visualizing the chemical incompatibility of halide and sulfide-based electrolytes in solid-state batteries *Adv. Energy Mater.* **13** 2203673
- [47] Zhao W, Lavrinenko A K, Tu M F, Huet L, Vasileiadis A, Famprakis T, et al. 2025 Irreducible solid electrolytes: new perspectives on stabilizing high-capacity anodes in solid-state batteries *ACS Energy Lett.* **10** 5363–72
- [48] Wan H, Wang Z, Zhang W, He X and Wang C 2023 Interface design for all-solid-state lithium batteries *Nature* **623** 739–44
- [49] Aktekin B, Riegger L M, Otto S K, Fuchs T, Henss A and Janek J 2023 SEI growth on lithium metal anodes in solid-state batteries quantified with coulometric titration time analysis *Nat. Commun.* **14** 6946
- [50] Luo Y, Rao Z, Yang X, Wang C, Sun X and Li X 2024 Safety concerns in solid-state lithium batteries: from materials to devices *Energy Environ. Sci.* **17** 7543–65
- [51] Kim T, Kim K, Lee S, Song G, Jung M S and Lee K T 2022 Thermal Runaway Behavior of Li<sub>6</sub>PS<sub>5</sub>Cl Solid Electrolytes for LiNi<sub>0.8</sub>Co<sub>0.1</sub>Mn<sub>0.1</sub>O<sub>2</sub> and LiFePO<sub>4</sub> in All-Solid-State Batteries *Chem. Mater.* **34** 9159–71

- [52] Rui X, Ren D, Liu X, Wang X, Wang K, Lu Y, et al. 2023 Distinct thermal runaway mechanisms of sulfide-based all-solid-state batteries *Energy Environ. Sci.* **16** 3552–63
- [53] He Y, Wang J, Rong C, Li W, Gao Z, Wang D, et al. 2024 Status of cell-level thermal safety assessments toward optimization of all-solid-state batteries *Cell Reports Phys. Sci.* **5** 102056
- [54] Lu P, Wu D, Chen L, Li H and Wu F 2022 Air Stability of Solid-State Sulfide Batteries and Electrolytes *Electrochem. Energy Rev.* **5** 3
- [55] Ohno S and Zeier W G 2021 Toward Practical Solid-State Lithium–Sulfur Batteries: Challenges and Perspectives *Accounts Mater. Res.* **2** 869–80
- [56] Wang S, Lou C, Wu X, Lin J, Gautam A, Li S, et al. 2025 Large-scale manufacturing sulfide superionic conductor for advancing all-solid-state batteries *Matter* **8** 102135
- [57] Zhang Z, Shao Y, Lotsch B, Hu Y S, Li H, Janek J, et al. 2018 New horizons for inorganic solid state ion conductors *Energy Environ. Sci.* **11** 1945–76
- [58] Kerman K, Luntz A, Viswanathan V, Chiang Y-M and Chen Z 2017 Review—Practical Challenges Hindering the Development of Solid State Li Ion Batteries *J. Electrochem. Soc.* **164** A1731–44
- [59] Li X, Liang J, Yang X, Adair K R, Wang C, Zhao F, et al. 2020 Progress and perspectives on halide lithium conductors for all-solid-state lithium batteries *Energy Environ. Sci.* **13** 1429–61
- [60] Anantharamulu N, Koteswara Rao K, Rambabu G, Vijaya Kumar B, Radha V and Vithal M 2011 A wide-ranging review on Nasicon type materials *J. Mater. Sci.* **46** 2821–37
- [61] Wang Y, Song S, Xu C, Hu N, Molenda J and Lu L 2019 Development of solid-state electrolytes for sodium-ion battery—A short review *Nano Materials Science* **1** 91–100
- [62] Wu J, Li J and Yao X 2025 Exploring the Potential of Halide Electrolytes for Next-Generation All-Solid-State Lithium Batteries *Adv. Funct. Mater.* **35** 2416671
- [63] Fu J, Wang S, Liang J, Alahakoon S H, Wu D, Luo J, et al. 2023 Superionic Conducting Halide Frameworks Enabled by Interface-Bonded Halides *J. Am. Chem. Soc.* **145** 2183–94
- [64] Li X, Liang J, Luo J, Norouzi Banis M, Wang C, Li W, et al. 2019 Air-stable  $\text{Li}_3\text{InCl}_6$  electrolyte with high voltage compatibility for all-solid-state batteries *Energy Environ. Sci.* **12** 2665–71
- [65] Shi X, Zeng Z, Sun M, Huang B, Zhang H, Luo W, et al. 2021 Fast Li-ion Conductor of  $\text{Li}_3\text{HoBr}_6$  for Stable All-Solid-State Lithium-Sulfur Battery *Nano Lett.* **21** 9325–31
- [66] Li X, Liang J, Chen N, Luo J, Adair K R, Wang C, et al. 2019 Water-Mediated Synthesis of a Superionic Halide Solid Electrolyte *Angew. Chem. Int. Ed.* **58** 16427–32
- [67] Liang J, Li X, Wang S, Adair K R, Li W, Zhao Y, et al. 2020 Site-Occupation-Tuned Superionic  $\text{Li}_x\text{ScCl}_{3+x}$  Halide Solid Electrolytes for All-Solid-State Batteries *J. Am. Chem. Soc.* **142** 7012–22
- [68] Park K H, Kaup K, Assoud A, Zhang Q, Wu X and Nazar L F 2020 High-Voltage Superionic Halide Solid Electrolytes for All-Solid-State Li-Ion Batteries *ACS Energy Lett* **5** 533–9
- [69] Helm B, Schlem R, Wankmiller B, Banik A, Gautam A, Ruhl J, et al. 2021 Exploring Aliovalent Substitutions in the Lithium Halide Superionic Conductor  $\text{Li}_{3-x}\text{In}_{1-x}\text{Zr}_x\text{Cl}_6$  ( $0 \leq x \leq 0.5$ ) *Chem. Mater.* **33** 4773–82
- [70] Kim S Y, Kaup K, Park K H, Assoud A, Zhou L, Liu J, et al. 2021 Lithium Ytterbium-Based Halide Solid Electrolytes for High Voltage All-Solid-State Batteries *ACS Mater. Lett.* **3** 930–8

- [71] Asano T, Sakai A, Ouchi S, Sakaida M, Miyazaki A and Hasegawa S 2018 Solid Halide Electrolytes with High Lithium-Ion Conductivity for Application in 4 V Class Bulk-Type All-Solid-State Batteries *Adv. Mater.* **30** 1803075
- [72] Park J, Han D, Kwak H, Han Y, Choi Y J, Nam K W, et al. 2021 Heat treatment protocol for modulating ionic conductivity via structural evolution of  $\text{Li}_{3-x}\text{Yb}_{1-x}\text{M}_x\text{Cl}_6$  ( $\text{M} = \text{Hf}^{4+}, \text{Zr}^{4+}$ ) new halide superionic conductors for all-solid-state batteries *Chem. Eng. J.* **425** 130630
- [73] Combs S R, Todd P K, Gorai P and Maughan A E 2022 Editors' Choice—Review—Designing Defects and Diffusion through Substitutions in Metal Halide Solid Electrolytes *J. Electrochem. Soc.* **169** 040551
- [74] Liu Z, Chien P H, Wang S, Song S, Lu M, Chen S, et al. 2024 Tuning collective anion motion enables superionic conductivity in solid-state halide electrolytes *Nat. Chem.* **16** 1584–91
- [75] Schlem R, Banik A, Ohno S, Suard E and Zeier W G 2021 Insights into the Lithium Substructure of Superionic Conductors  $\text{Li}_3\text{YCl}_6$  and  $\text{Li}_3\text{YBr}_6$  *Chem. Mater.* **33** 327–37
- [76] Schlem R, Muy S, Prinz N, Banik A, Shao-Horn Y, Zobel M, et al. 2020 Mechanochemical Synthesis: A Tool to Tune Cation Site Disorder and Ionic Transport Properties of  $\text{Li}_3\text{MCl}_6$  ( $\text{M} = \text{Y}, \text{Er}$ ) Superionic Conductors *Adv. Energy Mater.* **10** 1903719
- [77] Park D, Kim K, Chun G H, Wood B C, Shim J H and Yu S 2021 Materials design of sodium chloride solid electrolytes  $\text{Na}_3\text{MCl}_6$  for all-solid-state sodium-ion batteries *J. Mater. Chem. A* **9** 23037–45
- [78] Qie Y, Wang S, Fu S, Xie H, Sun Q and Jena P 2020 Yttrium-Sodium Halides as Promising Solid-State Electrolytes with High Ionic Conductivity and Stability for Na-Ion Batteries *J. Phys. Chem. Lett.* **11** 3376–83
- [79] Kwak H, Lyoo J, Park J, Han Y, Asakura R, Remhof A, et al. 2021  $\text{Na}_2\text{ZrCl}_6$  enabling highly stable 3 V all-solid-state Na-ion batteries *Energy Storage Mater.* **37** 47–54
- [80] Zhao T, Kraft M A and Zeier W G 2023 Synthesis-Controlled Polymorphism and Anion Solubility in the Sodium-Ion Conductor  $\text{Na}_3\text{InCl}_{6-x}\text{Br}_x$  ( $0 \leq x \leq 2$ ) *Inorg. Chem.* **62** 11737–45
- [81] Zhao T, Sobolev A N, Schlem R, Helm B, Kraft M A and Zeier W G 2023 Synthesis-Controlled Cation Solubility in Solid Sodium Ion Conductors  $\text{Na}_{2+x}\text{Zr}_{1-x}\text{In}_x\text{Cl}_6$  *ACS Appl. Energy Mater.* **6** 4334–41
- [82] Schlem R, Banik A, Eckardt M, Zobel M and Zeier W G 2020  $\text{Na}_{3-x}\text{Er}_{1-x}\text{Zr}_x\text{Cl}_6$ -A halide-based fast sodium-ion conductor with vacancy-driven ionic transport *ACS Appl. Energy Mater.* **3** 10164–73
- [83] Zhao T, Sobolev A N, de Irujo Labalde X M, Kraft M A and Zeier W G 2024 On the influence of the coherence length on the ionic conductivity in mechanochemically synthesized sodium-conducting halides,  $\text{Na}_{3-x}\text{In}_{1-x}\text{Zr}_x\text{Cl}_6$  *J. Mater. Chem. A* **12** 7015–24
- [84] Martinez de Irujo-Labalde X, Zhao T, Samanta B, Bernges T, Faka V, Sobolev A N, et al. 2024 How crystal structure and microstructure can influence the sodium-ion conductivity in halide perovskites *J. Mater. Chem. A* **12** 33707–22
- [85] Okada Y, Kimura T, Motohashi K, Sakuda A and Hayashi A 2023 Mechanochemical Synthesis and Characterization of  $\text{Na}_{3-x}\text{In}_{1-x}\text{Zr}_x\text{Cl}_6$  Solid Electrolyte *Electrochemistry* **91** 077009
- [86] Huang Z, Yoshida S, Akamatsu H, Hayashi K and Ohno S 2024  $\text{NaMCl}_6$  ( $\text{M} = \text{Nb}$  and  $\text{Ta}$ ): A New Class of Sodium-Conducting Halide-Based Solid Electrolytes *ACS Mater. Lett.* **6** 1732–8
- [87] Hu Y, Fu J, Xu J, Luo J, Zhao F, Su H, et al. 2024 Superionic amorphous  $\text{NaTaCl}_6$  halide electrolyte for highly reversible all-solid-state Na-ion batteries *Matter* **7** 1018–34

- [88] Motohashi K, Tsukasaki H, Sakuda A, Mori S and Hayashi A 2024 NaTaCl<sub>6</sub>: Chloride as the End-Member of Sodium-Ion Conductors *ACS Mater. Lett.* **6** 1178–83
- [89] Tanaka Y, Ueno K, Mizuno K, Takeuchi K, Asano T and Sakai A 2023 New Oxyhalide Solid Electrolytes with High Lithium Ionic Conductivity >10 mS cm<sup>-1</sup> for All-Solid-State Batteries *Angew. Chem. Int. Ed.* **62** e202217581
- [90] Newnham J A, Kondek J, Hartel J, Rosenbach C, Li C, Faka V, et al. 2025 Correlation between the Coherence Length and Ionic Conductivity in LiNbOCl<sub>4</sub> via the Anion Stoichiometry *Chem. Mater.* **37** 4130–44
- [91] Zhang S, Zhao F, Chen J, Fu J, Luo J, Alahakoon S H, et al. 2023 A family of oxychloride amorphous solid electrolytes for long-cycling all-solid-state lithium batteries *Nat. Commun.* **14** 3780
- [92] Zhang S, Zhao F, Chang L Y, Chuang Y C, Zhang Z, Zhu Y, et al. 2024 Amorphous Oxyhalide Matters for Achieving Lithium Superionic Conduction *J. Am. Chem. Soc.* **146** 2977–85
- [93] Lin X, Zhao Y, Wang C, Luo J, Fu J, Xiao B, et al. 2024 A Dual Anion Chemistry-Based Superionic Glass Enabling Long-Cycling All-Solid-State Sodium-Ion Batteries *Angew. Chem. Int. Ed.* **136** e202314181
- [94] Zhao T, Samanta B, de Irujo-Labalde X M, Whang G, Yadav N, Kraft M A, et al. 2024 Sodium Metal Oxyhalides NaMOCl<sub>4</sub> (M = Nb, Ta) with High Ionic Conductivities *ACS Mater. Lett.* **6** 3683–9
- [95] Zhou L, Bazak J D, Li C and Nazar L F 2024 4 V Na Solid State Batteries Enabled by a Scalable Sodium Metal Oxyhalide Solid Electrolyte *ACS Energy Lett.* **9** 4093–101
- [96] Kageyama H, Hayashi K, Maeda K, Attfield J P, Hiroi Z, Rondinelli J M, et al. 2018 Expanding frontiers in materials chemistry and physics with multiple anions *Nat. Commun.* **9** 772
- [97] Riegger L M, Schlem R, Sann J, Zeier W G and Janek J 2021 Lithium-Metal Anode Instability of the Superionic Halide Solid Electrolytes and the Implications for Solid-State Batteries *Angew. Chem. Int. Ed.* **60** 6718–23
- [98] Tao B, Zhong D, Li H, Wang G and Chang H 2023 Halide solid-state electrolytes for all-solid-state batteries: structural design, synthesis, environmental stability, interface optimization and challenges *Chem. Sci.* **14** 8693–722
- [99] Goodwin L E, Ziegler M, Till P, Nazer N, Adelhelm P, Zeier W G, et al. 2024 Halide and Sulfide Electrolytes in Cathode Composites for Sodium All-Solid-State Batteries and their Stability *ACS Appl. Mater. Interfaces* **16** 19792–805
- [100] Cheng Z, Zhao W, Wang Q, Zhao C, Lavrinenko A K, Vasileiadis A, et al. 2025 Beneficial redox activity of halide solid electrolytes empowering high-performance anodes in all-solid-state batteries *Nat. Mater.* **24** 1763–72
- [101] Ridley P, Duong G, Ko S L, An Sam Oh J, Deysher G, Griffith K J, et al. 2025 Tailoring Chloride Solid Electrolytes for Reversible Redox *J. Am. Chem. Soc.* **147** 19508–19
- [102] Kmiec S, Ruoff E and Manthiram A 2025 A New Class of Oxyhalide Solid Electrolytes NaNbCl<sub>6-2x</sub>O<sub>x</sub> for Solid-state Sodium Batteries *Angew. Chem. Int. Ed.* **64** e20241697
- [103] Ferrari S, Falco M, Munoz-Garcia A B, Bonomo M, Brutti S, Pavone M, et al. 2021 Solid-State Post Li Metal Ion Batteries: A Sustainable Forthcoming Reality? *Adv. Energy Mat.* **11** 2100785
- [104] Fampiriskis T, Canepa P, Dawson J A, Islam M A and Masquelier C 2019 Fundamentals of inorganic solid-state electrolytes for batteries *Nat. Mater.* **18** 1278–91

- 1 [105] Iton Z W B and See K Z 2022 Multivalent ion conduction in inorganic solids *Chem. Mater.* **34**  
2 881–98  
3
- 4 [106] Grill J, Steensen S K, Castro D L Q, Castelli I E and Popovic-Neuber J 2024 Solid-state  
5 inorganic electrolytes for next generation potassium batteries *Comm. Mater.* **5** 127  
6
- 7 [107] Lu Z, Qiu P, Zhai H, Zhang G G, Chen X W, Lu Z, et al. 2024 Facile synthesis of potassium  
8 decahydrido-monocarpa-closo-decaborate imidazole complex electrolyte for all-solid-state  
9 potassium metal batteries *Angew. Chem. Int. Ed.* **63** e202412401  
10
- 11 [108] Grill J and Popovic-Neuber J. 2025 Bulk and interphase properties of W-doped  $K_3SbS_4$  solid-  
12 state electrolyte *J. Ener. Chem.* **111** 274–8  
13
- 14 [109] Chen Y, Wang P, Truong E, Ogbolu B, Jin Y, Oyekunle I, et al. 2024 Superionic Conduction in  
15  $K_3SbS_4$  enabled by Cl-modified anion lattice *Angew. Chem. Int. Ed.* **136** e202408574  
16
- 17 [110] Jaschin P W, Gao Y, Li Y and Bo S H 2020 A materials perspective on magnesium-ion-based  
18 solid-state electrolytes *J. Mater. Chem.* **8** 2875–97  
19
- 20 [111] Kisu K, Kim S, Inukai M, Oguchi H, Takagi H and Orimo S 2020 Magnesium borohydrate  
21 ammonia borane as a magnesium ionic conductor *ACS Appl. Energy Mater.* **3** 3174–9  
22
- 23 [112] Amdisen M B, Grinderslev J B, Skov L N and Jensen T R 2023 Methylamine magnesium  
24 borohydrides as electrolytes for all-solid-state magnesium batteries *Chem. Mater.* **35** 1440–8  
25
- 26 [113] Glaser, C, Sotouden M, Dillenz M., Sarkar K., Bark J S, Singh S, et al. 2025 High room-  
27 temperature magnesium ion conductivity in spinel-type  $MgYb_2Se_4$  solid electrolyte *Chem.*  
28 *Mater.* **37** 3353–62  
29
- 30 [114] Shinohara T, Kisu K, Takagi S and Orimo S 2024 Investigating the ion conductivity and  
31 synthesis conditions of calcium monocarborane solid-state electrolytes *Energy Adv.* **3** 2758–63  
32
- 33 [115] Amidsen M B and Jensen T 2025 Urea calcium borohydrides as  $Ca^{2+}$  solid-state electrolytes  
34 *Chem. Mater.* **37** 1183–94  
35
- 36 [116] Grinderslev J B, Skov L N, Kristensen L R and Jensen T R 2025 Advancing solid-state calcium  
37 batteries: Achieving fast ionic conductivity at near ambient conditions in calcium  
38 hydridoborates *Angew. Chem. Int. Ed.* **64** e202510493  
39
- 40 [117] Mercadier B, Coles S W, Duttine M, Legein M, Body M, Borkiewicz O J, et al. 2023 Dynamic  
41 lone pairs and fluoride-ion disorder in cubic- $BaSnF_4$  *J. Am. Chem. Soc.* **145** 23739–54  
42
- 43 [118] Mori K, Sato S, Ogawa T, Kuwabara A, Song A, Saito T, et al. 2024 Experimental  
44 visualization of F-ion diffusion pathways and geometric frustration-induced positional disorder  
45 in  $CaF_2$ - $BaF_2$  solid electrolytes *ACS Appl. Energy Mater.* **7** 7787–97  
46
- 47 [119] Mohammad I, Witter R, Fichtner M and Reddy M A 2018 Room-temperature, rechargeable  
48 solid-state fluoride-ion batteries *ACS Appl. Energy Mater.* **1** 4766–75  
49
- 50 [120] Hou T, Xu W, Pei X, Jiang L, Yaghi, O M and Persson K A 2022 Ionic Conduction Mechanism  
51 and Design of Metal–Organic Framework Based Quasi-Solid-State Electrolytes *J. Am. Chem.*  
52 *Soc.* **144** 13446–50  
53
- 54 [121] Paskevicius M, Pitt M P, Brown D H, Sheppard D A, Chumphongphan S and Buckley C E  
55 2013 First-order phase transition in the  $Li_2B_{12}H_{12}$  system *Phys. Chem. Chem. Phys.* **15** 15825–8.  
56
- 57 [122] Udovic T J, Matsuo M, Unemoto A, Verdal N, Stavila V, Skripov A V, et al. 2014 Sodium  
58 superionic conduction in  $Na_2B_{12}H_{12}$  *Chem. Commun.* **50** 3750–2  
59
- 60 [123] Duchêne L, Kühnel R-S, Rentsch D, Remhof A, Hagemann H and Battaglia C 2017 A highly  
stable sodium solid-state electrolyte based on a dodeca/deca-borate equimolar mixture *Chem.*  
*Commun.* **53** 4195–8

- [124] Duchêne L, Lunghammer S, Burankova S, Liao W S, Embs J P, Copéret C, et al. 2019 Ionic Conduction Mechanism in the  $\text{Na}_2(\text{B}_{12}\text{H}_{12})_{0.5}(\text{B}_{10}\text{H}_{10})_{0.5}$  closo-Borate Solid-State Electrolyte: Interplay of Disorder and Ion-Ion Interactions *Chem. Mater.* **31** 3449–60
- [125] Kweon K E, Varley J B, Shea P, Adelstein N, Mehta P, Heo T W, et al. 2017 Structural, Chemical, and Dynamical Frustration: Origins of Superionic Conductivity in closo-Borate Solid Electrolytes *Chem. Mater.* **29** 9142–53
- [126] Tang W S, Yoshida K, Soloninin A V, Skoryunov R V, Babanova O A, Skripov A V, et al. 2016 Stabilizing Superionic-Conducting Structures via Mixed-Anion Solid Solutions of Monocarbocloso-borate Salts *ACS Energy Lett.* **1** 659–64
- [127] Payandeh S, Rentsch D, Łodziana Z, Asakura R, Bigler L, Černý R, et al. 2021 Nido-Hydroborate-Based Electrolytes for All-Solid-State Lithium Batteries *Adv. Funct. Mater.* **31** 2010046
- [128] Gulino V, Brighi M, Murgia F, Ngene P, de Jongh P, Černý R, et al. 2021 Room-Temperature Solid-State Lithium-Ion Battery Using a  $\text{LiBH}_4$ – $\text{MgO}$  Composite Electrolyte *ACS Appl. Energy Mater.* **4** 1228–36
- [129] Kim S, Kisu K, Takagi S, Oguchi H and Orimo S-I 2020 Complex Hydride Solid Electrolytes of the  $\text{Li}(\text{CB}_9\text{H}_{10})$ – $\text{Li}(\text{CB}_{11}\text{H}_{12})$  Quasi-Binary System: Relationship between the Solid Solution and Phase Transition, and the Electrochemical Properties *ACS Appl. Energy Mater.* **3** 4831–9
- [130] Garcia A, Müller G, Černý R, Rentsch D, Asakura R, Battaglia C, et al. 2023  $\text{Li}_4\text{B}_{10}\text{H}_{10}\text{B}_{12}\text{H}_{12}$  as solid electrolyte for solid-state lithium batteries *J. Mater. Chem. A* **11** 18996–19003
- [131] Duchêne L, Kühnel R S, Stilp E, Cuervo Reyes E, Remhof A, Hagemann H, et al. 2017 A stable 3 V all-solid-state sodium-ion battery based on a closo-borate electrolyte *Energy Environ. Sci.* **10** 2609–15
- [132] Braun H, Asakura R, Remhof A and Battaglia C 2024 Hydroborate Solid-State Lithium Battery with High-Voltage NMC811 Cathode *ACS Energy Lett.* **9** 707–14
- [133] Asakura R, Reber D, Duchêne L, Payandeh S, Remhof A, Hagemann H, et al. 2020 4 V room-temperature all-solid-state sodium battery enabled by a passivating cathode/hydroborate solid electrolyte interface *Energy Environ. Sci.* **13** 5048–58
- [134] Duchêne L, Kim D H, Song Y B, Jun S, Moury R, Remhof A, et al. 2020 Crystallization of closo-borate electrolytes from solution enabling infiltration into slurry-casted porous electrodes for all-solid-state batteries *Energy Storage Mater.* **26** 543–9
- [135] Muetterties E L, Balthis J H, Chia Y T, Knoth W H and Miller H C 1964 Chemistry of Boranes. VIII. Salts and Acids of  $\text{B}_{10}\text{H}_{10}^{2-}$  and  $\text{B}_{12}\text{H}_{12}^{2-}$  *Inorg. Chem.* **3** 444–51
- [136] Asakura R, Łodziana Z, Grissa R, Rentsch D, Battaglia C and Remhof A 2025 Unveiling Solid-State Electrochemical Oxidation of  $\text{LiBH}_4$  and  $\text{Li}_2\text{B}_{12}\text{H}_{12}$  for High-Voltage All-Solid-State Batteries *ACS Appl. Energy Mater.* **8** 9637–45
- [137] Bay M-C, Grissa R, Egorov K V, Asakura R and Battaglia C 2022 Low  $\text{Na}$ - $\beta''$ -alumina electrolyte/cathode interfacial resistance enabled by a hydroborate electrolyte opening up new cell architecture designs for all-solid-state sodium batteries *Mater. Futures* **1** 031001
- [138] Gigante A, Duchêne L, Moury R, Pupier M, Remhof A and Hagemann H 2019 Direct Solution-Based Synthesis of  $\text{Na}_4(\text{B}_{12}\text{H}_{12})(\text{B}_{10}\text{H}_{10})$  Solid Electrolyte *ChemSusChem* **12** 4832–7
- [139] Berger A, Buckley C E, Paskevicius M 2021 Synthesis of closo- $\text{CB}_{11}\text{H}_{12}$ –Salts Using Common Laboratory Reagents *Inorg. Chem.* **60** 14744–51
- [140] Kulenkampff J, Armbruster C, Drolshagen J, Regnat C, Wienold T, Spari L, et al. 2024 Video Documented Upscaled Synthesis of Salts of the Parent Carbaborate Ion  $[\text{CB}_{11}\text{H}_{12}]^-$ , its

- 1 Undecafluorinated Form  $[\text{CHB}_{11}\text{F}_{11}]^-$  and Useful Starting Materials for its Introduction *Chem.*  
2 *Methods* **4** e202400011  
3
- 4 [141] Cheng D, Wynn T A, Wang X, Wang S, Zhang M, Shimizu R, et al. 2020 Unveiling the Stable  
5 Nature of the Solid Electrolyte Interphase between Lithium Metal and LiPON via Cryogenic  
6 Electron Microscopy *Joule* **4** 2484–500  
7
- 8 [142] Turrell S J, Liang Y, Cai T, Jagger B and Pasta M 2025 Origin of Stability in the Solid  
9 Electrolyte Interphase formed between Lithium and Lithium Phosphorus Oxynitride *Chem.*  
10 *Mater.* **13** 3504–18  
11
- 12 [143] Wenzel S, Sedlmaier S J, Dietrich C, Zeier W G and Janek J 2018 Interfacial reactivity and  
13 interphase growth of argyrodite solid electrolytes at lithium metal electrodes *Solid State Ion.*  
14 **318** 102–12  
15
- 16 [144] Nazri G 1989 Preparation, structure and ionic conductivity of lithium phosphide *Solid State Ion.*  
17 **34** 97–102  
18
- 19 [145] Alpen U v, Rabenau A and Talat G H 1977 Ionic conductivity in  $\text{Li}_3\text{N}$  single crystals *Appl.*  
20 *Phys. Lett.* **15** 621–3  
21
- 22 [146] Li W, Li M, Wang S, Chien P H, Luo J, Fu J, et al. 2025 Superionic conducting vacancy-rich  $\beta$ -  
23  $\text{Li}_3\text{N}$  electrolyte for stable cycling of all-solid-state lithium metal batteries *Nat. Nanotechnol.*  
24 **20** 265–75  
25
- 26 [147] Dawson J A, Famprakis T and Johnston K E 2021 Anti-perovskites for solid-state batteries:  
27 recent developments, current challenges and future prospects *J. Mater. Chem A* **9** 18746–72  
28
- 29 [148] Wang Z, Xia J, Ji X, Liu Y, Zhang J, He X, et al. 2024 Lithium anode interlayer design for all-  
30 solid-state lithium-metal batteries *Nat. Energy.* **9** 251–62  
31
- 32 [149] Li W, Li M, Chien P H, Wang S, Yu C, King G, et al. 2023 Lithium-compatible and air-stable  
33 vacancy-rich  $\text{Li}_9\text{N}_2\text{Cl}_3$  for high-areal capacity, long-cycling all-solid-state lithium metal  
34 batteries *Sci. Adv.* **9** eadh4626.  
35
- 36 [150] Landgraf V, Famprakis T, de Leeuw J, Bannenberg L J, Ganapathy S and Wagemaker M 2023  
37  $\text{Li}_5\text{NCl}_2$ : A Fully-Reduced, Highly-Disordered Nitride-Halide Electrolyte for Solid-State  
38 Batteries with Lithium-Metal Anodes *ACS Appl. Energy Mater.* **6** 1661–72  
39
- 40 [151] Landgraf V, Tu M, Cheng Z, Vasileiadis A, Wagemaker M and Famprakis T 2025  
41 Compositional flexibility in irreducible antifluorite electrolytes for next-generation battery  
42 anodes *J. Mater. Chem A* **13** 3562–74  
43
- 44 [152] Szczuka C, Karasulu B, Groh M F, Sayed F N, Sherman T J, Bocarsly J D, et al. 2022 Forced  
45 Disorder in the Solid Solution  $\text{Li}_3\text{P-Li}_2\text{S}$ : A New Class of Fully Reduced Solid Electrolytes for  
46 Lithium Metal Anodes *J. Am. Chem. Soc.* **144** 16350–65  
47
- 48 [153] Landgraf V, Tu M, Zhao W, Lavrinenko A K, Cheng Z, Canals J, et al. 2025 Disorder-  
49 Mediated Ionic Conductivity in Irreducible Solid Electrolytes *J. Am. Chem. Soc.* **147** 18840–52  
50
- 51 [154] Yu P, Zhang H, Hussain F, Luo J, Tang W, Lei J, et al. 2024 Lithium Metal-Compatible  
52 Antifluorite Electrolytes for Solid-State Batteries *J. Am. Chem. Soc.* **146** 12681–90  
53
- 54 [155] Schmid M, Pielnhofer F, Pfitzner A 2025 The cubic structure of  $\text{Li}_3\text{As}$  stabilized by pressure or  
55 configurational entropy via the solid solution  $\text{Li}_3\text{As-Li}_2\text{Se}$  *RSC Mechanochem.* **2** 193–200  
56
- 57 [156] Tu M, Landgraf V, Zhao W, Cheng Z, Famprakis T, Wang X, et al. 2025 Highly-conductive  
58 irreducible electrolytes for next generation low-potential anodes *doi:10.26434/chemrxiv-2025-  
59 rvccf*  
60
- [157] Lorgier S, Usiskin R and Maier J 2019 Transport and Charge Carrier Chemistry in Lithium  
Oxide *J. Electrochem. Soc.* **166** A2215–20

- 1 [158] Longer S, Usiskin R E and Maier J 2019 Transport and Charge Carrier Chemistry in Lithium  
2 Sulfide *Adv. Funct. Mater.* **29** 1807688
- 3
- 4 [159] Geschwind G 1969 Anion reduced ionic conductivity in LiF *J. Phys. Chem. Solids.* **30** 1631–5
- 5
- 6 [160] Sharon M and Pradhananga R R 1981 Ionic Conductivity of MCI of Pure and Ca<sup>2+</sup>- and Sr<sup>2+</sup>-  
7 Doped Single Crystals *J. Solid State Chem.* **40** 20–7
- 8
- 9 [161] Schlaikjer C R and Liang C C 1971 Ionic Conduction in Calcium Doped Polycrystalline  
10 Lithium Iodide *J. Electrochem. Soc.* **118** 1447–50
- 11
- 12 [162] Gao S, Broux T, Fujii S, Tassel C, Yamamoto K, Xiao Y, et al. 2021 Hydride-based  
13 antiperovskites with soft anionic sublattices as fast alkali ionic conductors *Nat. Commun.* **12**  
14 201
- 15
- 16 [163] Richards W D, Miara L J, Wang Y, Kim J C and Ceder G 2016 Interface Stability in Solid-  
17 State Batteries *Chem. Mater.* **28** 266–73
- 18
- 19 [164] Lavrinenko A K, Famprikis T, Quirk J A, Landgraf V, Groszewicz P B, Heringa J R, et al.  
20 2024 Optimizing ionic transport in argyrodites: a unified view on the role of sulfur/halide  
21 distribution and local environments *J. Mater Chem. A* **12** 26596–611
- 22
- 23 [165] Simonov A and Goodwin A L 2020 Designing disorder into crystalline materials *Nat. Rev.*  
24 *Chem.* **4** 657–73
- 25
- 26 [166] Schmaltz T, Hartmann F, Wicke T, Weymann L, Neef C and Janek J 2023 A Roadmap for  
27 Solid-State Batteries *Adv. Energy Mater.* **13** 2301886
- 28
- 29 [167] Zhao Q, Stalin S, Zhao C-Z and Archer L A 2020 Designing solid-state electrolytes for safe,  
30 energy-dense batteries *Nat. Rev. Mater.* **5** 229–52
- 31
- 32 [168] Tian Y, Zeng G, Rutt A, Shi T, Kim H, Wang J, et al. 2021 Promises and Challenges of Next-  
33 Generation “Beyond Li-ion” Batteries for Electric Vehicles and Grid Decarbonization *Chem.*  
34 *Rev.* **121** 1623–69
- 35
- 36 [169] Neudecker B J, Dudney N J and Bates J B 2000 “Lithium-Free” Thin-Film Battery with In Situ  
37 Plated Li Anode *J. Electrochem. Soc.* **147** 517–23
- 38
- 39 [170] Chi X, Zhang Y, Hao F, Kmiec S, Dong H, Xu R, et al. 2022 An electrochemically stable  
40 homogeneous glassy electrolyte formed at room temperature for all-solid-state sodium batteries  
41 *Nat. Commun.* **13** 2854
- 42
- 43 [171] Mei A, Wang X-L, Lan J-L, Feng Y-C, Geng H-X, Lin Y-H, et al. 2010 Role of amorphous  
44 boundary layer in enhancing ionic conductivity of lithium–lanthanum–titanate electrolyte  
45 *Electrochim. Acta* **55** 2958–63
- 46
- 47 [172] Di L, Pan J, Gao L, Zhu J, Wang L, Wang X, et al. 2023 Effect of grain boundary resistance on  
48 the ionic conductivity of amorphous xLi<sub>2</sub>S-(100-x)LiI binary system *Front. Chem.* **11** 1230187
- 49
- 50 [173] Jung S-K, Gwon H, Yoon G, Miara L J, Lacivita V and Kim J-S 2021 Pliable lithium  
51 superionic conductor for all-solid-state batteries *ACS Energy Lett.* **6** 2006–15
- 52
- 53 [174] Yang X, Gupta S, Chen Y, Sari D, Hau H M, Cai Z, et al. 2024 Fast Room-Temperature  
54 Mg-Ion Conduction in Clay-Like Halide Glassy Electrolytes *Adv. Energy Mater.* **14** 2400163
- 55
- 56 [175] Bates J B, Dudney N J, Gruzalski G R, Zuhr R A, Choudhury A, Luck C F, et al. 1992  
57 Electrical properties of amorphous lithium electrolyte thin films *Solid State Ion.* **53** 647–54
- 58
- 59 [176] Yu X, Bates J B, Jellison Jr. G E and Hart F X 1997 A Stable Thin-Film Lithium Electrolyte:  
60 Lithium Phosphorus Oxynitride *J. Electrochem. Soc.* **144** 524–32

- [177] Senevirathne K, Day C S, Gross M D, Lachgar A and Holzwarth N A W 2013 A new crystalline LiPON electrolyte: Synthesis, properties, and electronic structure *Solid State Ion.* **233** 95–101
- [178] Zou Z, Xiao Z, Lin Z, Zhang B, Zhang C and Wei F 2024 Lithium Phosphorous Oxynitride as an Advanced Solid-State Electrolyte to Boost High-Energy Lithium Metal Battery *Adv. Funct. Mater.* **34** 2409330
- [179] Atwal S, Bhasin V, Nayak C, Nagendra A, Karki V, Sahoo P K, et al. 2025 Spectroscopic Ellipsometry Study of TiO<sub>2</sub>/LiPON and LNMC/LiPON Solid Electrode/Electrolyte Interfaces of Solid-State Batteries *ACS Appl. Energy Mater.* **8** 7730–43
- [180] Kwon G, Gwon H, Bae Y, Jung C, Ko D S, Kim M G, et al. 2025 Disorder-driven sintering-free garnet-type solid electrolytes *Nat. Commun.* **16** 3256
- [181] Zhu Y, Hood Z D, Paik H, Groszewicz P B, Emge S P, Sayed F N, et al. 2024 Highly disordered amorphous Li-battery electrolytes *Matter* **7** 500–2
- [182] Kuwata N, Lu X, Miyazaki T, Iwai Y, Tanabe T and Kawamura J 2016 Lithium diffusion coefficient in amorphous lithium phosphate thin films measured by secondary ion mass spectroscopy with isotope exchange methods *Solid State Ion.* **294** 59–66
- [183] Kazyak E, Chen K-H, Davis A L, Yu S, Sanchez A J, Lasso J, et al. 2018 Atomic layer deposition and first principles modeling of glassy Li<sub>3</sub>BO<sub>3</sub>–Li<sub>2</sub>CO<sub>3</sub> electrolytes for solid-state Li metal batteries *J. Mater. Chem. A* **6** 19425–37
- [184] Hayashi A, Hama S, Morimoto H, Tatsumisago M and Minami T 2004 Preparation of Li<sub>2</sub>S–P<sub>2</sub>S<sub>5</sub> Amorphous Solid Electrolytes by Mechanical Milling *J. Am. Ceram. Soc.* **84** 477–9
- [185] Tsukasaki H, Mori S, Morimoto H, Hayashi A and Tatsumisago M 2017 Direct observation of a non-crystalline state of Li<sub>2</sub>S–P<sub>2</sub>S<sub>5</sub> solid electrolytes *Sci. Rep.* **7** 4142
- [186] Lee B, Jun K, Ouyang B and Ceder G 2023 Weak Correlation between the Polyanion Environment and Ionic Conductivity in Amorphous Li–P–S Superionic Conductors *Chem. Mater.* **35** 891–9
- [187] Chen Z, Du T, Krishnan N M A, Yue Y and Smedskjaer M M 2025 Disorder-induced enhancement of lithium-ion transport in solid-state electrolytes *Nat. Commun.* **16** 1057
- [188] Xu R, Yao J, Zhang Z, Li L, Wang Z, Song D, et al. 2022 Room Temperature Halide-Eutectic Solid Electrolytes with Viscous Feature and Ultrahigh Ionic Conductivity *Adv. Sci.* **9** e2204633
- [189] Spannenberger S, Miß V, Klotz E, Kettner J, Cronau M, Ramanayagam A, et al. 2029 Annealing-induced vacancy formation enables extraordinarily high Li<sup>+</sup> ion conductivity in the amorphous electrolyte 0.33LiI + 0.67Li<sub>3</sub>PS<sub>4</sub> *Solid State Ion.* **341** 115040
- [190] Lin X, Zhang S, Yang M, Xiao B, Zhao Y, Luo J, et al. 2025 A family of dual-anion-based sodium superionic conductors for all-solid-state sodium-ion batteries *Nat. Mater.* **24** 83–91
- [191] Jang Y J, Seo H, Lee Y S, Kang S, Cho W, Cho Y, et al. 2023 Lithium Superionic Conduction in BH<sub>4</sub>-Substituted Thiophosphate Solid Electrolytes *Adv. Sci.* **10** e2204942
- [192] Braga M H, Ferreira J A, Stockhausen V, Oliveira J E and El-Azab A 2014 Novel Li<sub>3</sub>ClO based glasses with superionic properties for lithium batteries *J. Mater. Chem. A* **2** 5470–80
- [193] Seino Y, Ota T, Takada K, Hayashi A and Tatsumisago M 2014 A sulphide lithium super ion conductor is superior to liquid ion conductors for use in rechargeable batteries *Energy Environ. Sci.* **7** 627–31
- [194] Ishiguro Y, Ueno K, Nishimura S, Iida G and Igarashib Y 2023 TaCl<sub>5</sub>-glassified Ultrafast Lithium Ion-conductive Halide Electrolytes for High-performance All-solid-state Lithium Batteries *Chem. Lett.* **52** 237–41

- [195] Mizuno F, Hayashi A, Tadanaga K and Tatsumisago M 2006 High lithium ion conducting glass-ceramics in the system  $\text{Li}_2\text{S}-\text{P}_2\text{S}_5$  *Solid State Ion.* **177** 2721–5
- [196] Guo H, Wang Q, Urban A and Artrith N 2022 Artificial Intelligence-Aided Mapping of the Structure-Composition-Conductivity Relationships of Glass-Ceramic Lithium Thiophosphate Electrolytes *Chem. Mater.* **34** 6702–12
- [197] Kam R L, Jun K, Barroso-Luque L, Yang J H, Xie F and Ceder G 2023 Crystal Structures and Phase Stability of the  $\text{Li}_2\text{S}-\text{P}_2\text{S}_5$  System from First Principles *Chem. Mater.* **35** 9111–26
- [198] Wang Y, Qu H, Liu B, Li X, Ju J, Li J, et al. 2023 Self-organized hetero-nanodomains actuating super  $\text{Li}^+$  conduction in glass ceramics *Nat. Commun.* **14** 669
- [199] Ohtomo T, Mizuno F, Hayashi A, Tadanaga K and Tatsumisago M 2005 Mechanochemical synthesis of lithium ion conducting glasses and glass-ceramics in the system  $\text{Li}_2\text{S}-\text{P}-\text{S}$  *Solid State Ion.* **176** 2349–53
- [200] Wu Z, Xie Z, Yoshida A, Wang Z, Hao X, Abudula A, et al. 2019 Utmost limits of various solid electrolytes in all-solid-state lithium batteries: A critical review *Renew. Sustain. Energy Rev.* **109** 367–85
- [201] Schweiger L, Hogrefe K, Gadermaier B, Rupp J L M and Wilkening H M R 2022 Ionic Conductivity of Nanocrystalline and Amorphous  $\text{Li}_{10}\text{GeP}_2\text{S}_{12}$ : The Detrimental Impact of Local Disorder on Ion Transport *J. Am. Chem. Soc.* **144** 9597–609
- [202] Smith J G and Siegel D J 2020 Low-temperature paddlewheel effect in glassy solid electrolytes *Nat. Commun.* **11** 1483
- [203] Qi J, Banerjee S, Zuo Y, Chen C, Zhu Z, Holekevi Chandrappa M L, et al. 2021 Bridging the gap between simulated and experimental ionic conductivities in lithium superionic conductors *Mater. Today Phys.* **21** 100463
- [204] Sastre J, Futscher M H, Pompizi L, Aribia A, Priebe A, Overbeck J, et al. 2021 Blocking lithium dendrite growth in solid-state batteries with an ultrathin amorphous  $\text{Li-La-Zr-O}$  solid electrolyte *Commun. Mater.* **2** 76
- [205] Kalita D, Lee S, Lee K, Ko D and Yoon Y 2012 Ionic conductivity properties of amorphous  $\text{Li-La-Zr-O}$  solid electrolyte for thin film batteries *Solid State Ion.* **229** 14–9
- [206] Zheng Z, Fang H, Yang F, Liu Z-K and Wang Y 2014 Amorphous  $\text{LiLaTiO}_3$  as Solid Electrolyte Material *J. Electrochem. Soc.* **161** A473–9
- [207] Aguesse F, Roddatis V, Roqueta J, García P, Pergolesi D, Santiso J, et al. 2015 Microstructure and ionic conductivity of LLTO thin films: Influence of different substrates and excess lithium in the target *Solid State Ion.* **272** 1–8
- [208] Lee T, Qi J, Gadre C A, Huyan H, Ko S-T, Zuo Y, et al. 2023 Atomic-scale origin of the low grain-boundary resistance in perovskite solid electrolyte  $\text{Li}_{0.375}\text{Sr}_{0.4375}\text{Ta}_{0.75}\text{Zr}_{0.25}\text{O}_3$  *Nat. Commun.* **14** 1940
- [209] Ling Q, Yu Z, Xu H, Zhu G, Zhang X, Zhao Y, et al. 2016 Preparation and electrical properties of amorphous  $\text{Li-Al-Ti-P-O}$  thin film electrolyte *Mater. Lett.* **169** 42–5
- [210] Luo C, Yi M, Cao Z, Hui W and Wang Y 2024 Review of Ionic Conductivity Properties of NASICON Type Inorganic Solid Electrolyte LATP *ACS Appl. Electron. Mater.* **6** 641–57
- [211] Wei B, Huang S, Wang X, Liu M, Huang C, Liu R, et al. 2025 Intermediate phase induced in situ self-reconstruction of amorphous NASICON for long-life solid-state sodium metal batteries *Energy Environ. Sci.* **18** 831–40

- [212] Ishiguro Y, Iida G, Ueno K, Nishimura S and Igarashib Y 2023 All-Solid-State Lithium Batteries in Cold Environments of  $-20^{\circ}\text{C}$  Enabled by Amorphous Halide-Based Electrolytes  $\text{LiNbCl}_5\text{X}$  and  $\text{LiTaCl}_5\text{X}$  <https://doi.org/10.21203/rs.3.rs-3072105/v1>
- [213] Gupta S, Yang X and Ceder G 2023 What dictates soft clay-like lithium superionic conductor formation from rigid salts mixture *Nat. Commun.* **14** 6884
- [214] Li R, Xu K, Wen S, Tang X, Lin Z, Guo X, et al. 2025 A sodium superionic chloride electrolyte driven by paddle wheel mechanism for solid state batteries *Nat. Commun.* **16** 6633
- [215] Choudhary S and Banerjee S 2025 Ion coordination and migration mechanisms in alkali metal complex borohydride-based solid electrolytes *Commun. Chem.* **8** 123
- [216] Roy A, Sotoudeh M, Dinda S, Tang Y, Kübel C, Groß A, et al. 2024 Improving rechargeable magnesium batteries through dual cation co-intercalation strategy *Nat. Commun.* **15** 492
- [217] Dong Z L, Yuan Y, Martins V, Jin E, Gan Y, Lin X, et al. 2024 Structural insight and modulating of sulfide-based solid-state electrolyte for high-performance solid-state sodium sulfur batteries *Nano Energy* **128** 109871
- [218] Cha G H and Jung S C 2022 Cation-assisted lithium ion diffusion in a lithium oxythioborate halide glass solid electrolyte *Electrochim. Acta* **426** 140806
- [219] Qian L, Tu S, Wang Y, Yang X, Ye C and Qiao S Z 2025 Near-Saturated Coordinated Cations in Oxyhalide Superionic Conductors Boost High-Rate All-Solid-State Batteries *J. Am. Chem. Soc.* **147** 23170–9
- [220] Dong Z L, Gan Y, Martins V, Wang X, Fu B, Jin E, et al. 2025 Novel Sulfide-Chloride Solid-State Electrolytes with Tunable Anion Ratio for Highly Stable Solid-State Sodium-Ion Batteries *Adv. Mater.* **37** e2503107
- [221] Lacivita V, Artrith N and Ceder G 2018 Structural and Compositional Factors That Control the Li-Ion Conductivity in LiPON Electrolytes *Chem. Mater.* **30** 7077–90
- [222] Baba T and Kawamura Y 2016 Structure and Ionic Conductivity of  $\text{Li}_2\text{S}-\text{P}_2\text{S}_5$  Glass Electrolytes Simulated with First-Principles Molecular Dynamics *Front. Energy Res.* **4** 22
- [223] Ohara K, Mitsui A, Mori M, Onodera Y, Shiotani S, Koyama Y, et al. 2016 Structural and electronic features of binary  $\text{Li}_2\text{S}-\text{P}_2\text{S}_5$  glasses *Sci. Rep.* **6** 21302
- [224] Wang D, Jhang L J, Kou R, Liao M, Zheng S, Jiang H, et al. 2023 Realizing high-capacity all-solid-state lithium-sulfur batteries using a low-density inorganic solid-state electrolyte *Nat. Commun.* **14** 1895
- [225] Faka V, Agne M T, Till P, Bernges T, Sadowski M, Gautam A, et al. 2023 Pressure dependence of ionic conductivity in site disordered lithium superionic argyrodite  $\text{Li}_6\text{PS}_5\text{Br}$  *Energy Adv.* **2** 1915–25
- [226] Torres V, Philipp P, Kmiec S and Martin S W 2024 Ionic Conductivity of and Structure and Property Relationships in  $\text{Li}_2\text{S} + \text{SiS}_2 + \text{LiPO}_3$  Glassy Solid Electrolytes *Chem. Mater.* **36** 5521–33
- [227] Kim Y and Martin S 2006 Ionic conductivities of various  $\text{GeS}_2$ -based oxy-sulfide amorphous materials prepared by melt-quenching and mechanical milling methods *Solid State Ion.* **177** 2881–7
- [228] Tanibata N, Noi K, Hayashi A and Tatsumisago M 2018 Preparation and characterization of  $\text{Na}_3\text{PS}_4-\text{Na}_4\text{GeS}_4$  glass and glass-ceramic electrolytes *Solid State Ion.* **320** 193–8
- [229] Zhang Z, Li H, Kaup K, Zhou L, Roy P-N and Nazar L F 2020 Targeting Superionic Conductivity by Turning on Anion Rotation at Room Temperature in Fast Ion Conductors *Matter* **2** 1667–84

- [230] Zhang Z, Roy P-N, Li H, Avdeev M and Nazar L F 2019 Coupled Cation–Anion Dynamics Enhances Cation Mobility in Room-Temperature Superionic Solid-State Electrolytes *J. Am. Chem. Soc.* **141** 19360–72
- [231] Jun K, Lee B, Kam R L and Ceder G 2024 The nonexistence of a paddlewheel effect in superionic conductors *Proc. Natl. Acad. Sci.* **121** e2316493121
- [232] Li F, Cheng X, Lu G, Yin Y C, Wu Y C, Pan R, et al. 2023 Amorphous Chloride Solid Electrolytes with High Li-Ion Conductivity for Stable Cycling of All-Solid-State High-Nickel Cathodes *J. Am. Chem. Soc.* **145** 27774–87
- [233] Qian L, Singh B, Yu Z, Chen N, King G, Arthur Z, et al. 2024 Unlocking lithium ion conduction in lithium metal fluorides *Matter* **7** 3587–607
- [234] Sun Y, Ouyang B, Wang Y, Zhang Y, Sun S, Cai Z, et al. 2022 Enhanced ionic conductivity and lack of paddle-wheel effect in pseudohalogen-substituted Li argyrodites *Matter* **5** 4379–95
- [235] Zhang Z and Nazar L F 2022 Exploiting the paddle-wheel mechanism for the design of fast ion conductors *Nat. Rev. Mater.* **7** 389–405
- [236] Jun K and Ceder G 2025 Reply to Smith and Siegel: Most lithium hops in paddlewheel-claimed conductors occur without spatially and temporally correlated anion-group rotations *Proc. Natl. Acad. Sci.* **122** e2423194122
- [237] Smith J G and Siegel D J 2025 A proper definition of the paddlewheel effect affirms its existence *Proc. Natl. Acad. Sci.* **122** e2419892122
- [238] Wang Y, Richards W D, Ong S P, Miara L J, Kim J C, Mo Y, et al. 2015 Design principles for solid-state lithium superionic conductors *Nat. Mater.* **14** 1026–31
- [239] Yu S, Noh J, Kim B, Song J-H, Oh K, Yoo J, et al. 2023 Design of a trigonal halide superionic conductor by regulating cation order-disorder *Science* **382** 573–9
- [240] He Y, Scivally E, Shaji A, Ouyang B and Zeng Y 2025 Unraveling the Fast Ionic Conduction in NASICON-Type Materials *Adv. Energy Mater.* **15** 2403877
- [241] Liu Y, Wang S, Nolan A M, Ling C and Mo Y 2020 Tailoring the Cation Lattice for Chloride Lithium-Ion Conductors. *Adv. Energy Mater.* **10** 2002356
- [242] Dheerasinghe M J, Gan Y, Wang L, He Y, He Z, Xu G-L, et al. 2025 High throughput screening of high entropy spinel electrolytes for multivalent batteries *Chem. Commun.* **61** 11199–202
- [243] Wang J, He T, Yang X, Cai Z, Wang Y, Lacivita V, et al. 2023 Design principles for NASICON super-ionic conductors *Nat. Commun.* **14** 5210
- [244] Ouyang B, Wang J, He T, Bartel C J, Huo H, Wang Y, et al. 2021 Synthetic accessibility and stability rules of NASICONs *Nat. Commun.* **12** 5752
- [245] Chen Y, Zhao X, Chen K, Koirala K P, Giovine R, Yang X, et al. 2025 Coherent-Precipitation-Stabilized Phase Formation in Over-Stoichiometric Rocksalt-Type Li Superionic Conductors *Adv. Mater.* **37** e2416342
- [246] Chen Y, Lun Z, Zhao X, Koirala K P, Li L, Sun Y, et al. 2024 Unlocking Li superionic conductivity in face-centred cubic oxides via face-sharing configurations *Nat. Mater.* **23** 535–42
- [247] Liu X, Ouyang B and Zeng Y 2025 Balancing autonomy and expertise in autonomous synthesis laboratories *Nat. Comput. Sci.* **5** 92–4
- [248] Wang L, He Z and Ouyang B 2023 Data driven design of compositionally complex energy materials *Comput. Mater. Sci.* **230** 112513

- [249] Bera P K, Medvedev G A, Caruthers J M and Ediger M D 2024 Structural Relaxation Time of a Polymer Glass during Deformation *Phys. Rev. Lett.* **132** 208101
- [250] Málek J 2023 Structural Relaxation Rate and Aging in Amorphous Solids *J. Phys. Chem. C* **127** 6080–7
- [251] Wang X, Wang J and Ruan H 2023 Ergodicity breaking of an inorganic glass aging near  $T_g$  probed by elasticity relaxation *Phys. Rev. B* **107** 024205
- [252] Höland W and Beall G H 2012 *Glass-ceramic technology*: Wiley Online Library.
- [253] Fu L, Engqvist H and Xia W 2020 Glass–ceramics in dentistry: A review *Materials* **13** 1049.
- [254] Su H, Zhong Y, Wang C, Liu Y, Hu Y, Li J, et al. 2024 Deciphering the critical role of interstitial volume in glassy sulfide superionic conductors *Nat. Commun.* **15** 2552
- [255] Krauskopf T, Richter F H, Zeier W G and Janek J 2020 Physicochemical concepts of the lithium metal anode in solid-state batteries *Chem. Rev.* **120** 7745–94
- [256] Minami T, Hayashi A and Tatsumisago M 2006 Recent progress of glass and glass-ceramics as solid electrolytes for lithium secondary batteries *Solid State Ion.* **177** 2715–20
- [257] Kwak H, Wang S, Park J, Liu Y, Kim K T, Choi Y, et al. 2022 Emerging halide superionic conductors for all-solid-state batteries: Design, synthesis, and practical applications *ACS Energy Lett.* **7** 1776–805
- [258] Kwak H, Han D, Lyoo J, Park J, Jung S H, Han Y, et al. 2021 New cost-effective halide solid electrolytes for all-solid-state batteries: mechanochemically prepared  $\text{Fe}^{3+}$ -substituted  $\text{Li}_2\text{ZrCl}_6$  *Adv. Energy Mater.* **11** 2003190
- [259] Yang J, Lin J, Brezesinski T and Strauss F 2024 Emerging Superionic Sulfide and Halide Glass–Ceramic Solid Electrolytes: Recent Progress and Future Perspectives *ACS Energy Lett.* **9** 5977–90
- [260] Patel S V, Lacivita V, Liu H, Truong E, Jin Y, Wang E, et al. 2023 Charge-clustering induced fast ion conduction in  $2\text{LiX-GaF}_3$ : A strategy for electrolyte design *Sci. Adv.* **9** eadj9930
- [261] Dai T, Wu S, Lu Y, Yang Y, Liu Y, Chang C, et al. 2023 Inorganic glass electrolytes with polymer-like viscoelasticity *Nat. Energy* **8** 1221–8
- [262] Kim W, Han S, Lee S, Yoo J, Park C, Yu S, et al. 2025 Oxygen-tuned aluminum-based halide solid electrolytes enabling low-voltage anode compatibility in all-solid-state batteries *Energy Environ. Sci.* **18** 2039–51
- [263] Chaupatnaik A, Rouse G, Perez A J, Morozov A V, Elkaïm E, Avdeev M, et al. 2024 Synthesis, Structure, and Electrochemistry of Crystallized Layered Chlorides,  $\text{LiMCl}_6$  ( $\text{M} = \text{Ta/Nb}$ ) *Adv. Energy Mater.* **14** 2402555
- [264] Kwak H, Kim J-S, Han D, Kim J S, Park J, Kwon G, et al. 2023 Boosting the interfacial superionic conduction of halide solid electrolytes for all-solid-state batteries *Nat. Commun.* **14** 2459
- [265] Wang G, Zhang S, Wu H, Zheng M, Zhao C, Liang J, et al. 2025 Oxychloride Polyanion Clustered Solid-State Electrolytes via Hydrate-Assisted Synthesis for All-Solid-State Batteries *Adv. Mater.* **37** 2410402
- [266] You I, Singh B, Cui M, Goward G, Qian L, Arthur Z, et al. 2025 A facile route to plastic inorganic electrolytes for all-solid state batteries based on molecular design *Energy Environ. Sci.* **18** 478–91
- [267] Duan H, Wang C, Zhang X-S, Fu J, Li W, Wan J, et al. 2024 Amorphous  $\text{AlOCl}$  compounds enabling nanocrystalline  $\text{LiCl}$  with abnormally high ionic conductivity *J. Am. Chem. Soc.* **146** 29335–43

- [268] Yuan L, Peng W, Zhan Z, Wang J, Feng Y, Yan Y, et al. 2025 Enhancing Ion Transport at Primary Interparticle Boundaries of Polycrystalline Lithium-Rich Oxide in All-Solid-State Batteries *Angew. Chem. Int. Ed.* **64** e202508605
- [269] Schlautmann E, Weiß A, Maus O, Ketter L, Rana M, Puls S, et al. 2023 Impact of the solid electrolyte particle size distribution in sulfide-based solid-state battery composites *Adv. Energy Mater.* **13** 2302309
- [270] Woo J, Song Y B, Kwak H, Jun S, Jang B Y, Park J, et al. 2023 Liquid-Phase Synthesis of Highly Deformable and Air-Stable Sn-Substituted  $\text{Li}_3\text{PS}_4$  for All-Solid-State Batteries Fabricated and Operated under Low Pressures *Adv. Energy Mater.* **13** 2203292
- [271] Ohsaki S, Yano T, Hatada A, Nakamura H and Watano S 2021 Size control of sulfide-based solid electrolyte particles through liquid-phase synthesis *Powder Technol.* **387** 415–20
- [272] Kim Y-S, Jeon S H, Cho W, Kim K, Yu J, Yi J, et al. 2022 Surficial sulfur loss of jet-milled  $\text{Li}_6\text{PS}_5\text{Cl}$  powder under mild-temperature heat treatment *ACS Appl. Energy Mater.* **5** 15442–51
- [273] Shannon R and Prewitt C 1970 Revised values of effective ionic radii *Structural Sci.* **26** 1046–8
- [274] Lei P, Wu G, Liu H, Qi X, Wu M, Li D, et al. 2025 Boosting Ion Conduction and Moisture Stability Through  $\text{Zn}^{2+}$  Substitution of Chloride Electrolytes for All-Solid-State Lithium Batteries *Adv. Energy Mater.* **15** 2405760
- [275] Kim K T, Woo J, Kim Y S, Sung S, Park C, Lee C, et al. 2023 Ultrathin Superhydrophobic Coatings for Air-Stable Inorganic Solid Electrolytes: Toward Dry Room Application for All-Solid-State Batteries *Adv. Energy Mater.* **13** 2301600
- [276] Samanta S, Bera S, Biswas R K, Mondal S, Mandal L and Banerjee A 2024 Ionocovalency of the Central Metal Halide Bond-Dependent Chemical Compatibility of Halide Solid Electrolytes with  $\text{Li}_6\text{PS}_5\text{Cl}$  *ACS Energy Lett.* **9** 3683–93
- [277] Xia W, Zhao Y, Zhao F, Adair K, Zhao R, Li S, et al. 2022 Antiperovskite electrolytes for solid-state batteries *Chem. Rev.* **122** 3763–819
- [278] Li W, Li M, Ren H, Kim J T, Li R, Sham T-K, et al. 2025 Nitride solid-state electrolytes for all-solid-state lithium metal batteries *Energy Environ. Sci.* **18** 4521–54
- [279] Shen L, Wang Z, Xu S, Law H M, Zhou Y and Ciucci F 2025 Harnessing database-supported high-throughput screening for the design of stable interlayers in halide-based all-solid-state batteries *Nat. Commun.* **16** 3687
- [280] Xiao Y, Wang Y, Bo S H, Kim J C, Miara L J and Ceder G 2020 Understanding interface stability in solid-state batteries *Nat. Rev. Mater.* **5** 105–26
- [281] Wang Y, Ye L, Fitzhugh W, Chen X and Li X 2023 Interface Coating Design for Dynamic Voltage Stability of Solid-State Batteries *Adv. Energy Mater.* **13** 2302288
- [282] Hwang T, Bae J H, Lee S R, Park H, Park J W, Ha Y C, et al. 2024 Oxygen Substitution to Enhance Chemo-Mechanical Stability at the Cathode-Sulfide Electrolyte Interface in All-Solid-State Batteries *ACS Nano* **18** 23320–30
- [283] Zhang S, Zhao F, Wang S, Liang J, Wang J, Wang C, et al. 2021 Advanced High-Voltage All-Solid-State Li-Ion Batteries Enabled by a Dual-Halogen Solid Electrolyte *Adv. Energy Mater.* **11** 2100836
- [284] Strauss F, Stepien D, Maibach J, Pfaffmann L, Indris S, Hartmann P, et al. 2020 Influence of electronically conductive additives on the cycling performance of argyrodite-based all-solid-state batteries *RSC Adv.* **10** 1114–9
- [285] Tan D H S, Wu E A, Nguyen H, Chen Z, Marple M A T, Doux J M, et al. 2019 Elucidating Reversible Electrochemical Redox of  $\text{Li}_6\text{PS}_5\text{Cl}$  Solid Electrolyte *ACS Energy Lett.* **4** 2418–27

- [286] Suzuki K, Mashimo N, Ikeda Y, Yokoi T, Hirayama M and Kanno R 2018 High Cycle Capability of All-Solid-State Lithium–Sulfur Batteries Using Composite Electrodes by Liquid-Phase and Mechanical Mixing *ACS Appl. Energy Mater.* **1** 2373–7
- [287] Wang S, Zhang Y, Zhang X, Liu T, Lin Y H, Shen Y, et al. 2018 High-Conductivity Argyrodite  $\text{Li}_6\text{PS}_5\text{Cl}$  Solid Electrolytes Prepared via Optimized Sintering Processes for All-Solid-State Lithium–Sulfur Batteries *ACS Appl. Mater. Interfaces* **10** 42279–85
- [288] Song H, Münch K, Liu X, Shen K, Zhang R, Weintraut T, et al. 2025 All-solid-state Li–S batteries with fast solid–solid sulfur reaction *Nature* **637** 846–53
- [289] Nikodimos Y, Su W N and Hwang B J 2023 Halide Solid-State Electrolytes: Stability and Application for High Voltage All-Solid-State Li Batteries *Adv. Energy Mater.* **13** 2202854
- [290] Song Z, Dai Y, Wang T, Yu Q, Ye X, Wang L, et al. 2024 An Active Halide Catholyte Boosts the Extra Capacity for All-Solid-State Batteries *Adv. Mater.* **36** 2405277
- [291] Fu J, Wang C, Wang S, Reid J W, Liang J, Luo J, et al. 2025 A cost-effective all-in-one halide material for all-solid-state batteries *Nature* **643** 111–8
- [292] Zhang G, Liu Z, Ma Y, Pepas J, Bai J, Zhong H, et al. 2024  $\text{Li}_{2.9}\text{Fe}_{0.9}\text{Zr}_{0.1}\text{Cl}_6$  as Redox-Active Catholyte for Solid-State Li-Ion Batteries *Chem. Mater.* **36** 10104–12
- [293] Wang K, Gu Z, Xi Z, Hu L and Ma C 2023  $\text{Li}_3\text{TiCl}_6$  as ionic conductive and compressible positive electrode active material for all-solid-state lithium-based batteries *Nat. Commun.* **14** 1396
- [294] Kmiec S, Ruoff E and Manthiram A 2025 A New Class of Oxyhalide Solid Electrolytes  $\text{NaNbCl}_{6-2x}\text{O}_x$  for Solid-state Sodium Batteries *Angew. Chem. Int. Ed.* **64** e202416979
- [295] Ruoff E, Kmiec S and Manthiram A 2025 Redox-Active Halide Catholytes for Enhanced Energy Density in Solid-State Sodium Batteries *ACS Appl. Mater. Interfaces* **17** 18420–29
- [296] Schwietert T K, Arszlewska V A, Wang C, Yu C, Vasileiadis A, de Klerk N J J, et al. 2020 Clarifying the relationship between redox activity and electrochemical stability in solid electrolytes *Nat. Mater.* **19** 428–35
- [297] Zhang X, Wang S, Xue C, Xin C, Lin Y, Shen Y, et al. 2019 Self-suppression of lithium dendrite in all-solid-state lithium metal batteries with poly(vinylidene difluoride)-based solid electrolytes *Adv. Mater.* **31** 1806082
- [298] Piana G, Bella F, Geobaldo F, Meligrana G and Gerbaldi C 2019 PEO/LAGP hybrid solid polymer electrolytes for ambient temperature lithium batteries by solvent-free, “one pot” preparation *J. Energy Storage* **26** 100947
- [299] Ren Y, Deng H, Chen R, Shen Y, Lin Y and Nan C-W 2015 Effects of Li source on microstructure and ionic conductivity of Al-contained  $\text{Li}_{6.75}\text{La}_3\text{Zr}_{1.75}\text{Ta}_{0.25}\text{O}_{12}$  ceramics *J. Eur. Ceram. Soc.* **35** 561–72
- [300] Zhou R, Gautam A, Suard E, Li S, Ganapathy S, Chen K, et al. 2025 Boosting ionic conductivity and air stability in bromide-rich thioarsenate argyrodite solid electrolytes *Adv. Funct. Mater.* **35** 2420971
- [301] Zhang Z and Kennedy J H 1990 Synthesis and characterization of the  $\text{B}_2\text{S}_3\text{-Li}_2\text{S}$ , the  $\text{P}_2\text{S}_5\text{-Li}_2\text{S}$  and the  $\text{B}_2\text{S}_3\text{-P}_2\text{S}_5\text{-Li}_2\text{S}$  glass systems *Solid State Ion.* **38** 217–24
- [302] Yu C, van Eijck L, Ganapathy S and Wagemaker M 2016 Synthesis, structure and electrochemical performance of the argyrodite  $\text{Li}_6\text{PS}_5\text{Cl}$  solid electrolyte for Li-ion solid state batteries *Electrochim. Acta* **215** 93–9
- [303] Mizuno F, Hayashi A, Tadanaga K and Tatsumisago M 2005 New, highly ion-conductive crystals precipitated from  $\text{Li}_2\text{S-P}_2\text{S}_5$  glasses *Adv. Mater.* **17** 918–21

- [304] Wang S, Gautam A, Wu X, Li S, Zhang X, He H, et al. 2024 Effect of processing on structure and ionic conductivity of chlorine-rich lithium argyrodites *Adv. Energy Sustain. Res.* **5** 2200197
- [305] Li S, Lin J, Schaller M, Indris S, Zhang X, Brezesinski T, et al. 2023 High-entropy lithium argyrodite solid electrolytes enabling stable all-solid-state batteries *Angew. Chem. Int. Ed.* **62** e202314155
- [306] Zhou L, Zuo T-T, Kwok C Y, Kim S Y, Assoud A, Zhang Q, et al. 2022 High areal capacity, long cycle life 4 V ceramic all-solid-state Li-ion batteries enabled by chloride solid electrolytes *Nat. Energy* **7** 83–93
- [307] Miura A, Rosero-Navarro N C, Sakuda A, Tadanaga K, Phuc N H H, Matsuda A, et al. 2019 Liquid-phase syntheses of sulfide electrolytes for all-solid-state lithium battery *Nat. Rev. Chem.* **3** 189–98
- [308] Li G, Wang S, Fu J, Liu Y and Chen Z 2023 Manufacturing high-energy-density sulfidic solid-state batteries *Batteries* **9** 347
- [309] Wang C, Liang J, Luo J, Liu J, Li X, Zhao F, et al. 2021 A universal wet-chemistry synthesis of solid-state halide electrolytes for all-solid-state lithium-metal batteries *Sci. Adv.* **7** eabh1896
- [310] Liu Y, Xu B, Zhang W, Li L, Lin Y and Nan C 2020 Composition modulation and structure design of inorganic-in-polymer composite solid electrolytes for advanced lithium batteries *Small* **16** 1902813
- [311] Li S, Yang Z, Wang S-B, Ye M, He H, Zhang X, et al. 2024 Sulfide-based composite solid electrolyte films for all-solid-state batteries *Commun. Mater.* **5** 44
- [312] Zhang Z, Wu L, Zhou D, Weng W and Yao X 2021 Flexible sulfide electrolyte thin membrane with ultrahigh ionic conductivity for all-solid-state lithium batteries *Nano Lett.* **21** 5233–9
- [313] Wang C, Yu R, Duan H, Lu Q, Li Q, Adair K R, et al. 2022 Solvent-free approach for interweaving freestanding and ultrathin inorganic solid electrolyte membranes *ACS Energy Lett.* **7** 410–6
- [314] Fleischauer M D, Hatchard T D, Rockwell G P, Topple J M, Trussler S, Jericho S K, et al. 2003 Design and Testing of a 64-Channel Combinatorial Electrochemical Cell *J. Electrochem. Soc.* **150** A1465–9
- [315] Al-Maghrabi M A, van der Bosch N, Sanderson R J, Stevens D A, Dunlap R A and Dahn J R 2011 A New Design for a Combinatorial Electrochemical Cell Plate and the Inherent Irreversible Capacity of Lithiated Silicon *Electrochem. Solid-State Lett.* **14** A42–4
- [316] Beal M S, Hayden B E, Le Gall T, Lee C E, Lu X, Mirsaneh M, et al. 2011 High Throughput Methodology for Synthesis, Screening, and Optimization of Solid State Lithium Ion Electrolytes *ACS Comb. Sci.* **13** 375–81
- [317] Yada C, Lee C E, Laughman D, Hannah L, Iba H and Hayden B E 2015 A High-Throughput Approach Developing Lithium-Niobium-Tantalum Oxides as Electrolyte/Cathode Interlayers for High-Voltage All-Solid-State Lithium Batteries *J. Electrochem. Soc.* **162** A722–6
- [318] Szymanski N J, Rendy B, Fei Y, Kumar R E, He T, Milsted D, et al. 2023 An autonomous laboratory for the accelerated synthesis of novel materials *Nature* **624** 86–91
- [319] Jonderian A, Anderson E, Peng R, Xu P, Jia S, Cozea V, et al. 2022 Suite of high-throughput experiments for screening solid electrolytes for Li batteries *J. Electrochem. Soc.* **169** 050504
- [320] Jonderian A, Rehman S, Card Gormley M, Jia S, Ma S B, Kwon G, et al. 2024 Pioneering combinatorial investigation to unlock the potential of lithium borosilicate glasses as solid electrolytes *ACS Appl. Energy Mater.* **7** 11278–87

- [321] Anderson E, Zolfaghar E, Jonderian A, Khaliullin R and McCalla E 2024 Comprehensive Dopant Screening in  $\text{Li}_7\text{La}_3\text{Zr}_2\text{O}_{12}$  Garnet Solid Electrolyte *Adv. Energy Mater.* **14** 230425
- [322] Johari N S M, Jonderian A, Jia S, Cozea V, Yao E, Adnan S B R S, et al. 2022 High-throughput development of  $\text{Na}_2\text{ZnSiO}_4$ -based hybrid electrolytes for sodium-ion batteries *J. Power Sources* **541** 231706
- [323] McCalla E 2023 Semiautomated experiments to accelerate the design of advanced battery materials: combining speed, low cost, and adaptability *ACS Engineering Au* **3** 391–402
- [324] Manna S, Paul P, Manna S S, Das S and Pathak B 2025 Utilizing Machine Learning to Advance Battery Materials Design: Challenges and Prospects *Chem. Mater.* **37** 1759–87
- [325] McCalla E 2024 Braving the elements: learning from 60+ dopants in battery materials *J. Phys. Chem. C* **128** 16831–43
- [326] S. Shukla, G. Anand and S. Agarwal 2025 Advancements in Solid-State Batteries for Electric Vehicles: A Comprehensive Review. *IJSSIC* **2** 1–14
- [327] Zeinali Galabi N, Liu C, Jain M, Kamel M, Jia S, Bengio J, et al. 2025 Navigating ternary doping in Li-ion cathodes with closed-loop multi-objective Bayesian optimization <https://doi.org/10.26434/chemrxiv-2025-9f5ts>
- [328] Vahdatkhah P, Zolfaghar Y and McCalla E 2025 Adapting High-Throughput Synthesis for Aggressively Air-Sensitive Halide Solid Electrolytes *247<sup>th</sup> ECS conference* A03-0197, <https://ecs.confex.com/ecs/247/meetingapp.cgi/Paper/200609>
- [329] Zolfaghar E, Vahdatkhah P and McCalla E 2025 Development of High-Throughput Solid-State Synthesis and Screening of Halide Solid Electrolytes *247<sup>th</sup> ECS conference* A03-0404, <https://ecs.confex.com/ecs/247/meetingapp.cgi/Paper/202568>
- [330] Projects for Graduate Students in CEDER group, <https://ceder.berkeley.edu/wp-content/uploads/2024/02/Projects-for-Graduate-Students-in-CEDER-group-UC-Berkeley.pdf>, accessed on July 22, 2025
- [331] Gendron D M, Torabi A, Wanees M, Dsouza M S, Feddersen B, et al. 2025 Method—A High-Throughput Technique for Unidirectional Critical Current Density Testing of Solid Electrolyte Materials *J. Electrochem. Soc.* **172** 020511
- [332] Atkins D, Capria E, Edström K, Famprikis T, Grimaud A, Jacquet Q, et al. 2022 Accelerating Battery Characterization Using Neutron and Synchrotron Techniques: Toward a Multi-Modal and Multi-Scale Standardized Experimental Workflow *Adv. Energy Mater.* **12** 2102694
- [333] Strauss F, Kitsche D, Ma Y, Teo J H, Goonetilleke D, Janek J, et al. 2021 Operando Characterization Techniques for All-Solid-State Lithium-Ion Batteries *Adv. Energy Sustainability Res.* **2** 2100004
- [334] Huang Y, Perlmutter D, Fei-Huei Su A, Quenum J, Shevchenko P, Parkinson D Y, et al. 2023 Detecting lithium plating dynamics in a solid-state battery with operando X-ray computed tomography using machine learning *Npj Comput. Mater.* **9** 93
- [335] Ning Z, Jolly D S, Li G, De Meyere R, Pu S D, Chen Y, et al. 2021 Visualizing plating-induced cracking in lithium-anode solid-electrolyte cells *Nat. Mater.* **20** 1121–9
- [336] Ji T, Zhang Y, Torres J, Mijailovic A S, Tang Y, Zhao X, et al. 2025 Operando neutron imaging-guided gradient design of Li-ion solid conductor for high-mass-loading cathodes *Nat. Commun.* **16** 7667
- [337] Bradbury R, Kardjilov N, Dewald G F, Tengattini A, Helfen L, Zeier W G, et al. 2023 Visualizing Lithium Ion Transport in Solid-State Li–S Batteries Using  $^6\text{Li}$  Contrast Enhanced Neutron Imaging *Adv. Funct. Mater.* **33** 2302619

- [338] Yadav N G, Folastre N, Bolmont M, Jamali A, Morcrette M and Davoisne C 2022 Study of failure modes in two sulphide-based solid electrolyte all-solid-state batteries via in situ SEM *J. Mater. Chem A* **10** 17142–55
- [339] Zhao L, Feng M, Wu C, Guo L, Chen Z, Risal S, et al. 2025 Imaging the evolution of lithium-solid electrolyte interface using operando scanning electron microscopy *Nat. Commun.* **16** 4283
- [340] Basak S, Migunov V, Tavabi A H, George C, Lee Q, Rosi P, et al. 2020 Operando Transmission Electron Microscopy Study of All-Solid-State Battery Interface: Redistribution of Lithium among Interconnected Particles *ACS Appl. Energy Mater.* **3** 5101–6
- [341] Perrenot P, Bayle-Guillemaud P, Jouneau P H, Boulineau A and Villevieille C 2024 Operando Focused Ion Beam–Scanning Electron Microscope (FIB-SEM) Revealing Microstructural and Morphological Evolution in a Solid-State Battery *ACS Energy Lett.* **9** 3835–40
- [342] Brant W R, Li D, Gu Q and Schmid S 2016 Comparative analysis of ex-situ and operando X-ray diffraction experiments for lithium insertion materials *J. Power Sources* **302** 126–34
- [343] Korjus O, Anil Kumar S, Gendrin L, Vial S, Villevieille C and Suard E 2025 Enabling Operando Neutron Diffraction for Solid-State Battery Studies *ACS Mater. Lett.* **7** 2725–31
- [344] Choudhary K, Santos Mendoza I O, Nadeina A, Becker D, Lombard T, Sez nec V, et al. 2023 Operando X-ray diffraction in transmission geometry « at home » from tape casted electrodes to all-solid-state battery *J. Power Sources* **553** 232270
- [345] Boulet-Roblin L, Borel P, Sheptyakov D, Tessier C, Novák P and Villevieille C 2016 Operando Neutron Powder Diffraction Using Cylindrical Cell Design: The Case of  $\text{LiNi}_{0.5}\text{Mn}_{1.5}\text{O}_4$  vs Graphite *J. Phys. Chem C* **120** 17268–73
- [346] Bianchini M, Leriche J B, Laborier J L, Gendrin L, Suard E, Croguennec L, et al. 2013 A New Null Matrix Electrochemical Cell for Rietveld Refinements of In-Situ or Operando Neutron Powder Diffraction Data *J. Electrochem. Soc.* **160** A2176–83
- [347] Roberts M, Biendicho J J, Hull S, Beran P, Gustafsson T, Svensson G, et al. 2013 Design of a new lithium ion battery test cell for in-situ neutron diffraction measurements *J. Power Sources* **226** 249–55
- [348] Stavola A M, Sun X, Guida D P, Bruck A M, Cao D, Okasinski J S, et al. 2023 Lithiation Gradients and Tortuosity Factors in Thick NMC111-Argyrodite Solid-State Cathodes *ACS Energy Lett.* **8** 1273–80
- [349] Sottmann J, Di Michiel M, Fjellvåg H, Malavasi L, Margadonna S, Vajeeston P, et al. 2017 Chemical Structures of Specific Sodium Ion Battery Components Determined by Operando Pair Distribution Function and X-ray Diffraction Computed Tomography *Angew. Chem. Int. Ed.* **56** 11385–9
- [350] Li Z, Yin L, Mattei G S, Cosby M R, Lee B S, Wu Z, et al. 2020 Synchrotron Operando Depth Profiling Studies of State-of-Charge Gradients in Thick  $\text{Li}(\text{Ni}_{0.8}\text{Mn}_{0.1}\text{Co}_{0.1})\text{O}_2$  Cathode Films *Chem Mater.* **32** 6358–64
- [351] Hu J, Young R S, Lukic B, Broche L, Jervis R, Shearing P R, et al. 2025 Quantifying Heterogeneous Degradation Pathways and Deformation Fields in Solid-State Batteries *Adv. Energy Mater.* **15** 2404231
- [352] Finegan D P, Vamvakeros A, Tan C, Heenan T M M, Daemi S R, Seitzman N, et al. 2020 Spatial quantification of dynamic inter and intra particle crystallographic heterogeneities within lithium ion electrodes *Nat. Commun.* **11** 631
- [353] Ulvestad A, Singer A, Clark J N, Cho H M, Kim J W, Harder R, et al. 2015 Topological defect dynamics in operando battery nanoparticles *Science* **348** 1344–7

- [354] Jacquet Q, Cele J, Casiez L, Tardif S, Medjaheh A, Pouget M B, et al. 2025 Operando microimaging of crystal structure and orientation in all components of all-solid-state-batteries *Nat. Commun.* **16** 11524
- [355] Villevieille C, Thompson O and Vaughan G 2024 Revealing the spatial distribution of decomposition products upon ageing on Li<sub>6</sub>PS<sub>5</sub>Cl solid electrolyte via X-ray diffraction computed tomography *Research Square* <https://doi.org/10.21203/rs.3.rs-5191594/v1>
- [356] Villevieille C 2025 The challenge of studying interfaces in battery materials *Nat. Nanotechnol.* **20** 2–5
- [357] Chen Y T, Jang J, Oh J A S, Ham S Y, Yang H, Lee D J, et al. 2024 Enabling Uniform and Accurate Control of Cycling Pressure for All-Solid-State Batteries *Adv. Energy Mater.* **14** 2304327
- [358] Lee C, Kim J Y, Bae K Y, Kim T, Jung S J, Son S, et al. 2024 Enhancing electrochemomechanics: How stack pressure regulation affects all-solid-state batteries *Energy Storage Mater.* **66** 103196
- [359] Reif B, Ashbrook S E, Emsley L and Hong M 2021 Solid-state NMR spectroscopy *Nat. Rev. Methods Primers* **1** 2
- [360] Chandran C V and Heitjans P 2016 Solid-state NMR studies of lithium ion dynamics across materials classes *Ann. Rep. NMR Spectr.* **89** 1–102
- [361] Harm S, Hatz A-K, Moudrakovski I, Eger R, Kuhn A, Hoch C, et al. 2019 Lesson learned from NMR: characterization and ionic conductivity of LGPS-like Li<sub>7</sub>SiPS<sub>8</sub> *Chem. Mater.* **31** 1280–8
- [362] Hogrefe K, Minafra N, Hanghofer I, Banik A, Zeier W G and Wilkening H M R 2022 Opening diffusion pathways through site disorder: the interplay of local structure and ion dynamics in the solid electrolyte Li<sub>6+x</sub>P<sub>1-x</sub>Ge<sub>x</sub>S<sub>5</sub>I as probed by neutron diffraction and NMR *J. Am. Chem. Soc.* **144** 1795–812
- [363] Böhmer R, Jeffrey K R and Vogel M 2007 Solid-state Li NMR with applications to the translational dynamics in ion conductors *Prog. Nucl. Magn. Reson. Spectrosc.* **50** 87–174
- [364] Hogrefe K, Minafra N, Zeier W G and Wilkening H M R 2021 Tracking ions the direct way: long-range Li<sup>+</sup> dynamics in the thio-LISICON family Li<sub>4</sub>MCh<sub>4</sub> (M = Sn, Ge; Ch = S, Se) as probed by <sup>7</sup>Li NMR relaxometry and <sup>7</sup>Li spin-alignment echo NMR *J. Phys. Chem. C* **125** 2306–17
- [365] Hogrefe K, Stainer F, Minafra N, Zeier W G and Wilkening H M R 2024 NMR down to cryogenic temperatures: accessing the rate-limiting step of Li transport in argyrodite electrolytes *Chem. Mater.* **36** 6527–34
- [366] Wilkening M and Heitjans P 2006 Extremely slow cation exchange processes in Li<sub>4</sub>SiO<sub>4</sub> probed directly by two-time <sup>7</sup>Li stimulated-echo nuclear magnetic resonance spectroscopy *J. Phys.: Condes. Matter* **18** 9849–62
- [367] Gamon J, Duff B B, Dyer M S, Collins C, Daniels L M, Surta T W, et al. 2019 Computationally guided discovery of the sulfide Li<sub>3</sub>AlS<sub>3</sub> in the Li–Al–S Phase field: Structure and lithium conductivity *Chem. Mater.* **31** 9699–714
- [368] Marko A, Hogrefe K, Schweiger L, Stainer F, Königsreiter J, Spsychala J, et al. 2025 Mapping the various Li<sup>+</sup> jump pathways in Li<sub>10</sub>GeP<sub>2</sub>S<sub>12</sub>: from ultraslow exchange to high-temperature diffusion *J. Am. Chem. Soc.* **147** 38215–24
- [369] Patel S V, Banerjee S, Liu H, Wang P, Chien P-H, Feng X, et al. 2021 Tunable lithium-ion transport in mixed-halide argyrodites Li<sub>6-x</sub>PS<sub>5-x</sub>ClBr<sub>x</sub>: an unusual compositional space *Chem. Mater.* **33** 1435–43

- [370] Hanghofer I, Brinek M, Eisbacher S, Bitschnau B, Volck M, Hennige V, et al. 2019 Substitutional disorder: structure and ion dynamics of the argyrodites  $\text{Li}_6\text{PS}_5\text{Cl}$ ,  $\text{Li}_6\text{PS}_5\text{Br}$  and  $\text{Li}_6\text{PS}_5\text{I}$  *Phys. Chem. Chem. Phys.* **21** 8489–507
- [371] Tapler D, Gadermaier B, Spychala J, Stainer F, Marko A, Königsreiter J, et al. 2025 Unraveling ultrafast Li-ion dynamics in the solid electrolyte  $\text{LiTi}_2(\text{PS}_4)_3$  by NMR down to cryogenic temperatures *J. Am. Chem. Soc.* **147** 20023–32
- [372] Banik A, Famprikis T, Ghidui M, Ohno S, Kraft M A and Zeier W G 2021 On the underestimated influence of synthetic conditions in solid ionic conductors *Chem. Sci.* **12** 6238–63
- [373] Stainer F, Gadermaier B and Wilkening H M R 2025 Local and long-range diffusion in  $\text{Li}_3\text{InCl}_6$ : impact of preparation method on ion dynamics *Chem. Mater.* **37** 2650–63
- [374] Lunghammer S and Wilkening H M R 2025  $\text{Na}^+$  self-diffusion and ionic transport in sodium  $\beta''$ -alumina *Solid State Ion.* **422** 116809
- [375] Bottke P, Freude D and Wilkening M 2013 Ultraslow Li exchange processes in diamagnetic  $\text{Li}_2\text{ZrO}_3$  as monitored by EXSY NMR *J. Phys. Chem. C* **117** 8114–9
- [376] Bottke P, Hogrefe K, Kohl J, Nakhal S, Wilkening A, Heitjans P, et al. 2023 Energetically preferred  $\text{Li}^+$  ion jump processes in crystalline solids: site-specific hopping in  $\beta$ - $\text{Li}_3\text{VF}_6$  as revealed by high-resolution  $^6\text{Li}$  2D EXSY NMR *Mater. Res. Bull.* **162** 112193
- [377] Gombotz M, Hogrefe K, Zettl R, Gadermaier B and Wilkening H M R 2021 Fuzzy logic: about the origins of fast ion dynamics in crystalline solids *Phil. Trans. A* **379** 20200434
- [378] Jiang Y, Zhao M, Peng Z and Zhong G 2024 Progress in in-situ electrochemical nuclear magnetic resonance for battery research *Magn. Res. Lett.* **4** 200099
- [379] Heitjans P 1986 Use of beta radiation-detected NMR to study ionic motion in solids *Solid State Ion.* **18-19** 50-64
- [380] MacFarlane W A 2015 Implanted-ion  $\beta\text{NMR}$ : a new probe for nanoscience *Solid State Nucl. Magn. Reson.* **68-69** 1–12
- [381] MacFarlane W A 2022 Status and progress of ion-implanted  $\beta\text{NMR}$  at TRIUMF *Z. Phys. Chem.* **236** 757–98
- [382] Zhang X and Huo H 2021 Nuclear magnetic resonance studies of organic-inorganic composite solid electrolytes *Magn. Res. Lett.* **1** 142–52
- [383] Zagórski J, López del Amo J M, Cordill M J, Aguesse F, Buannic L and Llordés A 2019 Garnet-polymer composite electrolytes: new insights on local Li-ion dynamics and electrodeposition stability with Li metal anodes *ACS Appl. Energy Mater.* **2** 1734–46
- [384] Heitjans P and Indris S 2003 Diffusion and ionic conduction in nanocrystalline ceramics *J. Phys.: Condes. Matter* **15** R1257–89
- [385] Breuer S, Uitz M and Wilkening H M R 2018 Rapid Li ion dynamics in the interfacial regions of nanocrystalline solids *J. Phys. Chem. Lett.* **9** 2093–7
- [386] Gombotz M, Pree K P, Pregartner V, Hanzu I, Gadermaier B, Hogrefe K, et al. 2021 Insulator:conductor interfacial regions — Li ion dynamics in the nanocrystalline dispersed ionic conductor  $\text{LiF}:\text{TiO}_2$  *Solid State Ion.* **369** 115726
- [387] Breuer S, Pregartner V, Lunghammer S and Wilkening H M R 2019 Dispersed solid conductors: fast interfacial Li-ion dynamics in nanostructured  $\text{LiF}$  and  $\text{LiF}:\text{g-Al}_2\text{O}_3$  composites *J. Phys. Chem. C* **123** 5222–30
- [388] Marko A, Scheiber T, Gadermaier B and Wilkening H M R 2025 Interfacial lithiation of lithium aluminum titanium phosphate explored by  $^7\text{Li}$  NMR *Commun. Chem.* **8** 102

- 1 [389] Huang Y, Wu X, Nie L, Chen S, Sun Z, He Y, et al. 2020 Mechanism of lithium  
2 electrodeposition in a magnetic field *Solid State Ion.* **345** 115171
- 3
- 4 [390] Hanghofer I, Gadermaier B and Wilkening H M R 2019 Fast Rotational Dynamics in  
5 Argyrodite-Type  $\text{Li}_6\text{PS}_5\text{X}$  (X: Cl, Br, I) as Seen by  $^{31}\text{P}$  Nuclear Magnetic Relaxation — On  
6 Cation–Anion Coupled Transport in Thiophosphates *Chem. Mater.* **31** 4591–7
- 7
- 8 [391] Hogrefe K, Gadermaier B, Schneider C, Bette S, Lotsch B V and Wilkening H M R 2025 A  
9 dynamically induced phase transition in  $\text{Na}_4\text{P}_2\text{S}_6$ : ultrafast  $\text{Na}^+$  mobility triggering rotor phase  
10 formation *J. Am. Chem. Soc.* **147** 28799–809
- 11
- 12 [392] Blanc F, Leskes M and Grey C P 2013 In situ solid-state NMR spectroscopy of electrochemical  
13 cells: batteries, supercapacitors, and fuel cells *Acc. Chem. Res.* **46** 1952–63
- 14
- 15 [393] Maity A, Svirinovsky-Arbeli A, Buganim Y, Oppenheim C and Leskes M 2024 Tracking  
16 dendrites and solid electrolyte interphase formation with dynamic nuclear polarization NMR  
17 spectroscopy *Nat. Commun.* **15** 9956
- 18
- 19 [394] Freytag A I, Pauric A D, Krachkovskiy S A and Goward G R 2019 In situ magic-angle  
20 spinning  $^7\text{Li}$  NMR analysis of a full electrochemical lithium-ion battery using a jelly roll cell  
21 design *J. Am. Chem. Soc.* **141** 13758–61
- 22
- 23 [395] Marbella L E, Zekoll S, Kasemchainan J, Emge S P, Bruce P G and Grey C P 2019  $^7\text{Li}$  NMR  
24 chemical shift imaging to detect microstructural growth of lithium in all-solid-state batteries  
25 *Chem. Mater.* **31** 2762–9
- 26
- 27 [396] Liu H, Chen Y, Chien P-H, Amouzandeh G, Hou D, Truong E, et al. 2025 Dendrite formation  
28 in solid-state batteries arising from lithium plating and electrolyte reduction *Nat. Mater.* **24**  
29 581–8
- 30
- 31 [397] Hope M A, Rinkel B L D, Gunnarsdóttir A B, Märker K, Menkin S, Paul S, et al. 2020  
32 Selective NMR observation of the SEI–metal interface by dynamic nuclear polarisation from  
33 lithium metal *Nat. Commun.* **11** 2224
- 34
- 35 [398] Fan E, Li L, Wang Z, Lin J, Huang Y, Yao Y, et al. 2020 Sustainable Recycling Technology  
36 for Li-Ion Batteries and Beyond: Challenges and Future Prospects *Chem. Rev.* **120** 7020–63
- 37
- 38 [399] Rasoulnia P, Chen Q, Yang X and He C 2025 Recovery of valuable metals from end-of-life Li-  
39 ion batteries: Technologies, progress, and perspectives *Resour. Conserv. Recycl.* **223** 108497
- 40
- 41 [400] Xu P, Tan D H S, Jiao B, Gao H, Yu X and Chen Z 2023A Materials Perspective on Direct  
42 Recycling of Lithium-Ion Batteries: Principles, Challenges and Opportunities *Adv. Funct.*  
43 *Mater.* **33** 2213168
- 44
- 45 [401] Schirmer T, Qiu H, Goldmann D, Stallmeister C and Friedrich B 2022 Influence of P and Ti on  
46 Phase Formation at Solidification of Synthetic Slag Containing Li, Zr, La, and Ta *Minerals* **12**  
47 310
- 48
- 49 [402] Schwich L, Küpers M, Finsterbusch M, Schreiber A, Fattakhova-Rohlfing D, Guillon O, et al.  
50 2020 Recycling Strategies for Ceramic All-Solid-State Batteries—Part I: Study on Possible  
51 Treatments in Contrast to Li-Ion Battery Recycling *Metals* **10** 1523
- 52
- 53 [403] Waidha A I, Salihovic A, Jacob M, Vanita V, Aktekin B, Brix K, et al. 2023 Recycling of All-  
54 Solid-State Li-ion Batteries: A Case Study of the Separation of Individual Components Within  
55 a System Composed of LTO, LLZTO, and NMC *ChemSusChem* **16** e202202361
- 56
- 57 [404] Bertau M and Martin G 2019 Integrated Direct Carbonation Process for Lithium Recovery from  
58 Primary and Secondary Resources *Mater. Sci. Forum.* **959** 69–73
- 59
- 60

- 1 [405] Ihrig M, Kuo L-Y, Lobe S, Laptev A M, Lin C-A, Tu C-H, et al. 2023 Thermal Recovery of the  
2 Electrochemically Degraded  $\text{LiCoO}_2/\text{Li}_7\text{La}_3\text{Zr}_2\text{O}_{12}:\text{Al},\text{Ta}$  Interface in an All-Solid-State  
3 Lithium Battery *ACS Appl. Mater. Interfaces* **15** 4101–12
- 4 [406] Tan D H S, Xu P, Yang H, Kim M-C, Nguyen H, Wu E A, et al. 2020 Sustainable design of  
5 fully recyclable all solid-state batteries *MRS Energy & Sustainability* **7** E23
- 6 [407] Wissel K, Hu Z, Wu X, Jacob M, Küster K, Starke U, et al. 2025 Towards Recycling of All-  
7 Solid-State Batteries with Argyrodite Sulfide Electrolytes: Insights into Electrolyte and  
8 Electrode Degradation in Dissolution-Based Separation Processes *ChemSusChem* **18**  
9 e202402128
- 10 [408] Wissel K, Haben A, Küster K, Starke U, Kautenburger R, Ensinger W, et al. 2024 Direct  
11 Recycling of  $\beta\text{-Li}_3\text{PS}_4$ -Based All-Solid-State Li-Ion Batteries: Interactions of Electrode  
12 Materials and Electrolyte in a Dissolution-Based Separation Process *Adv. Energy Sustainability*  
13 *Res.* **5** 2300280
- 14 [409] Ghidui M, Ruhl J, Culver S P and Zeier W G 2019 Solution-based synthesis of lithium  
15 thiophosphate superionic conductors for solid-state batteries: a chemistry perspective *J. Mater.*  
16 *Chem. A* **7** 17735–53
- 17 [410] Jacob M, Moreno Fernandez H, Haben A, Waidha A I, Özel S, Hofmann J P, et al. 2025 Direct  
18 Recycling of All-Solid-State Batteries with a Halide Solid Electrolyte via Water-Based  
19 Separation: Interactions of Electrode Materials in Aqueous  $\text{Li}_3\text{InCl}_6$  Solutions *Batter.*  
20 *Supercaps* **8** e202500189
- 21 [411] Azhari L, Bong S, Ma X and Wang Y 2020 Recycling for All Solid-State Lithium-Ion Batteries  
22 *Matter* **3** 1845–61
- 23 [412] Jacob M, Wissel K and Clemens O 2024 Recycling of solid-state batteries—challenge and  
24 opportunity for a circular economy? *Mater. Futures.* **3** 012101
- 25 [413] Pehlivan İ B, Marsal R, Niklasson G A, Granqvist C G and Georén P 2010 PEI–LiTFSI  
26 electrolytes for electrochromic devices: Characterization by differential scanning calorimetry  
27 and viscosity measurements *Sol. Energy Mater. Sol. Cells* **94** 2399–404
- 28  
29  
30  
31  
32  
33  
34  
35  
36  
37  
38  
39  
40  
41  
42  
43  
44  
45  
46  
47  
48  
49  
50  
51  
52  
53  
54  
55  
56  
57  
58  
59  
60